

Electronic Thesis and Dissertation Repository

7-26-2017 12:00 AM

Cardiac repair post-myocardial infarction: Roles of the primary cilium and the long non-coding RNA Malat1

Jessica N. Blom
The University of Western Ontario

Supervisor
Dr. Qingping Feng
The University of Western Ontario

Graduate Program in Physiology and Pharmacology
A thesis submitted in partial fulfillment of the requirements for the degree in Doctor of Philosophy
© Jessica N. Blom 2017

Follow this and additional works at: <https://ir.lib.uwo.ca/etd>



Part of the [Medical Physiology Commons](#)

Recommended Citation

Blom, Jessica N., "Cardiac repair post-myocardial infarction: Roles of the primary cilium and the long non-coding RNA Malat1" (2017). *Electronic Thesis and Dissertation Repository*. 4897.
<https://ir.lib.uwo.ca/etd/4897>

This Dissertation/Thesis is brought to you for free and open access by Scholarship@Western. It has been accepted for inclusion in Electronic Thesis and Dissertation Repository by an authorized administrator of Scholarship@Western. For more information, please contact wlsadmin@uwo.ca.

Abstract

Complete occlusion of a coronary artery causes myocardial infarction (MI), resulting in cardiomyocyte cell death. The surviving myocardium undergoes a deleterious remodeling process which causes further injury, and can ultimately result in heart failure. Despite therapeutic advances that have prolonged life, MI remains a leading cause of death worldwide and imparts a significant economic burden. The advancement of treatments to improve cardiac repair post-MI requires the discovery of new targeted treatment strategies. Epicardial-to-mesenchymal transition (EMT) occurs post-MI as a mechanism to support neovascularization and cardiac healing. However, the endogenous EMT is not enough to support sufficient repair. The transcription factor Wilms' tumor 1 (Wt1) and the primary cilium regulate EMT by altering gene expression. Furthermore, the long non-coding RNA (lncRNA) *Malat1* is not only known to regulate EMT, but also mitigates cell death from injury. Little is known about the roles of Wt1, primary cilia, and *Malat1* in relation to neonatal cardiac regeneration and adult cardiac repair post-MI. The aim of this thesis was to investigate cardiac repair mechanisms related to EMT, primary cilia, and *Malat1*. To study the effects of Wt1 and *Malat1* deficiency, a reproducible model of cardiac regeneration using coronary artery ligation to induce MI was developed in neonatal mice. We demonstrated the robust capacity for neonatal cardiac regeneration as neither Wt1 nor *Malat1* deficiency affected the regenerative response. In the adult mouse, MI was induced to investigate the role of the primary cilium in EMT and repair post-MI, and the effects of *Malat1* deficiency on acute MI pathology. We found that indeed epicardial cells are ciliated, and primary ciliary disassembly supports EMT post-MI, which enhances the contribution of epicardium-derived cells (EPDCs) to

neovascularization. This reduced deleterious cardiac remodeling and preserved cardiac function. Contrastingly, *Malat1* deficiency augmented cardiac cell death from MI. Rather than affecting apoptosis, *Malat1* deficiency enhanced necroptotic cell death post-MI. Overall, this thesis is the first to show that in the adult heart, the primary cilium regulates epicardial EMT and the lncRNA *Malat1* governs the propensity for necroptosis from ischemic injury. Both the primary cilium and *Malat1* may serve as targets in the development of therapeutics to treat MI.

Keywords: Myocardial infarction; cardiac remodeling; cardiac regeneration; coronary artery ligation; epicardium-derived cells; epithelial-to-mesenchymal transition; angiogenesis; Wt1; primary cilium; long non-coding RNA; *Malat1*

Co-Authorship Statement

The studies outlined in **Chapters 2-4** were performed by Jessica Blom in the laboratory of Dr. Qingping Feng, with the assistance of co-authors listed below.

Dr. Qingping Feng contributed to experimental design, data interpretation, and manuscript preparation for all experiments. Additionally, Dr. Xiangru Lu assisted with scientific training and troubleshooting in all experiments.

Chapter 2: Dr. Xiangru Lu assisted with experimental training, and with Evan's blue perfusion experiments. Paul Arnold assisted with obtaining images of the surgical procedure.

Chapter 3: Outside of experimental training and assistance with troubleshooting, Dr. Xiangru Lu performed 70% of adult MI surgeries for the study while Jessica Blom performed the other 30%. Dr. Xiangru Lu also propagated both the Ad-shIf88 and Ad-GFP adenovirus. Ms. Mella Kim worked as an undergraduate student and assisted with tissue processing and histology, as well as intramyocardial adenoviral injection.

Chapter 4: The *Malat1*^{-/-} mouse was a generous gift from Dr. David L. Spector from Cold Spring Harbor Laboratory, New York. Dr. Xiangru Lu performed 75% of the MI surgeries for the study while Jessica Blom performed the other 25%. Dr. Xiangru Lu performed all functional measurements using the Millar pressure-conductance catheter. Additionally, Dr. Xiangru Lu helped with PI imaging, and Western blotting.

Acknowledgments

I would like to express great appreciation for the support and guidance of numerous individuals, without whom completing my PhD would not have been possible. Firstly, I have deep appreciation and great respect for **Dr. Qingping Feng**. Dr. Feng has offered continual support and guidance throughout my PhD studies, always offering an open door when needed. His enthusiasm for research and commitment to excellence have made me not only a better researcher, but also a better person. Dr. Feng's always positive attitude and passion for the pursuit of knowledge has kept me motivated. Although there were numerous setbacks throughout my studies, Dr. Feng's confidence in our research did not waver. Dr. Feng, thank you so much for your excellent mentorship over the years. I have learned numerous valuable skills that I will continue to develop in my future career. I would also like to thank the members of my advisory committee, Drs. Andy Babwah, Tom Drysdale, Cheryle Seguin, and Zia Khan for your mentorship. Our discussions and your valuable suggestions have strengthened my research and broadened my understanding of scientific discovery.

I am extremely grateful to members of the Feng laboratory for the consistently supportive and positive atmosphere. Most significantly, I would like to thank **Dr. Sharon Lu**, who taught me almost all the experimental procedures I have used. More importantly though, Sharon is a wonderful teacher and friend who would never hesitate to help troubleshoot and answer laboratory questions, and was always happy to tell stories and have a laugh in the lab. Thank you Sharon for your guidance and friendship. Likewise, graduate school would not have been as enjoyable nor gratifying without the friendship

of the past and present Feng lab members. Anish Engineer, Edward Kim, Mella Kim, Katherine Lee, Dr. Carmen Leung, Tana Saiyin, and MengQi Zhang, your friendship and the memories we have made are what I cherish most from graduate school. Our jokes and laughter made long days and late nights in the lab endurable. I could have not asked for a better lab environment. You became a family away from home that was always comforting and supportive. Also our friendly neighbor Evelyn Ng, thanks for always being my study buddy!

Finally, I would like to thank my wonderful family and close friends. Thank you to Georgia and Britt, my sisters who always make me cry from laughter, no matter what the scenario. James, thank you for sharing all the ups and downs with me, and encouraging me no matter what. And thank you for calling me every night, even just for a hello. Erica, Jamie, Lily and Jake, hanging with you is not only so warm and loving, but also always reminds me what is important in life. Erica, thank you for being the most inspiring, strong, and hilarious sister, but most importantly, thank you for moving back home!

Thanks especially to my mom and dad, who have always supported whatever dream I have wanted to pursue. Their love and support has always been unconditional and over the top. I would not be where I am today without the years of encouragement, no matter what hill I decided to climb, nor how many. They taught me the fundamentals of work ethic and work-life balance, not to mention grammar and the value of a good chow mein cookie. They have always inspired me as role models, which has been instrumental to not only my success in graduate school, but my success as a person.

Table of Contents

Abstract.....	i
Co-Authorship Statement.....	iii
Acknowledgments.....	iv
Table of Contents.....	vi
List of Tables.....	xi
List of Figures.....	xii
List of Abbreviations.....	xv
1 Introduction.....	2
1.1 Heart Disease.....	2
1.2 Heart Physiology.....	3
1.3 Myocardial Infarction (MI).....	4
1.4 Cell death after MI.....	4
1.4.1 Apoptosis.....	6
1.4.2 Necrosis.....	9
1.4.3 Necroptosis.....	10
1.4.4 Role of apoptosis, necrosis and necroptosis post-MI.....	13
1.5 Cardiac remodeling after MI.....	14
1.6 Progression to heart failure.....	16
1.7 Current treatments for MI and heart failure.....	18
1.7.1 Revascularization.....	18
1.7.2 Pharmacologic management post-MI and for heart failure.....	19
1.8 Augmenting healing post-MI.....	20
1.9 Models of Cardiac Injury.....	22
1.10 Possible mechanisms to support repair.....	24

1.11	Mechanisms supporting neonatal cardiac regeneration	25
1.11.1	Epithelial-to-mesenchymal transition (EMT)	27
1.12	Wilms' tumor 1	29
1.13	The primary cilium	30
1.13.1	Structure of the primary cilium.....	30
1.13.2	Primary cilium in signal transduction.....	34
1.13.3	The primary cilium in development and the heart.....	40
1.14	EMT and Non-coding RNA.....	41
1.14.1	Non-coding RNA	42
1.14.2	RNA interference	43
1.14.3	Long non-coding RNA	44
1.14.4	Non-coding RNA in cardiovascular disease	45
1.15	<i>MALATI</i>	47
1.15.1	A role for <i>MALATI</i> in EMT and angiogenesis	47
1.15.2	Effects of <i>MALATI</i> on cell proliferation, and cell death	48
1.16	Rationale and hypothesis	49
1.16.1	Aim 1: Cardiac regeneration in neonatal mice	51
1.16.2	Aim 2: The primary cilium and EMT	51
1.16.3	Aim 3: <i>Malat1</i> and ischemic cell death	52
1.17	References.....	53
2	Chapter 2	72
2.1	Chapter Summary	72
2.2	Introduction.....	73
2.2.1	Models of cardiac repair	74
2.2.2	Angiogenesis in the regenerating myocardium.....	76

2.2.3	Modulators of epithelial-to-mesenchymal transition	77
2.3	Methods.....	79
2.3.1	Animals.....	79
2.3.2	Surgery.....	80
2.3.3	Measurement of Myocardial Infarct Size 4-6 hours Post-MI	85
2.3.4	Measurement of Cardiac Function Post-MI.....	86
2.3.5	Measurement of Myocardial Infarct Size 24 hours Post-MI	87
2.4	Results.....	88
2.5	Discussion.....	99
2.6	References.....	103
Chapter 3	107
3	Chapter 3.....	108
3.1	Chapter summary.....	108
3.2	Introduction.....	109
3.3	Methods.....	111
3.3.1	Animals.....	111
3.3.2	Adenoviruses.....	111
3.3.3	Coronary artery ligation and <i>in vivo</i> adenoviral injection	111
3.3.4	Echocardiography	113
3.3.5	Cell culture and adenovirus infection <i>in vitro</i>	113
3.3.6	EPDC EMT assay <i>in vitro</i>	115
3.3.7	Histological analysis	115
3.3.8	Immunohistochemical analysis.....	116
3.3.9	Real-time qPCR	117
3.3.10	Statistical Analysis.....	119

3.4	Results.....	119
3.4.1	Outgrowth of cultured EPDCs	119
3.4.2	Epicardial EMT <i>ex-vivo</i>	123
3.4.3	Ift88 knockdown in a post-regenerative <i>in vivo</i> model.....	125
3.4.4	Cardiac function post-MI in adult mice	128
3.4.5	Epicardial activation and growth factor release 3 days post-MI in adult mice.....	130
3.4.6	Capillary and arteriole density 5 and 21 days post-MI.....	136
3.4.7	Cardiac hypertrophy 21 days post-MI in adult mice	139
3.5	Discussion.....	141
3.6	References.....	146
4	Chapter 4.....	151
4.1	Chapter summary	151
4.2	Introduction.....	152
4.3	Methods.....	153
4.3.1	Animals.....	153
4.3.2	Murine model of myocardial ischemia	154
4.3.3	Hemodynamic Measurements.....	154
4.3.4	Infarct Size	155
4.3.5	Cell Death by Caspase-3 and Caspase-8 Activity and Propidium Iodide.....	155
4.3.6	Quantitative RT-qPCR.....	156
4.3.7	Western Blotting	157
4.3.8	Statistical Analysis.....	158
4.4	Results.....	159
4.4.1	<i>Malat1</i> expression is increased post-MI	159
4.4.2	Deficiency in <i>Malat1</i> augments myocardial damage post-MI.....	160

4.4.3	Deficiency in <i>Malat1</i> reduces expression of cardioprotective genes.....	164
4.4.4	Deficiency in <i>Malat1</i> does not affect myocardial caspase activity post-MI.....	166
4.4.5	<i>Malat1</i> prevents necrotic cell death post-MI	167
4.5	Discussion.....	171
4.6	References.....	176
5	Chapter 5	180
5.1	Summary of Major Findings.....	180
5.2	Study Limitations.....	184
5.2.1	Mouse models	184
5.2.2	Genetically altered mice	186
5.2.3	Methods for <i>Ift88</i> knockdown	189
5.2.4	Suggestions for future research.....	190
5.2.5	Conclusions.....	193
5.3	References.....	195
	Appendix.....	199
	Curriculum Vitae	200

List of Tables

Table 2.1. Genotyping PCR primer sequences.....	80
Table 3.1 Real-time RT-PCR primer sequences.....	118
Table 4.1. The PCR primer sequences.....	157
Table 4.2. Hemodynamic parameters of WT and <i>Malat1</i> ^{-/-} mice 1 day after coronary artery ligation (MI) or sham operation.....	163

List of Figures

Figure 1.1. Cell death by apoptosis.....	8
Figure 1.2. Cell death by necrosis and necroptosis.....	12
Figure 1.3. Structure of the cilium.....	32
Figure 1.4. Signaling associated with the primary cilium.	39
Figure 2.1. Coronary artery is visible during neonatal CAL procedure.	90
Figure 2.2 Evidence of complete cardiac regeneration after neonatal LAD ligation.	91
Figure 2.3. Neonatal LAD ligation results in cardiac damage at 24 hours post-MI.	93
Figure 2.4. Neonatal LAD ligation results in cardiac damage at 48 hours post-MI.	94
Figure 2.5. Neonatal LAD ligation is 100% reproducible.....	96
Figure 2.6. Neonatal LAD ligation results in reliable infarct area percentage.	97
Figure 2.7. The neonatal mouse maintains a robust propensity for cardiac regeneration.	98
Figure 3.1 <i>In vitro</i> culture of EPDCs.....	120
Figure 3.2. Ad-shIft88 reduces Ift88 expression, ciliary number, cilia length, and cellular E-cadherin mRNA in EPDCs.....	122
Figure 3.3. Inhibition of Ift88 promotes EPDC EMT.....	124
Figure 3.4. Inhibition of Ift88 attenuates cardiac functional impairment post-myocardial infarction in neonatal mice.....	126
Figure 3.5. Inhibition of Ift88 attenuates infarct size post-myocardial infarction in neonatal mice.	127

Figure 3.6. Inhibition of Ift88 attenuates cardiac functional impairment post-myocardial infarction in adult mice.	128
Figure 3.7. Inhibition of Ift88 attenuates cardiac functional impairment post-myocardial infarction in adult mice.	129
Figure 3.8. Inhibition of Ift88 augments Wt1 expression in the peri-infarct area post-MI.	131
Figure 3.9. Expression of EMT markers is upregulated post-MI in hearts treated with Ad-shIft88.	134
Figure 3.10. Ad-shIft88 treatment increases myocardial expression of HIF-1 α and its downstream targets that are implicated in neovascularization and EMT.	135
Figure 3.11. Inhibition of Ift88 improves myocardial capillary density in the peri-infarct area post-MI.	137
Figure 3.12. Inhibition of Ift88 improves arteriolar density in the peri-infarct area post-MI.	138
Figure 3.13. Inhibition of Ift88 attenuates cardiac hypertrophy 21 days post-MI.	140
Figure 3.14. Schematic diagram of enhanced epicardial EMT via Ift88 inhibition post-myocardial infarction (MI).	142
Figure 4.1. <i>Malat1</i> expression is significantly increased in the infarct area post-MI.	159
Figure 4.2. <i>Malat1</i> deficiency increases infarct size after myocardial infarction.	161
Figure 4.3. <i>Malat1</i> deficiency significantly attenuates cardioprotective gene expression in the peri-infarct area post-MI.	165
Figure 4.4. <i>Malat1</i> deficiency did not affect caspase activity 1 day post-MI.	166
Figure 4.5. <i>Malat1</i> deficiency promotes necrotic cell death in the infarct area one day post-MI.	168

Figure 4.6 *Malat1* deficiency augments *TNF- α* and *RIP3* expression 1 day post-MI... 170

Figure 5.1. Summary of the cardiac response to myocardial infarction and the effects of primary ciliary disassembly and *Malat1* deficiency..... 183

List of Abbreviations

AAVs: adeno-associated viruses

ACEi: angiotensin-converting-enzyme inhibitor

Ang II: angiotensin II

ANP: atrial natriuretic peptide

Apaf-1: apoptotic protease-activating factor 1

ARBs: angiotensin receptor blockers

AT₁: angiotensin II receptor

BAX: Bcl-2-associated-X protein

Bcl-2: B-cell lymphoma 2

bFGF: basic fibroblast growth factor

BH3: Bcl-2 homology domain 3 only protein

BMSCs: bone marrow-derived haematopoietic stem cells

BNP: brain natriuretic peptide

BNPs: biological nanoparticles

CABG: coronary artery bypass graft

CARL: cardiac apoptosis-related lncRNA

CARMEN: Cardiac Mesoderm Enhancer-associated Non-coding RNA

Chast: cardiac hypertrophy-associated transcript

CHRF: cardiac hypertrophy related factor

circRNA: circular RNA

CypD: cyclophilin D

DISC: death-inducing complex

Dvl: Dishevelled

EndMT: endocardial-to-mesenchymal transition

EMT: epithelial-to-mesenchymal transition

EPDCs: epicardium-derived cells

ET-1: endothelin-1

FADD: Fas-associated death domain

FasL: Fas-ligand

fRNA: functional RNA

Fz: Frizzled

G-CSF: granulocyte-colony stimulating factor

GFP: green fluorescent protein

GPCR: g-protein-coupled receptor

HGF: hepatocyte growth factor

Hh: Hedgehog

HIF-1 α : hypoxia-inducible factor-1 alpha

HR: heart rate

IFT: intraflagellar transport

IFT88: intraflagellar transport protein 88

IGF-1: insulin-like growth factor 1

IL: interleukin

I/R: ischemia/ reperfusion injury

Jbn: Joubertin

IV: intravenous

LAD: left anterior descending coronary artery

LV +dP/dt: left ventricular contractility

LV -dP/dt: left ventricular relaxation

LVEDP: left ventricular end diastolic pressure

LVSP: left ventricular end systolic pressure

lncRNA: long non-coding RNA

MAC: mitochondrial apoptosis-induced channel

Malat1: metastasis-associated lung adenocarcinoma transcript 1

MAP: mean arterial pressure

MAPK: mitogen-activated protein kinase

MCP-1: monocyte chemoattractant protein-1

MI: myocardial infarction

miRNA: micro RNA

MLKL: mixed lineage kinase domain-like protein

mPTP: mitochondrial permeability transition pore

mRNA: messenger RNA

ncRNA: non-coding RNA

NE: norepinephrine

NEAT2: nuclear enriched abundant transcript 2

PCI: percutaneous coronary intervention

PDGF: platelet-derived growth factor

PI3K: phosphatidylinositol 3-kinase

piRNA: piwi-interacting RNA

Ptch: Patched

RA: retinoic acid

RAS: renin-angiotensin system

RAAS: renin-angiotensin-aldosterone system

RHIM: receptor interacting protein homotypic interaction motif domain

RIP1: receptor interacting protein 1

RIP3: receptor interacting protein 3

RNA: ribonucleic acid

RNAi: RNA interference

ROS: reactive oxygen species

rRNA: ribosomal RNA

scaRNA: small cajal body specific RNA

SCF: stem cell factor

SDF-1: stromal cell-derived factor 1

Shh: Sonic hedgehog

shRNA: short hairpin RNA

siRNA: small interfering RNA

Smo: Smoothed

snRNA: small nuclear RNA

snoRNA: small nucleolar RNA

Tbx18: T-box transcription factor 18

TGF- β : Transforming growth factor beta

TNF- α : tumor necrosis factor alpha

TNFR1: TNF- α receptor 1

tRNA: transfer RNA

TTC: 2,3,5-triphenyltetrazolium chloride

TUNEL: terminal deoxynucleotidyl transferase-mediated dUTP nick end-labeling

VEGF: vascular endothelial growth factor

Wnt: wingless-type integration site

Wt1: Wilms' tumor 1

Chapter 1

Portions of this chapter are in preparation for submission.

Blom JN, Feng Q.

“Enhancing cardiac repair by epicardial epithelial-to-mesenchymal transition”

1 Introduction

1.1 Heart Disease

Diseases of the heart are the second leading cause of death in Canada and the leading cause of death worldwide.^{1, 2} Specifically, myocardial infarction (MI), often caused by coronary artery disease, is the most common form of sudden cardiac injury.³ There has been significant improvement in therapeutic options for patients to treat MI and the subsequent disease associated with post-MI cardiac compensation. As a result, the number of Canadians who survive their in hospital stay after acute MI has increased from about 70% to over 90% in the last 60 years.⁴⁻⁶ Despite therapeutic advancement, MI and post-MI morbidity poses a significant financial burden for the health care system of most nations. In Canada, MI is the third leading cause of hospitalization and the largest driver of prescription drug use.⁷ In 2011 the annual estimated direct and indirect cost of ischemic heart disease amounted to over \$20.9 billion in Canada alone.⁸ The advent of percutaneous intervention as well as the use of vasodilators and thrombolytics has reduced the incidence of death from post-MI complications five-fold since the 1950s, however, 35% of patients still progress to heart failure.⁹ Furthermore, the number of patients for whom conventional revascularization techniques fail is increasing (due to widespread coronary block, immediate post-intervention vessel occlusion, or late restenosis). As such, the approach to the treatment of heart failure is continuously evolving, and clinical trials continue to investigate emerging treatment options from stem cells to gene therapy.

1.2 Heart Physiology

The heart is the driving force moving the supply of oxygen and nutrients to meet the metabolic demands of every tissue in the body. This fist sized muscular organ pumps blood through the large vessels of the circulatory system. The wall of the heart consists of three layers: the epicardium, a thin serous membrane on the outer layer of the heart; a contractile thick middle muscular layer; and a thin inner layer of endothelial cells called the endocardium. Cardiomyocytes are the cells responsible for generating the contractile force of the heart. In mice, the middle muscular layer of the heart contains myocytes (56%), cardiac fibroblasts (27%), endothelial cells (7%), and vascular smooth muscle cells (10%) as well as elastin and connective tissue.¹⁰ However, evidence from human autopsy tissues indicate that cardiomyocytes occupy about 75% of human cardiac tissue by volume, but only 30-40% by cell number.¹¹ The non-myocyte cells in these samples are predominantly fibroblasts.

Every tissue in the body requires a supply of blood to maintain its function – this includes the heart itself. As such, the heart not only pumps blood to the rest of the body through the aorta and subsequent great vessels, but also pumps blood to its own thick muscular walls through the coronary circulation. The heart consumes approximately 5% of the total cardiac output, making the coronary circulation essential to maintaining heart function.¹² When part of this coronary circulation is narrowed, constricted, or blocked, an ischemic event occurs where there is inadequate supply of oxygen to the portion of the cardiac muscle supplied by that artery. This causes damage and impaired cardiac function. A source of oxygen is paramount to allowing oxidative phosphorylation for not only continued cardiomyocyte contraction, but also cell homeostasis.

1.3 Myocardial Infarction (MI)

A “heart attack,” or acute MI, is a sudden form of cardiac injury, whereby obstruction to blood flow results in a perfusion imbalance between supply and demand that is long enough (several hours) to invoke myocyte death. Symptoms may present immediately, and include severe crushing chest pain, diaphoresis, dyspnea, fatigue, nausea and syncope. Many patients experience angina (chest pain) in the weeks to months leading up to an ischemic event due to narrowing of the coronary arterial lumen from atherosclerosis. However, the MI event is much more severe, resulting in complete deprivation of the cardiac tissue from oxygen.

The most common cause of MI is the blockage of a coronary artery resulting from a primary coronary event such as an atherosclerotic plaque rupture.¹³ This most often affects the left ventricle, with the majority of coronary occlusions occurring in the left anterior descending coronary artery (LAD). Importantly, no matter the artery affected, coronary artery occlusions typically occur in the proximal third of the coronary vessels, unfortunately resulting in higher morbidity and mortality from necrosis of a large myocardial territory.¹⁴ Thus, occlusion of the LAD is often referred to as the “widowmaker” lesion due to the poor prognosis of patients losing blood supply to such a large portion of their left ventricle.

1.4 Cell death after MI

The acute ventricular molecular response to MI results in tissue damage and cardiomyocyte loss. The gravity and duration of the ischemic period, as well as the propensity for cell death, determines the extent of tissue loss to infarction. The process

begins with a rapid decline of cellular homeostasis and permanent cardiomyocyte cell death leading to a cascade of processes involved in infarct healing. Oxidative phosphorylation generates over 95% of the energy required for myocyte function.¹⁵ Oxygen depletion in cardiomyocytes decreases the generation of high energy phosphates leading to loss of contractility (within 60 seconds) as well as the failure of membrane pumps and subsequent electrolyte imbalance.³ Both necrosis (Type I cell death; oncosis) and apoptosis (Type II cell death) occur acutely in the infarct region. The onset of passive cell death by necrosis, an un-programmed event caused by enzymatic degradation (autolysis), marks irreversible tissue injury. Signs of necrosis are evident within 4-6 hours after the onset of ischemia as demonstrated by the accumulation of water and electrolytes causing rapid swelling, destruction of cellular organelles, and early plasma membrane rupture causing inflammation.¹⁶ However, coagulative necrosis in the infarct region peaks 1 day post-infarction and is likely preceded by apoptosis.¹⁷ Programmed apoptotic cell death is energy dependent and is characterized by nuclear chromatin condensation, DNA fragmentation, cell shrinkage, budding of apoptotic bodies, and phagocytosis by neighboring cells. This process begins in the ischemic zone as early as 2-3 hours post-infarction and peaks at 4.5 hours.¹⁷ Traditionally, necrosis was viewed as the predominant form of cell death from MI. Subsequently, the discovery of the mechanisms of apoptosis turned the focus to this regulated form of cell death post-MI.¹⁷ However, limitations of assays including the annexin V assay, caspase staining, and terminal deoxynucleotidyl transferase-mediated dUTP nick end-labeling (TUNEL) impede the ability to definitively distinguish between the types of cell death.^{18, 19} For example, these assays have been developed to detect apoptotic cells, however depending on the timing of

use they may also detect late phase necrotic cells due to exposure of the inner plasma membrane and cellular contents to the outer environment upon cell lysis. More recently, owing to new discoveries surrounding the mechanisms of necrosis, it has been repeatedly suggested that necrosis is in fact responsible for the majority of cell death associated with the initial infarct.²⁰

1.4.1 Apoptosis

Programmed apoptotic cell death is a finely regulated process, and proceeds via one of several conserved “suicide” mechanisms. Cellular injury triggers the activation of cysteine proteases, called caspases, which in turn cause proteolytic cleavage of a spectrum of intracellular targets. Once an initiator caspase (Caspase-8 and Caspase-9) is activated, a proteolytic pathway ensues whereby downstream effector caspases (e.g., Caspase-3) are cleaved to the active state. Caspase proteases can be activated by an extrinsic (death ligand) or an intrinsic (mitochondrial) apoptotic pathway (**Figure 1.1**). The interaction of extracellular death signal proteins, such as tumor necrosis factor (TNF- α) and/or Fas-ligand (FasL) (both up-regulated in cardiac ischemia),²¹ with target membrane receptors causes extrinsic pathway activation by recruitment of intracellular adaptor proteins. FasL interacts with the Fas-associated death domain protein (FADD), whereas TNF- α binds TNF- α receptor 1 (TNFR1) to activate the TNFR-associated death domain protein (TRADD). The associated adaptor protein in turn binds caspases and adaptor molecules such as receptor interacting protein (RIP1) to create the transient death-inducing complex (DISC) or complex I, and activate the proteolytic cascade.²²

In acute ischemia, however, the intrinsic mitochondrial pathway plays a dominant role.²³ Intracellular stress such as hypoxia or increased production of reactive oxygen species (ROS) results in the loss of mitochondrial membrane potential along with increased mitochondrial outer membrane permeabilization by both membrane breakdown and mitochondrial apoptosis-induced channel (MAC) formation by proapoptotic proteins.²⁴ This causes the release of calcium and mitochondrial membrane protein cytochrome c. Cytosolic cytochrome c binds proapoptotic proteins, such as apoptotic protease-activating factor 1 (Apaf-1), to proteolytically activate initiator caspases (caspase-9).²⁵ Apaf-1 has an ATP-binding site, which may explain why the presence of ATP critically important for the apoptotic program.²⁶

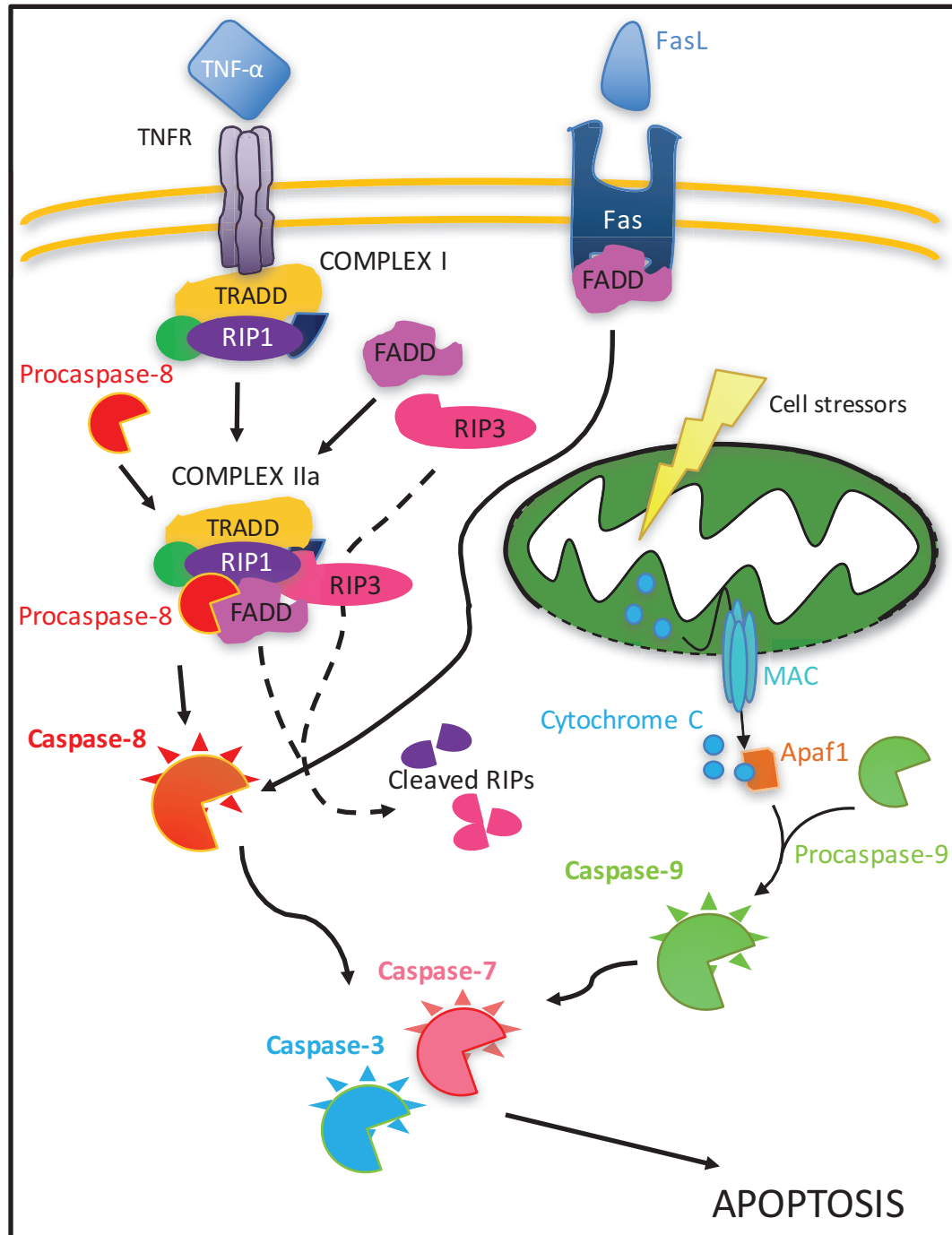


Figure 1.1. Cell death by apoptosis.

Apoptosis occurs via either an extrinsic ligand-mediated pathway or an intrinsic pathway. In the extrinsic pathway, TNF- α or FasL bind their receptors resulting in the activation of initiator caspases such as caspase-8. In the intrinsic pathway, intracellular stress such as hypoxia causes membrane destabilization, outer membrane pore opening, and mitochondrial apoptosis-induced channel formation (MAC), causing leak of cytochrome c into the cytosol, activation of apoptotic protease-activating factor (Apaf-1), and proteolytic cleavage of another initiator caspase, caspase-9. Caspase cleavage and activation results in protease activation and degrades the cell components.

Other proteins converge on the intrinsic caspase pathway to amplify or oppose the cascade. For example, Bcl-2-associated-X protein (BAX) and BH3 (Bcl-2 homology domain 3)-only proteins promote mitochondrial membrane destabilization and release of calcium, cytochrome c and other apoptogens by inserting themselves in the outer mitochondrial membrane.²⁷ Their natural antagonist and family member, Bcl-2, plays a protective role by sequestering and inhibiting pro-apoptotic proteins, thus preserving membrane integrity and inhibiting release of pro-apoptotic factors from the mitochondria.²⁸ Unfortunately, Bcl-2 is down-regulated in the hypoxic myocardium, worsening BAX mediated cell death.²⁹ Furthermore, upregulation of BAX post-infarction is also known to contribute to the development of heart failure.³⁰

1.4.2 Necrosis

In contrast to the tightly regulated apoptotic pathways, ordinary necrosis is relatively uncontrolled and ATP-independent (**Figure 1.2**). The culminating causal event contributing to necrosis is the opening of the mitochondrial permeability transition pore (mPTP) at the inner mitochondrial membrane. The formation of the mPTP is regulated by a calcium-dependent mechanism. A lack of oxygen during ischemia stimulates anaerobic glycolysis in the cardiomyocyte to provide ATP. This type of energy production causes the accumulation of H⁺ ions, which are in turn pumped out of the cell via the Na⁺/H⁺ exchanger. The increasing Na⁺ concentration forces the Na⁺/Ca²⁺ exchanger into reverse mode, thus elevating Ca²⁺ concentrations in the cytoplasm, and eventually the mitochondria through a Ca²⁺ uniporter. Elevated Ca²⁺ recruits proteins such as cyclophilin D (CypD), a component of the mPTP. The opening of the pore abrogates oxidative phosphorylation and ATP synthesis as hydrogen ions leak from the

mitochondria dissipating the proton gradient required for the process. Furthermore, the mPTP is large enough to allow free flow of water and solutes, thus causing mitochondrial swelling and rupture. The initiation of the release of inflammasomes and pro-inflammatory cytokines from necrotic cells induces inflammation and can trigger an immune response. This type of response is important for reactions to viral infection, but can be detrimental in cardiac repair. In acute MI, the recruitment of inflammatory cells, release of pro-apoptotic cytokines, and vascular dysfunction from inflammation amplifies cardiomyocyte destruction.^{31,32}

1.4.3 Necroptosis

While programmed cell death by apoptosis and unprogrammed cell death by necrosis have been traditionally recognized as causing the majority of cardiac cell loss during ischemia, accumulating evidence indicates that a substantial portion of necrotic cell death is in fact highly regulated and actively fulfilled. Programmed necrosis, termed necroptosis, is a form of necrotic cell death dependent on molecular signaling pathways. Like apoptosis, necroptosis can be initiated by both an intrinsic un-programmed pathway (as described above), or an extrinsic ligand mediated pathway. The binding of extrinsic ligands (ie: TNF- α) to their receptors, as in apoptosis, also induces the formation of complex I (transient), and subsequent conversion to complex II with the recruitment of receptor interacting protein 3 (RIP3) (**Figure 1.2**). In the presence of caspase-8, caspase activity causes cleavage of RIP1 and RIP3, abolishing their ability to signal necrosis; complex II is proteolytically cleaved and apoptosis is induced (**Figure 1.1**).³³ However, in the instance that caspase-8 is not present or its activity is inhibited, RIP3 interacts with RIP1 through homotypic interaction motif domains (RHIM), forming a RIP1-RIP3

pronecrotic complex, a necessary step for necroptosis (**Figure 1.2**).^{34, 35} The complex causes cross-phosphorylation of both RIP proteins, and phosphorylation of downstream kinases such as mixed lineage kinase domain-like protein (MLKL).³⁶ Phosphorylated MLKL can oligomerize and translocate to the plasma membrane. This causes pore formation, allowing the influx of Ca^{2+} into the cell, and membrane destabilization by an unknown mechanism, which triggers necroptosis.³⁷ Phosphorylation of numerous other catabolic enzymes, phospholipases, and sphingomyelinases elicits the production of ROS, the permeabilization of lysosomes, and also triggers necrosis.

RIP1 has been reported to be involved in Fas and TNF-mediated, caspase-8-dependent apoptosis as well as necroptosis. However, although RIP1 does promote caspase-8 activation, it is not necessarily required for apoptosis induced by Fas; RIP1 serine/threonine kinase activity is dispensable for the activation of apoptosis, but crucial in the necroptotic pathway.³⁸ Similarly, RIP3 knockout experiments indicate that its activity is not required for apoptosis induction.³⁹ Although RIP3 may be recruited to complex II in apoptosis, the complex is quickly degraded. The binding of RIP3 to RIP1 becomes more stable within a “pro-necrotic” complex II. Upon binding complex II, RIP3 is thought to act as a scaffold for RIP1 autophosphorylation. RIP3 is then phosphorylated at Ser199, activating its kinase activity. RIP1 alone cannot induce programmed necrosis.⁴⁰ However, RIP3 kinase activity is specifically implicated in caspase-independent, necroptotic cell death, distinguishing the pathways.⁴¹ The reduced necroptotic activity in $\text{RIP3}^{-/-}$ mice demonstrates the essential role of RIP3 as a mediator of necroptosis.³⁴ Necrostatin-1, a RIP1 inhibitor, is known to inhibit necroptosis, however this likely occurs by abolishing the RIP1-RIP3 complex formation, thus affecting RIP3 activity.³³

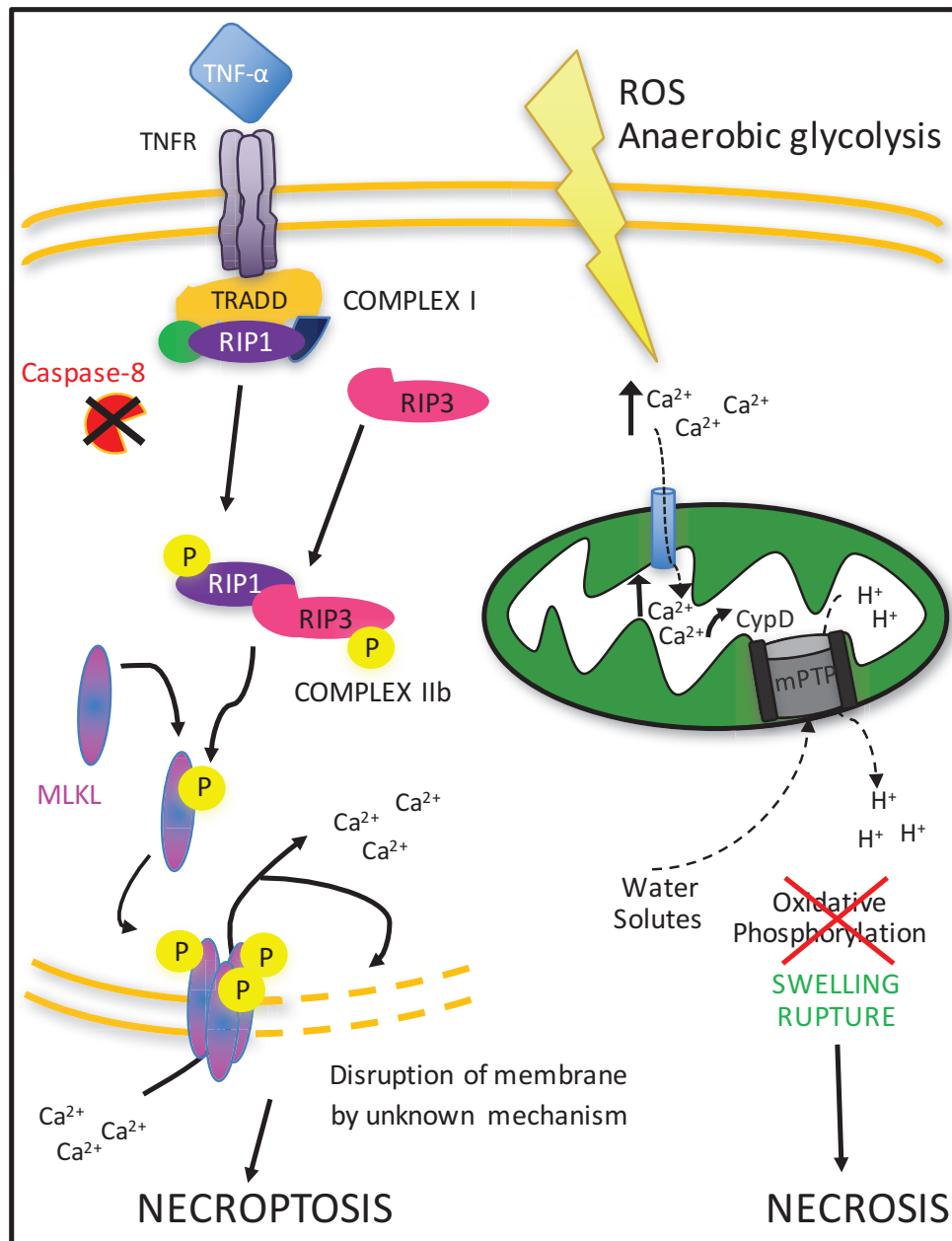


Figure 1.2. Cell death by necrosis and necroptosis.

Cell death stimuli cause excessive influx of calcium (Ca^{2+}) into the mitochondria, recruiting cyclophilin D (CypD), which leads to opening of the mitochondrial permeability transition pore (mPTP). Protons leak from the pore resulting in a loss of the gradient for oxidative phosphorylation. The mPTP also allows the influx of water and solutes into the mitochondria, causing swelling and rupture. Necroptosis is a form of regulated necrosis, where in the absence of caspase-8, TNF- α binding causes RIP1-RIP3 complex formation. RIP1 and RIP3 cross-phosphorylate each other. This causes MLKL recruitment and phosphorylation and subsequent pore formation at the plasma membrane, allowing Ca^{2+} entry into the cell and membrane destabilization by an unknown mechanism, resulting in cell death.

1.4.4 Role of apoptosis, necrosis and necroptosis post-MI

Apoptosis, necrosis and necroptosis have all been demonstrated to independently play a significant role in myocardial ischemia and the development of heart failure. As such, targeting mediators of these processes may contribute to a better understanding of their contribution to infarction while providing strategies for therapeutic interventions to limit tissue damage. To this end, much research has been conducted to determine the importance of mediators of the cell death pathways. The involvement of caspases and their contribution to cardiac apoptosis has been confirmed using a specific inhibitor of caspase activity, which reduces infarct size, apoptosis and caspase 3 levels in rabbits.⁴² However, inhibitors of caspase 1 and caspase 3 have been shown to reduce apoptosis but not infarct size in ischemia/reperfusion (I/R) injury, implicating another mechanism of cell death.⁴³ Nonetheless, mice lacking the Bax gene ($Bax^{-/-}$) did exhibit cardioprotection and reduced mitochondrial damage when subject to coronary artery ligation.⁴⁴ Similarly, cardiac specific over-expression of Bcl-2 reduced infarct size and apoptosis post-ischemic injury.⁴⁵ Mice deficient in Fas also have reduced infarct size as compared to WT control mice, indicating the importance of Fas in the response to MI.⁴⁶ Necrosis is also known to affect infarct size as mice lacking cyclophilin D are protected from I/R injury.⁴⁷ Finally, necroptosis has been demonstrated as a critical component of cell death in cardiac ischemic injury, which can be mitigated by its inhibition via necrostatin-1 (RIP1 inhibitor).⁴⁸ Indeed, knockout animals lacking RIP3 have attenuated cardiac damage (measured by troponin T levels). This led to enhanced cardiac function post-MI compared to controls, demonstrating the importance of necroptosis not only for infarct size but also for long term functional impairment.⁴⁹

1.5 Cardiac remodeling after MI

Remodeling after MI is a dynamic process whereby the ventricular architecture is altered significantly. Myocyte cell death results in cytotoxic spilling and the recruitment of inflammatory cells occurs in the first three or four days post-infarction. Injured myocytes act as a scaffold for complement activation (C5a) and release cytokines such as monocyte chemoattractant protein (MCP)-1 and transforming growth factor (TGF)- β 1, which attract macrophages and fibroblasts to the infarct region.⁵⁰ Neutrophils are also recruited via upregulation of cytokines such as interleukin (IL)-8.⁵⁰ Intracellular signaling and neurohormonal activation with inflammatory mediators is amplified as the inflammatory response is localized.

As cells are gradually lost in the early phase of remodeling, characteristic mural thinning occurs. By days three to five, the process of progressive infarct expansion is evident, where wall dilation occurs without additional necrosis. Recruited neutrophils release matrix metalloproteases and serine proteases, which digest local collagen.⁵¹ Myocyte alignment and intercellular myocyte connections are dependent on intracellular collagen struts and their breakdown results in myocyte sliding, termed “slippage.”⁵² Contributing to infarct expansion, myocytes bordering the infarct region (aka: border zone or peri-infarct area) exhibit signs of apoptosis beginning three hours after infarction, resulting from signaling by inflammatory mediators as well as moderate ischemia and changes in pressure load.⁵³ Apoptosis in this region peaks one day post-MI, but remains high for up to twelve weeks.⁵⁴ TUNEL staining in rats indicates that the majority of cell death by apoptosis occurs in the peri-infarct area, containing approximately 70% of apoptotic cells, while those in the infarct region account for only about 25%.⁵⁴

Over weeks to months, thinning and expansion causes ventricular dilation, which is initially beneficial, compensating for a reduced stroke volume. Ejection fraction, however is persistently depressed and end diastolic pressure continues to rise. Consistent with the Frank-Starling mechanism, reactive compensatory hypertrophy of remaining viable cardiomyocytes occurs. Myocytes increase in both diameter and length and alter their gene expression profile in response to mechanoreceptor stimulation and in reaction to hormonal and cytokine signaling.⁵⁵ Augmented levels of endothelin-1 (ET-1) and norepinephrine (NE) are found in the infarcted myocardium.^{56, 57} Importantly, release of the hypertrophic mediator angiotensin II (Ang II) is stimulated via a variety of mechanisms.

Hypotension post-infarction triggers the renin-angiotensin system (RAS) (both local and systemic), while myocyte stretch causes Ang II release from cytoplasmic granules.⁵⁸ These molecules activate Gq-dependent signaling pathways and protein kinase cascades which promote transcription factor profile changes conducive to hypertrophy and variations in contractile protein production. Myosin heavy chain isoforms are altered by increased beta-chain production and down-regulation of alpha-chains, while there is a general increase in protein production.^{59, 60}

These cellular profile changes allow individual myocytes to work harder to conserve ventricular function, but at a cost of requiring additional blood supply to sustain cell metabolism. An essential component of the remodeling process is neoangiogenesis within the infarct region. Upregulation of pro-angiogenic agents like vascular endothelial growth factor (VEGF) and basic fibroblast growth factor (bFGF) within the ischemic area promotes endothelial cell migration and pericyte communication.⁶¹ However, without

additional therapy the growing capillary network cannot keep pace with the growing demands of hypertrophied myocardium; this evokes further myocyte necrosis.

Later in remodeling, a fibrin-fibronectin matrix forms, attracting myofibroblasts, which infiltrate the infarct region, proliferate and deposit collagen.⁶² Mast cells attract myofibroblasts to the infarct region, promote their proliferation and increase collagen synthesis. The RAS system is also involved in scar formation as aldosterone stimulates collagen type I and type III transcription.⁶³ Gradually, fibrous tissue deposited by fibroblasts entirely replaces necrotic myocytes.⁶⁴ Fibroblasts appear transiently during the formation of granulation tissue and undergo apoptosis when a nondistensible scar has formed. This entire process is completed within weeks to months. Despite healing, the added contractile mass in remaining cardiomyocytes and muscle cell hypertrophy is inadequate to compensate completely for the scarring and loss of contractile mass. De-compensation inevitably occurs; post-infarction cardiomyopathy commonly progresses to heart failure.⁶⁵

1.6 Progression to heart failure

In the myocardium remote from the ischemic zone, cell death continues for months.⁶⁶ TUNEL staining indicates that in a normal human heart the prevalence of cell death is between 0.001 and 0.01%. However, in heart failure, the prevalence of cell death increases to about 0.12-0.70%, significantly contributing to its pathogenesis.⁶⁷ Progressive loss of cardiomyocytes plays a major contributing role in the development of this chronic disease. Spurring this is continued volume overload and persistent elevated end-diastolic left ventricular pressure. While impaired left ventricular function is the primary abnormality contributing to heart failure, the fall in cardiac output leads to

activation of multiple compensatory mechanisms aimed at improving function. As heart failure progresses, the neural sympathetic system is stimulated by baroreceptor activation; the sympathetic system attempts to maintain cardiac output and blood pressure by increasing heart rate and contractility (ionotropic support) while vasoconstricting peripherally. Not only is the response to catecholamines blunted in a failing heart, but worse, excessive sympathetic activity at the beta adrenergic receptor can provoke additional cardiomyocyte apoptosis and necrosis.^{68, 69} Furthermore, prolonged NE intensifies generalized sympathetic tone, thereby increasing both cardiac afterload and preload. A failing heart cannot respond to this increase as the Frank-Starling curve is flattened, and there is a lack of increased contractile force in response to afterload. This is a result of abnormal calcium cycling and an altered myofilament response to calcium in the failing ventricle.⁷⁰ Indeed, patients who have raised plasma NE concentrations in congestive heart failure have a worse prognosis.⁷¹ The stiffness of the ventricular wall continues to increase, eventually causing diastolic dysfunction by impaired relaxation.

The renin-angiotensin-aldosterone system (RAAS) is also activated to cause vasoconstriction by Ang II and increase blood pressure by provoking water retention with aldosterone. This natural compensatory elevation in Ang II levels also provokes cardiomyocyte hypertrophy by binding angiotensin II receptors (AT₁). Although the elevation in Ang II levels is a natural physiologic response to provoke hypertrophy and protect homeostasis in the setting of reduced cardiac output, this is to the detriment of the cardiomyocyte as activity at AT₁ eventually provokes further apoptosis.⁷²

There are also many beneficial cytokines and hormones released from the heart post-MI and through the progression into heart failure. Atrial natriuretic peptide (ANP)

and brain natriuretic peptide (BNP), for example, are released from stretched atrial and ventricular cells respectively, and oppose the effects of Ang II on the vasculature and kidney.⁷³ As mentioned above, TGF- β is a secreted cytokine up-regulated post-MI. TGF- β is involved in many cellular functions, and its upregulation not only supports recruitment of inflammatory mediators, but also exerts a cardioprotective effect by limiting myocardial necrosis.⁷⁴ TGF- β promotes myogenic differentiation of pools of stem cells, further implicating it in cardiac repair.⁷⁵ bFGF is also increased in the perinfarct area, contributing to angiogenesis. bFGF supports endothelial cell migration and proliferation, while also inhibiting oxidative injury and attenuating left ventricular contractile dysfunction post-MI.^{76, 77} Similarly, hepatocyte growth factor (HGF) and insulin-like growth factor 1 (IGF-1) are cardioprotective factors released in the infarct region post-MI. These factors reduce ventricular dilation and wall stress and are thought to regulate anti-apoptotic signaling.^{78, 79} The chemokine stromal cell-derived factor 1 (SDF-1) is also up-regulated post-MI and impedes myocyte death, promotes angiogenesis, and recruits stem cells for repair.⁸⁰ Unfortunately, patients who do not express adequate levels of these factors are at increased risk of developing the unrelenting clinical symptoms of heart failure.⁸¹

1.7 Current treatments for MI and heart failure

1.7.1 Revascularization

The most optimal and common initial treatment post-MI is to re-open a perfusion pathway for oxygen delivery to the ischemic cardiac muscle by reperfusion therapy with fibrinolysis, percutaneous coronary intervention (PCI), or in rare cases, an urgent coronary artery bypass graft (CABG).⁸² Reperfusion therapy reduces the relative

incidence of death from acute MI by over 25% by restoring oxygen delivery to cardiomyocytes and reducing initial infarct size from ischemia.⁸³ The in-hospital fatality rate for MI has dropped to 10.6% due to these immediate treatments.⁸⁴

1.7.2 Pharmacologic management post-MI and for heart failure

Beyond the acute MI, patients who survive are often prescribed antithrombotic (glycoprotein IIb/IIIa inhibitor/antagonist; e.g., abciximab) and antiplatelet (e.g., aspirin) agents to prevent rethrombosis. Within 24 hours post-MI, oral beta-adrenergic receptor blockers (β -blockers), adjunct calcium channel blockers (e.g., verapamil) to reduce oxygen demand, and anti-anginal drugs such as nitroglycerin (nitrates) are prescribed. Statins are also initiated to lower cholesterol and reduce risk of recurrent MI from atherosclerosis.⁸⁵

Despite optimal management, over 35% of patients with acute MI begin to develop symptoms of heart failure, a chronic disease requiring life-long management.⁹ Beyond lifestyle modification suggestions, these patients receive pharmacotherapy to improve long term prognosis by limiting cardiac remodeling. The first line pharmacologic therapy is an angiotensin-converting-enzyme inhibitor (ACEi), which reduces the multiple pathophysiological effects of Ang II on both systemic pressure and the heart.⁸⁶ Angiotensin receptor blockers (ARBs) may be used for patients who are intolerant to ACEis (often due to cough). Depending on the patient's volume status, they may receive loop diuretics (e.g., furosemide) to reduce dyspnea and edema, or β -blockers, which both reduce mortality and reverse ventricular remodeling.⁸⁷ For patients with class II heart failure, the addition of a mineralocorticoid receptor antagonist (MRA;

e.g., spironolactone) to compete with aldosterone at the MR has been demonstrated to provide survival benefit.⁸⁸ In patients who progress to class II to IV heart failure despite optimal therapy, the addition of digoxin, a sodium-potassium ATPase inhibitor, may be required to increase contractility of the heart while reducing heart rate by prolonging the cardiac action potential. Finally, in patients who continue to worsen, hydralazine (antihypertensive) and/or nitrates (vasodilator) may be required to reduce hypertension.

Although the current optimal treatments have extended patients' lives by reducing in-hospital mortality from heart failure complications by more than 2%, and 5 year mortality by over 9%, epidemiologic evidence, such as that from the Framingham study, has demonstrated no change in overall death rate from heart failure.^{89, 90} Thus, innovative approaches to limit cardiomyocyte loss from MI and impede deleterious cardiac remodeling are needed to improve prognosis for cardiac patients and create effective therapies for heart failure in the future.

1.8 Augmenting healing post-MI

Over the last 50 years, major efforts in cardiac research have focused on minimizing infarct expansion, fibroblast collagen deposition, and cardiac hypertrophy following MI. Methods such as inhibiting inflammation, reprogramming cardiac fibroblasts, activating cell cycle reentry, transferring skeletal myoblasts to the infarct region, and transplanting progenitor cells have been tested.⁹¹⁻⁹³ These methods have been met with conflicting results in *in vivo* models and in the clinic. Early studies in murine models suggested that bone marrow-derived haematopoietic stem cells (BMSCs) introduced into the myocardium following MI could differentiate into cardiomyocytes and aid in repair.⁹³ However, these cells did not differentiate or incorporate into the

myocardium in subsequent studies.⁹³ Furthermore, *Loffredo* et al. demonstrated that transplantation of BMSCs enhances cardiac repair, but not by engraftment; they could not discern the mechanism of action.⁹⁴ Results regarding the long-term efficacy and safety of transfer of bone marrow stem cells in human trials are inconsistent.⁹³ Also, the ability of these cells to differentiate into new muscle cells is limited.⁹⁵ A similar trend followed with experiments in mobilization of haematopoietic stem cells using granulocyte-colony stimulating factor (G-CSF); G-CSF was associated with improved stem cell recruitment and cardiac functionality post-MI in animal models, but was unable to demonstrate improvement in human trials.⁹⁶ Many traditional therapies were also directed at increasing infarct zone microvasculature and promoting angiogenesis. It is thought that if blood flow can be restored to the infarcted or “hibernating” myocardium, fewer cardiomyocytes will be lost. For example, augmented infarct zone angiogenesis has been demonstrated in animal models using VEGF and bFGF therapy,⁹⁷ however this was not associated with benefit in human trials.⁹⁸

Adult mammalian cardiomyocytes have classically been viewed as post-mitotic, and thus incapable of proliferating to replace damaged myocardium due to their terminally differentiated state.⁹⁹ Complete recovery from injury would be impeded by the replacement of lost cardiomyocytes with a fibrotic scar. To combat this deleterious response, research directed at blunting fibrosis and minimizing infarct expansion has been the primary focus in the field of cardiac repair. However, recent discoveries indicating a potential for cardiac regeneration have shifted the fundamental underlying assumptions around cardiac healing, deflecting research efforts towards regenerative strategies.¹⁰⁰ Normally, adult cardiac cells display little cell-cycle activity. Although

approximately 50% of cardiomyocytes are replaced in one's lifespan (0.45 - 1% annually),¹⁰¹ cardiac homeostasis after embryogenesis and initial neonatal maturation is mostly preserved by hypertrophic growth. However, resident cardiac progenitor cells are activated after cardiac injury, and these cells are able to proliferate and differentiate into fibrous cells, endothelial cells, smooth muscle cells and potentially even cardiomyocytes.¹⁰² This discovery is the cornerstone of current cardiac regeneration research as it offers the potential for stem cell induction therapy to promote infarct healing by directly replacing the injured myocardium. Isolated and purified resident cardiac progenitors can be injected after an ischemic event and differentiate into myocardial tissue in the region of necrosis.¹⁰³ While this form of cellular therapy seems an attractive option, techniques for isolating these types of cells remain to be optimized, and the relatively small number of cells available for autologous transplantation makes cell therapy too arduous for clinical use. Furthermore, results from conflicting clinical trials call into question the ability of transplanted cells to functionally integrate with the remaining viable myocardium and contribute to enhancing left ventricular function in the long term.¹⁰⁴ While cell replacement may not be the most realistic approach, therapeutic enhancement of the regenerative capacity of resident stem cells could provide a feasible non-invasive therapy.

1.9 Models of Cardiac Injury

To understand the biological mechanisms underlying any human disease, reliable models that mimic both typical disease pathogenesis and symptoms are required. An ideal model is physiologically very similar to the tissue of interest or recapitulates the human pathology, is inexpensive and reproducible, can be easily manipulated, and offers

large turnover in a short period of time (i.e., rapid gestation period, large litter size and relative quick growth). As summarized by *Garbern et al.*, cardiac disease has been studied using many different models ranging from computational to cell culture to large animal models.¹⁰⁵

The advancement in genomic editing and biotechnology has brought about the increasing availability of genetically manipulated mice, making the mouse a desirable animal to model various diseases. The most common murine models of cardiac disease include permanent or temporary occlusion of the left coronary artery (myocardial infarction or ischemia/reperfusion), aortic banding (pressure overload), electrocautery (focal infarctions), isoproterenol administration (diffuse myocardial necrosis), and genetic knock-in and knock-out mutations (arrhythmia, hypertrophy, congenital cardiac abnormalities). Surgical coronary ligation has been demonstrated to be a useful experimental technique in many animal models.^{106, 107} Originally used on dogs, and first applied in small animals by Johns and Olsen in 1954,¹⁰⁸ the coronary ligation model has become the most widely used in the field of heart failure.

While the types of murine injury listed above have served as prototypical models for the study of cardiac healing post-MI, each model results in permanent cardiac injury, without cardiac regeneration. Until recently, the dogma dictating an incapacity for complete mammalian cardiac healing left the study of *in vivo* regeneration to non-vertebrate models, such as that demonstrated by teleost fish from cardiac apex resection.¹⁰⁹ Recently, however, two groups have presented surgical models of mammalian cardiac regeneration in the neonatal mouse. First, *Porrello et al.* demonstrated complete cardiac regeneration after apex resection in mice at postnatal day

1 (P1).¹¹⁰ Subsequently, *Haubner* et al. presented complete cardiac regeneration after MI by coronary occlusion.¹¹¹ Unfortunately, in the first week of postnatal life, the tissue progenitor cell composition declines rapidly, and previously proliferative cells permanently exit the cell cycle.¹¹² As a result, the regenerative capacity in neonatal mice was retained only in the early neonatal period, and was lost shortly after birth by P7. Elucidating the mechanistic differences between the response to myocardial injury in the neonate and the adult could lead to novel targets which may be manipulated to therapeutically recapitulate neonatal regenerative capabilities in the adult human heart.

1.10 Possible mechanisms to support repair

The principles of tissue repair and regeneration are similar for almost any organ system, offering similar therapeutic targets for the treatment of disease. These are the fundamental processes affecting pathophysiological changes post-infarction and post-wounding. As summarized above, at the time of infarction, cell death occurs followed by an inflammatory cell response. In the long term, the infiltration of inflammatory cells, as well as collagen deposition and angiogenesis causes the development of a form of granulation tissue, a connective tissue matrix typically formed at the wound healing surface. Finally, a scar is produced and the surrounding tissue must compensate for the loss of this functional area. The mechanisms which could support regeneration include altering processes involved in wound healing response. Inhibiting apoptosis and necrosis are of primary importance to limit initial wounding. Secondly, the polarization of the inflammatory response contributes to the aggravation of wounding or improvement of the healing process. Neutrophils and macrophages are the first immune cells to arrive at the site of wounding. These immune cells engulf damaged tissue and cellular debris, but also

both respond to and secrete a variety of cytokines. Macrophages have been categorized into two major subtypes: pro-inflammatory M1 cells secrete mediators such as ROS which aggravate inflammation, while cells of the pro-regenerative M2 phenotype secrete cytokines which reduce inflammation and aid in angiogenesis. Thirdly, the ability to produce new vasculature is of utmost importance. Neovascularization supports cells at the wound site with nutrition and oxygen. Blood vessel growth occurs by three major mechanisms: angiogenesis, the formation of endothelial cell derived capillary sprouts from pre-existing capillary vessels; arteriogenesis, the remodeling of pre-existing arteriolar collaterals by increasing their size and caliber; and vasculogenesis, the formation of blood vessels *de novo* from progenitor cells (mesoderm derived) or angioblasts. Another important factor is the propensity for proliferation or cell replication to replace damaged tissue. A pro-proliferative microenvironment stimulates the division of existing viable cells to aid in the repopulation of the tissue. Finally, both resident stem cells and bone marrow derived stem cells are activated by cytokines and recruited to the site of injury. The differentiation of these cells into tissue resident cells, as well as their signaling for growth of resident healthy tissue is important for repair. Determining which of these mechanisms are up-regulated in the neonatal heart will provide a mechanistic framework for cardiac regeneration. Interestingly, many of these processes are hallmarks of cancer and metastasis.¹¹³ Thus, it may be prudent to learn from studies in cancer to direct therapies for cardiac repair.

1.11 Mechanisms supporting neonatal cardiac regeneration

Numerous studies have demonstrated the new myocardium post-injury in the neonate is derived from dividing cells. Recent insight into the mechanism of this process

comes from studies on lower vertebrates, such as urodele amphibians and teleost fish, which are known to possess the ability to regenerate organs following injury. Like in the zebrafish, cardiomyocytes of the vertebrate neonate are able to de-differentiate and proliferate to contribute to heart regeneration.^{109, 110} In fact, it has been demonstrated that cardiomyocytes are replaced throughout the human lifespan; however this replacement is at a rate of 5% per year in childhood and 0.5% per year in adulthood.¹⁰¹ This inherent cell division ability is not enough to compensate for injury. Thus, researchers have focused on inhibiting cell cycle arrest and up-regulating the proliferative potential.¹⁰⁰

Investigators have also demonstrated a polarized inflammatory response, and increased stem cell recruitment in the neonatal mouse contributing to its regenerative capacity.^{114, 115} Certainly, the importance of the regeneration of the contractile tissue cannot be undermined. However, the ability of cells to survive and proliferate is intimately linked with proponents for a vascular supply. This newly generated contractile tissue must retain a source of nutrients and oxygen; the regenerated cardiac tissue must also contain newly formed blood vessels. The source of this vasculature remains elusive.

In the zebrafish, ample evidence indicates that the epicardium is the cellular source of the regenerated vasculature after cardiac injury.¹¹⁶ Indeed, fetal epicardial markers are also re-expressed after MI in adult mice. This is particularly important in subsets of epicardium-derived cells (EPDCs) that express Wilms' tumor 1 (Wt1) and T-box transcription factor 18 (Tbx18), markers of embryonic cardiovascular progenitors.¹¹⁷ These cells are thought to contribute to angiogenesis and stem cell recruitment post-MI through paracrine effects by up-regulating molecules such as MCP-1, FGF and retinoic

acid (RA).^{118, 119} More importantly, EPDCs are able to recapitulate their embryonic profile and undergo a process called epithelial-to-mesenchymal transition (EMT).

1.11.1 Epithelial-to-mesenchymal transition (EMT)

EMT plays a critical role in early development. Beyond its role in the invasion of the uterine lining and the formation of the three germ layers, EMT is also responsible for cardiac formation. Originating in the proepicardial organ, cells that express *Wt1* in development migrate to the surface of the myocardium to become the epicardial layer (at about E9-E10.5 in mice).¹²⁰ Many of these cells then undergo EMT to delaminate from the epicardium and form EDPCs which migrate into the myocardium as the precursors of the cardiac structures (at about E11.5-12.5).¹²⁰ Specifically, EPDCs contribute to the subendocardial and atrioventricular cushion, cardiac interstitial fibroblasts, and the coronary vasculature (coronary smooth muscle cells and endothelial cells).¹²¹ This dormant fetal growth program is reactivated after adult MI by stimuli such as increased wall stress, which activates mechanical stretch receptors, triggering immediate early genes such as *c-jun*, *c-fos*, *c-myc* and *Egr-1*.¹²² Hypoxia from injury induces hypoxia-inducible factor-1 alpha (*HIF-1 α*), which is responsible for the upregulation of VEGF and other pro-angiogenic factors that are implicated in epicardial EMT in coronary vascular development.¹²³

Epicardial EMT involves cell junction disassembly, loss of epithelial cell polarity, and cytoskeletal reorganization via suppression of epithelial genes, and activation of a mesenchymal gene signature. The upregulated local expression of TGF- β and FGF-2 activated kinases and GTPases facilitates degradation of the basement membrane and promotes actin rearrangement and cell movement.¹²⁴ TGF- β stimulates the expression of

Snail and Slug transcription factors, which directly repress transcription of endothelial genes.¹²¹ For example, epithelial E-cadherin, a transmembrane protein that forms epithelial cellular junctions, is cleaved and its production suppressed in favor of N-cadherin and vimentin (mesenchymal proteins).^{121, 125} The cell assumes a mesenchymal phenotype and migrates away from the basement membrane. As discussed later, wntless-type integration site (Wnt) signaling and associated β -catenin nuclear translocation also contribute to this process. This embryonic reprogramming is responsible for detachment, inward movement and mitosis, which also occur in transitioning epicardial cells post-MI. Once transitioned, differentiated EPDCs lose Wt1 expression;¹²⁶ post-MI, epicardial cells express mesenchymal markers rather than epicardial ones, implying their mesenchymal transition.¹²¹

Many of the factors which promote EMT are also implicated in maintaining survival and integrity of cells for this newly formed vasculature. For example, TGF- β , a cytokine integral to the initiation of EMT, also promotes endothelial survival via phosphatidylinositol 3-kinase (PI3K) and mitogen-activated protein kinase (MAPK) signaling.¹²⁷ Platelet-derived growth factor (PDGF) is critical for epicardial EMT in development, but also participates in the recruitment of progenitors for angiogenesis and enhances survival of endothelial cells.^{128, 129} Additionally, bFGFs induce mesenchymal characteristics in endothelial cells and support epithelial migration and transition while inhibiting endothelial cell apoptosis via upregulation of the antiapoptotic proteins Bcl-2 and survivin.¹³⁰⁻¹³²

While genes for epicardial EMT are activated post-MI in the adult mammal, perhaps this activation is exacerbated in the neonate, contributing to its superior

regenerative response. Indeed, EMT genes are upregulated post-cardiac apex resection in the neonate.¹¹⁰ Data from zebrafish models designates the epicardium as the cellular source of the regenerated vascular compartment, corroborating this hypothesis.¹¹⁶

Enhancing the EMT process in the neonate and adult may augment infarct and peri-infarct angiogenesis, and by extension, cell division. Our laboratory recently demonstrated that the contribution of EPDC progenitors can be augmented in the adult by other factors related to embryogenesis, including stem cell factor (SCF).¹³³ The breakdown of the epicardial basement membrane post-MI allowed SCF expressed by the myocyte to interact with the *c-kit* receptor on the epicardium. This induced the expression of the key EMT regulator, TGF- β , enhancing epicardial activation and production of EPDCs, contributing to arteriogenesis.

1.12 Wilms' tumor 1

The involvement of Wt1 in promoting the EMT phenotype makes it a potential candidate to target EMT for regeneration. Wt1 is an epicardial transcription factor enriched in the embryonic heart, and is required for embryonic coronary artery formation and essential for EMT of EPDCs.^{126, 134} The Wt1 gene is located on chromosome 11p13, and codes for the Wt1 mRNA transcript, which is about 3.5 kb long.¹³⁵ Wt1 contains a DNA binding domain with a proline-glutamine rich region capable of regulating transcription. Early studies of Wt1 identified many potential target DNA binding sites including promoters of genes that encode IGF, PDGF-A, and TGF- β 1.¹³⁵ Subsequently, two of the major mediators of EMT, Snail (*Snail*) and E-cadherin (*Cdh1*), were both determined to be controlled through direct transcriptional regulation by Wt1, thereby

affecting cell differentiation.¹³⁶ After MI, Wt1 marks the activation of the epicardium and is expressed in the coronary vasculature.¹³⁷ However, the role of Wt1 in neonatal cardiac regeneration has not been elucidated.

1.13 The primary cilium

Receptors for cytokines that govern multiple signaling pathways integral to the initiation of EMT are found on small microtubule based sensory organelles called primary cilia.¹³⁸ Primary cilia are non-motile hair-like protrusions that emanate from the cell surface in an antenna-like fashion. Primary cilia are located on almost all polarized, and most non-polarized cell types.¹³⁹ Once considered vestigial organs, the function of the primary cilium is still being elucidated; the major function of primary cilia was hypothesized to be in calcium-responsive mechanical force sensation, however the involvement of calcium in this process was recently disproved.¹⁴⁰ Nevertheless, the hypothesis that primary cilia sense extracellular cues (chemical and mechanical) and transmit signals required for tissue homeostasis and tissue development persists. These organelles possess unique antenna-like properties which allow them to detect mechanical and sensory cues and transmit these signals from the cell surroundings to its interior.

1.13.1 Structure of the primary cilium

Primary cilia are immotile organelles comprised of microtubules in a structure called the axoneme, and a surrounding ciliary membrane (**Figure 1.3A**). The primary cilium grows to the outer surface of the cell from the centriole, which transforms into the base of the ciliary organ called the basal body. The requirement of the centriole to form the basal body makes the presence of the primary cilium mutually exclusive with

progression through the cell cycle; during mitosis the basal body detaches from the cell membrane region to enter the interior of the cell as the mother centriole of the centrosome.¹⁴¹ Centrioles are composed of nine microtubule triples, which give rise to microtubule doublets of acetylated α -tubulin to nucleate the axoneme of the primary cilium. For this reason, the basal body dictates the position and orientation of the cilium.¹⁴² At this transition zone between the basal body and axoneme are axonemal microtubules, transition fibers, and ciliary rootlets which anchor the basal body to the membrane and act as a barrier for selective passage of materials into the cilium; this region is known as the “ciliary necklace”.¹⁴³ During its formation, the primary cilium grows outward from the mother centriole to become encased by the lipid bilayer of the plasma membrane.¹⁴⁴ The plasma membrane of the cilium, however, is changed to contain an altered set of ion channels and membrane receptors which pass through the ciliary necklace by harboring specific ciliary targeting motifs.^{145, 146} Unlike the motile cilium which is comprised of a 9 + 2 microtubule structure (nine outer doublets with a central pair), the primary cilium lacks the central doublet, making a 9 + 0 structure (**Figure 1.3B**).

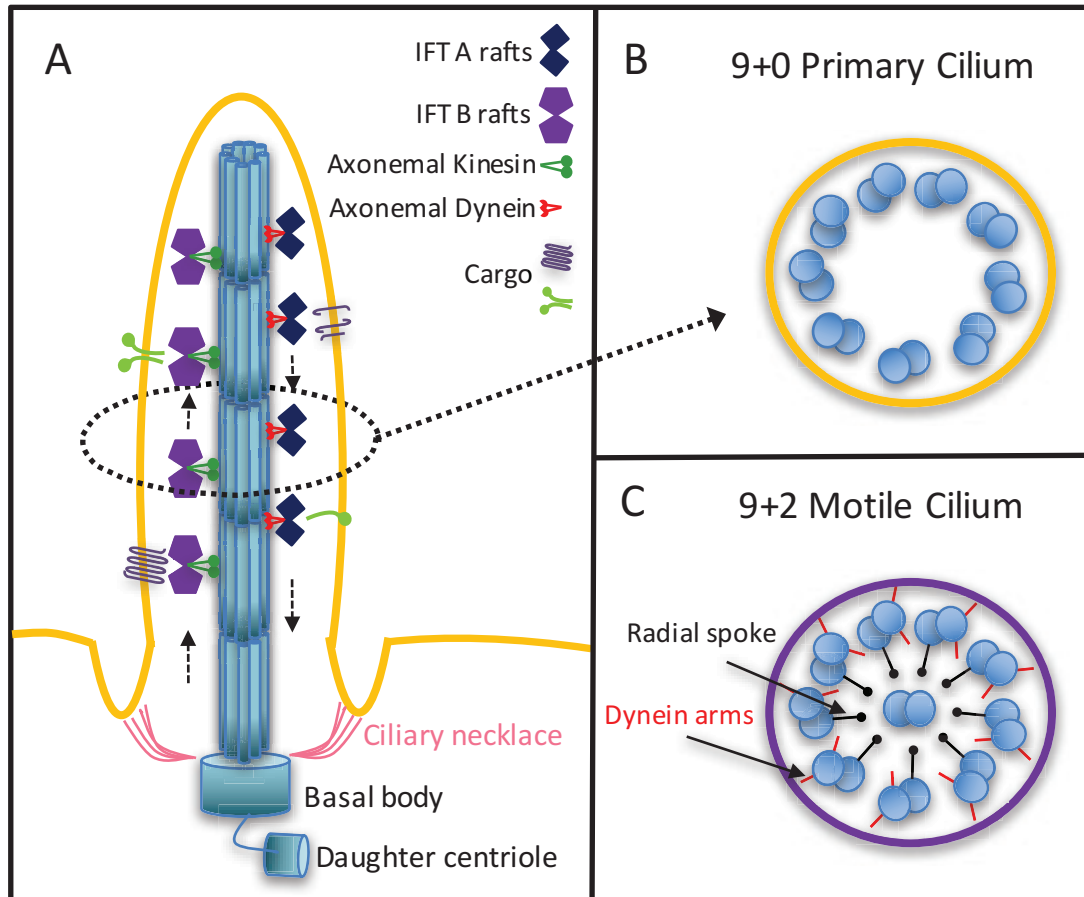


Figure 1.3. Structure of the cilium.

The primary cilium emanates from the basal body under the plasma membrane. The structure is membrane bound and composed mainly of the ciliary axoneme (A). Intraflagellar transport proteins (IFT) containing cargo are transported up the cilium with active kinesin. Ciliary turnover takes place in the ciliary tip, and inactive cargo is transported retrogradely on IFT particles by dynein. The ciliary axoneme differentiates the motile cilium from the primary cilium. In the motile cilium (C), a 9+2 arrangement of doublet microtubules surrounds a central microtubule pair. Attached to these microtubules are accessory structures involved in motility. On the other hand, the primary cilium (B) is also arranged with 9 outer doublet microtubules, however it does not contain the central pair or any accessory motility structures.

1.13.1.1 Intraflagellar transport

The machinery for protein synthesis does not reside within the cilium, thus all proteins necessary for ciliary function must be transported into the cilium from the cytoplasm. The ciliary axoneme is elongated, and continuously turned over via the process of intraflagellar transport (IFT). IFT is a bi-directional transport system which allows the trafficking of large protein complexes (IFT particles) along polarized microtubules in the axoneme.¹⁴⁷ Kinesin-2 motors carry particles along the outer doublet of microtubules from the base to the tip, and cytoplasmic dynein 2 returns the recycled products (e.g., inactive receptors) back to the cell body in a retrograde fashion (**Figure 1.3A**).^{148, 149} There are two distinct subcomplexes of IFT; IFT complex B is required for anterograde transport from the ciliary base to the axoneme tip, while IFT complex A allows retrograde movement from the axoneme tip back down to the ciliary base.^{150, 151} The IFT complexes serve as rafts for ciliary cargo such as tubulin, G protein coupled receptors (GPCRs), ion channels, and protein kinases.¹⁵² Dysregulation of IFT polypeptides leads to a plethora of human diseases, demonstrating the importance of these molecules for proper ciliary function. These “ciliopathies” are often pleiotropic disorders and include defects in numerous organ systems including the liver, kidney, airway, brain, pancreas, retina, adipose, and heart.¹³⁹

Intraflagellar transport protein 88 (Ift88) (*Tg737*; Polaris protein) is a complex B protein required for primary cilia formation. This requirement was discovered in *Chlamydomonas*, and subsequently determined to contribute to the failure of ciliary function in polycystic kidney disease.¹⁵¹ *Tg737* functionality was also shown to be required for various ciliary related processes including proper ependymal cell function in

brain ventricles and node cilia functioning in left-right patterning for embryonic development.¹⁵³ *Tg737* knock-out mice die at embryonic day 11.5 due to a variety of developmental abnormalities beyond those associated with left-right axis patterning defects, including cardiac insufficiency with pericardial sac ballooning.¹⁵⁴

1.13.2 Primary cilium in signal transduction

IFT allows the transport of signaling molecules and receptors, turning the cilium into a repository that can harbor proteins and coordinate signaling pathways. As a cell signaling center, the primary cilium integrates components of numerous signaling pathways, including Hedgehog (Hh), Wnt and PDGF (**Figure 1.4**), all molecules related to EMT.^{125, 155-157}

The Hh signaling pathway is required for adult tissue homeostasis, and is essential for axis determination and organ development during embryogenesis.¹⁵⁸ Gradients of Hh signal transduction dictate the developmental patterning of numerous tissues including the neural tube and limb bud. The primary modulator of the Hh pathway is Sonic hedgehog (Shh), which binds to its 12-transmembrane protein receptor Patched (Ptch) to initiate signaling.¹⁵⁹ Shh induces the expression of transcription factors required for cardiac development.¹⁶⁰ *Ift88*-null mice develop hearts with ventricular dilation, reduced myocardial trabeculation, and outflow tract abnormalities.¹⁶¹ *Clement et al.* demonstrated that Hh signaling is associated with the cilium in cardiomyocytes, and suggested its loss could be responsible for the observed cardiac phenotype of these *Ift88*-null mice. However, these authors also showed that Hh signaling is required for cardiac differentiation in pools of stem cells, suggesting that inhibition of *Ift88* (and consequently Hh) may allow for maintenance or return to a stem cell like phenotype. The downstream

positive mediator of Hh signaling is a seven-transmembrane GPCR protein called Smoothed (Smo), which modulates Gli transcription factors. Gli1 and Gli2 function as transcriptional activators while Gli3 is a repressor. Ptch, Smo, and Gli transcription factors are all present within the primary cilium and this localization of Ptch and Smo is mutually exclusive.^{162, 163} In a basal state, Ptch is localized to the primary cilium. In the absence of Shh, Ptch tonically inhibits Smo from its entrance into the cilium, thereby repressing Hh mediated transcription. In this instance, Smo cannot act on the Gli factors, and Gli2 is degraded while Gli3 is processed to its repressive form. Alternatively, in the presence of Shh, Ptch is internalized, allowing Smo to enter the primary cilium (**Figure 1.4A**). Within the cilium, Smo sends Gli3 to the proteasome for degradation, and activates the Gli2 transcription factor, which enters the nucleus to promote transcription. The involvement of the primary cilium in this process is demonstrated by the requirement of IFT for both Gli2 activator and Gli3 repressor processing. Loss of IFT results in reduced Gli2 activators and Gli3 repressors, causing aberrantly active low level Hh signaling.^{162, 164} During development, at which time high levels of Hh are required, this low level signaling results in apparent loss of function.¹⁵⁵ However, in the adult, Hh signaling plays a limited role, and reduced inhibition with abnormal low level activation results in a gain of function phenotype which may contribute to tumorigenesis.¹⁶⁵ Shh targets which may propagate tumor development include genes related to cell survival (*Bcl2*), self-renewal (*Nanog*), angiogenesis (*Vegf*), and EMT (*Snail1*).¹⁶⁶

Wnt signaling also contributes to normal mammalian development and adult tissue homeostasis. Wnts act through activation of two separate pathways: the canonical (β -catenin dependent) and non-canonical (β -catenin independent) pathway. In the

canonical pathway, Wnt ligands interact with the Frizzled (Fz) class of cell surface receptors, which in turn recruit the downstream signal mediator Dishevelled (Dvl) (**Figure 1.4B**). In the absence of Wnt ligand, β -catenin is constitutively phosphorylated and targeted for destruction. Conversely, when Wnt activates the canonical pathway, Dvl is recruited to Fz, and the β -catenin destruction complex is disassembled, allowing for β -catenin nuclear transport and subsequent activity as a transcription factor.¹⁶⁷ This type of Wnt/ β -catenin signaling is required for endocardial cushion formation during cardiac development.¹⁶⁸ Various lines of evidence indicate that the primary cilium plays an inhibitory role in Wnt signaling. Knockout mice for proteins required for primary cilia assembly exhibit hyperactive β -catenin-dependent signaling as compared to wild type controls.¹⁶⁹ It is thought that the β -catenin-positive regulator Joubertin (Jbn) is spatially sequestered in the cilium, constraining movement of β -catenin to the nucleus.¹⁵⁷ β -catenin is a known transcriptional activator of several EMT related genes, including Twist and ZEB1.¹⁷⁰

In the non-canonical (β -catenin independent) pathways, Wnts bind to either Fz or another transmembrane receptor, Vangl2, to activate small GTPases Rac1 and RhoA, which control planar cell polarity (PCP) pathways, resulting in cytoskeletal-actin rearrangements causing changes in cell shape.¹⁷¹ The PCP pathway causes polarized localization of proteins required for the establishment of polarized cell morphology. Unlike the canonical pathway, the primary cilium is thought to be required for PCP (non-canonical Wnt signaling).¹⁷² For example, conditional mutation of *Ift88* in the inner ear results in disorganization of the planar-polarized orientation of stereocilia.¹⁷³ Several core PCP proteins have been shown to localize to the primary cilium. For example, Vangl2 is

localized along the axoneme, likely contributing to its localization on the apical membrane in epithelia.¹⁷⁴ The interaction of Vangl2 with the ciliary/ basal body protein Bardet-Biedl syndrome 8 (BBS8) has been shown to be required for the establishment of left-right asymmetry.¹⁷⁵ On the other hand, it has been demonstrated that mediators of noncanonical Wnt/PCP signaling are required for primary cilia formation.¹⁷⁶ Regardless of whether the primary cilium is required for noncanonical Wnt signaling, or vice versa, the two appear to be closely connected, perhaps via various molecules. In either case, mutations in ciliary proteins attenuate Wnt/PCP signaling, resulting in loss of cell polarity – a feature of EMT.¹²⁵

Cell survival, proliferation, migration, and, importantly, angiogenesis are all also crucially regulated by PDGF signaling.^{177, 178} These pathways critically contribute to wound healing in adult tissues. Interestingly, *Schneider* et al. demonstrated that the primary cilium is essential for PDGF signaling in growth arrested cells through its receptor PDGFR $\alpha\alpha$, the homodimer of PDGFR α .¹⁵⁶ PDGFR $\alpha\alpha$ localized to the primary cilium, and in *Tg737* knockout mutants, embryonic fibroblast cell cycle entrance was blocked, delineating a role for the primary cilium and PDGF signaling in growth control. The same group also demonstrated the importance of this signaling pathway for directional wound healing, indicating that the primary cilium is required for chemotaxis towards PDGF-AA.¹⁷⁹ Defects in PDGF signaling are implicated in a range of diseases including epithelial cancers and vascular disorders.¹⁷⁸ Specifically, aberrant PDGF causes EMT and supports cancer metastasis.¹⁸⁰ PDGF signaling also plays a role in EMT of mesenchymal cells during cardiac development and the growth of the coronary vasculature.¹⁸¹ However, these authors demonstrated the importance of PDGF-B and

PDGFR $\beta\beta$, rather than PDGFR $\alpha\alpha$ in EMT for coronary artery development. Although *Schneider* et al. demonstrated that PDGF-AA signaling through PDGFR $\alpha\alpha$ is associated with the cilium, signaling through PDGFR $\beta\beta$ was unaffected by loss of the cilium (**Figure 1.4C**).¹⁵⁶ Interestingly, activation of PDGFR $\beta\beta$ has been shown to promote deciliation, a phenotype associated with ciliopathies.¹⁸² Furthermore, isolated deletion of PDGFR β results in an impairment of coronary vascular smooth muscle generation in development, while knockout of PDGFR α alone inhibits the generation of cardiac fibroblasts, differentiating the two PDGF receptors.¹²⁸ Thus, the type of PDGF may be an important consideration when determining the role of the cilium in PDGF signaling; specifically, it has been suggested that signaling through PDGF $\alpha\alpha$ requires the presence of the cilium, while PDGF $\beta\beta$ leads to activation of the downstream MEK/ERK mediators independent of the cilium.¹⁶¹

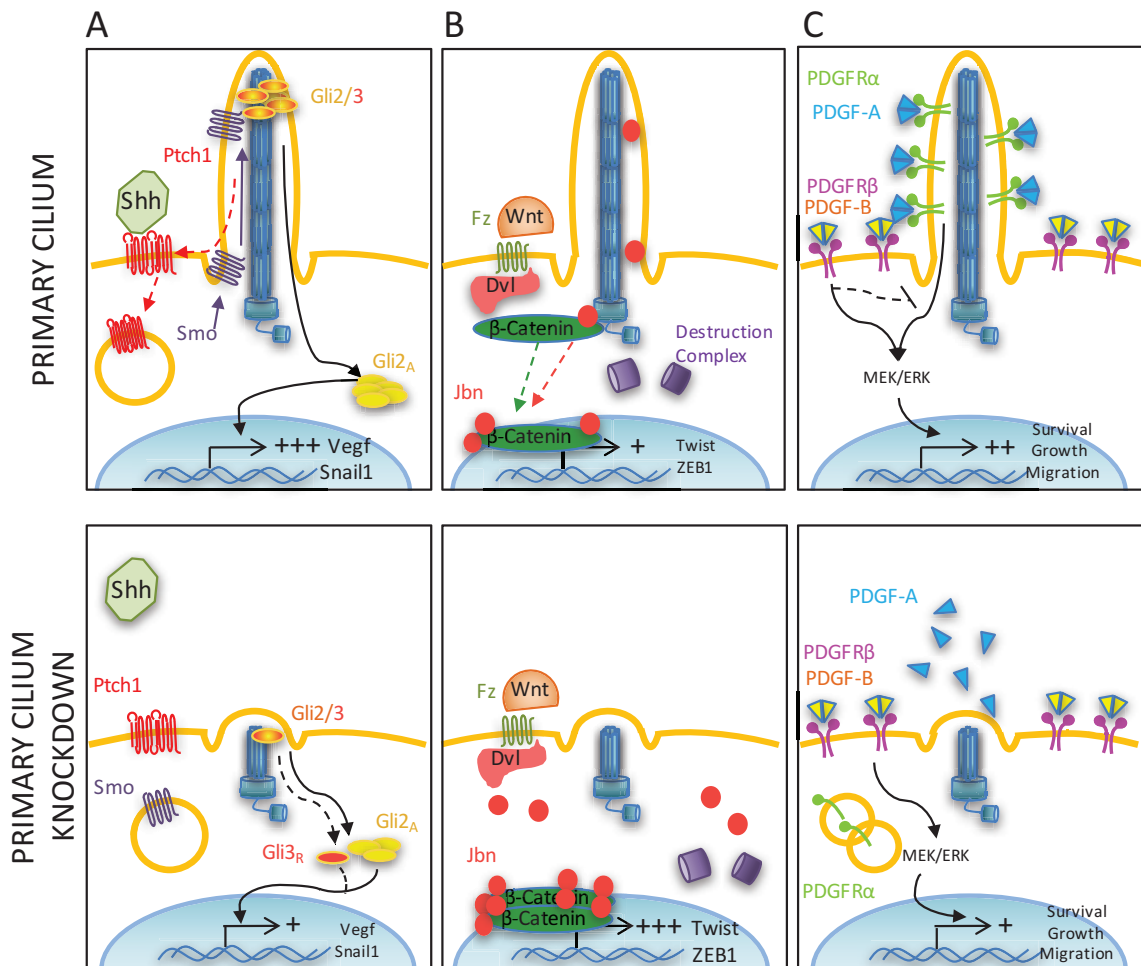


Figure 1.4. Signaling associated with the primary cilium.

A) Primary cilium harbors sonic hedgehog (Shh) signaling factors, and its degradation decreases Shh signaling. B) Wnt receptors are associated with the base of the primary cilium. In the absence of the cilium, Joubertin (Jbn) binds β -Catenin in the cytoplasm and its nuclear transport is uninhibited, causing hyperactive signaling. C) PDGF α receptors are associated on the cilium and PDGF β receptors on the plasma membrane. Loss of the cilium attenuates PDGF α mediated responses, but has no effect on PDGF β signaling.

Given the association between cilia and EMT related signaling, it is not surprising that altered ciliary function is associated with the progression of multiple types of cancer that require EMT for invasion and growth.¹⁶⁵ For example, EMT is a fundamental process in breast cancer development, and cilia loss is associated with breast carcinoma invasiveness and severity.¹⁸³ Specifically, genes related to intraflagellar transport proteins are downregulated in human breast cancer tissue as compared to tissue from normal patients. Similarly, cilia are lost in pre-invasive and invasive prostate cancer, leading to increased Wnt signaling.¹⁸⁴ Furthermore, as mentioned above, the presence of the cilium is also associated with cell cycle arrest, and ciliary resorption precedes cell cycle entry in many cell types, which may be associated with tumour growth.¹⁸⁵

1.13.3 The primary cilium in development and the heart

Ciliary function is also important for signaling during organogenesis and development.¹⁸⁶ Normal ciliary function is required for proper left-right patterning leading to proper situs and heart positioning in development.¹⁸⁷ Multiple human ciliopathies have related cardiac abnormalities such as dextrocardia, aortic stenosis, and septum defects.¹³⁸ Furthermore, mutations in cilia proteins in animal models result in congenital heart defects.^{161, 188} In concordance with this finding, patients with Bardet-Biedl syndrome, an autosomal recessive ciliopathy with multi-organ involvement, present with congenital heart defects, and echocardiography of adult patients demonstrated development of dilated cardiomyopathy.¹⁸⁹ Interestingly, FGF, the cardioprotective growth factor expressed post-MI, downregulates *Ift88* expression and reduces the ciliary length during development.¹⁹⁰ In the heart, both endocardial and epicardial cells are ciliated. However, under the influence of high shear stress (as in cardiac development, as

well as post-MI conditions), cells become devoid of cilia as the pressure signals the microtubules in these organelles to dissociate.¹⁹¹ In 2013, *Rozycki et al.* demonstrated that the resorption of the primary cilium is involved in regulating TGF- β mediated myofibroblast transition.¹⁹² Furthermore, the absence of ciliary Ift88 function in the embryonic mouse heart coincides with endocardial-to-mesenchymal transition (EndMT).¹⁹³ Therefore, stimulating ciliary disassembly by targeting the Ift88 protein may prove efficacious in recapitulating an embryonic phenotype conducive to promoting EMT for angiogenesis and cardiac regeneration post-MI.

1.14 EMT and Non-coding RNA

To target any regenerative mechanism, a suitable approach that is specific, efficient, efficacious, and cost effective with minimum side-effects is required. Protein expression can be up-regulated with the addition of recombinant proteins or adenoviral constructs containing the gene of interest, or silenced using gene-based interference technology. To enhance EMT, it is possible to prevent assembly of the primary cilium by inhibiting the translation of proteins necessary for the intraflagellar transport process. The understanding of the structure and function of ribonucleic acid (RNA), along with profiling of the mammalian transcriptome, has made knock-down or gene inhibition possible using RNA interference (RNAi). For example, short hairpin RNA (shRNA) can be used to inhibit messenger RNA from transcribed genes, or even other non-coding RNAs (to be discussed later). This is of particular importance in accessing targets for which conventional pharmaceutical agents such as small molecule agonists, antagonists or antibodies are currently not available.

1.14.1 Non-coding RNA

Genome wide analysis studies have determined that although the majority of the human (and mouse) genome is transcribed (80%), the bulk (62-75%) of these transcripts do not code for proteins.^{194, 195} RNA molecules that do not encode a molecular protein have been termed functional RNA (fRNA) or non-coding RNA (ncRNA). The advanced resolution with which data from genome wide analysis studies can be scrutinized along with careful examination of the transcriptome has led to an unprecedented understanding of the genomic organization of human life. Questioning the doctrine of the “central dogma” theory, ncRNA genes produce RNA molecules that are functional in and of themselves and are not merely intermediary molecules that encode proteins.

Early studies in biochemistry identified three RNAs involved in protein synthesis: messenger RNA (mRNA), transfer RNA (tRNA), and ribosomal RNA (rRNA), two of which are ncRNAs. However, the study of genomic organization through transcriptome analysis has allowed for the identification of several other forms of ncRNA. Broadly, these ncRNAs can be divided into two classes: small non-coding RNAs, less than 200 nucleotides in length, and longer non-coding RNAs, greater than 200 nucleotides in length. The types of small ncRNA include: piwi-interacting RNA (piRNA), involved in RNA destabilization and the formation of heterochromatin; small nucleolar RNAs (snoRNA), which are involved in rRNA modification; small cajal body specific RNA (scaRNA), a subset of the snoRNAs which guide biochemical modifications of rRNAs and snoRNAs; small nuclear RNAs (snRNA), which are involved in splicing; micro RNA (miRNA), which regulate (typically suppress) gene expression; and circular RNA (circRNA), which antagonize miRNA.¹⁹⁶ Longer ncRNAs include rRNA and other long

non-coding RNA (lncRNA), and these have heterogeneous biological functions such as mediating epigenetic modifications, transcription and post-transcriptional processing.¹⁹⁷

1.14.2 RNA interference

A number of molecular RNA tools have been developed in the research setting to exogenously alter gene expression, of which small interfering RNA (siRNA) and short hairpin RNA (shRNA) are of utmost interest for treatment of disease because they can cause gene silencing by RNA interference. These RNAs are advantageous as they are thought to have the ability to act on “non-druggable” targets which are inaccessible via typical means due to lack of enzymatic function, atypical protein conformation, or their presence inside the cell (beyond the plasma membrane). Furthermore, these molecules are typically more specific and potent than classical drugs, thereby reducing off-target side effects.¹⁹⁸

siRNA and shRNA are processed from either a double stranded (dsRNA) or hairpin RNA sequence. siRNAs are designed to have an almost perfect complementarity sequence to one mRNA, causing cleavage and degradation, rather than just repression of translation as occurs with endogenous miRNA. The specificity and efficiency of siRNA makes it a useful synthetic tool for gene silencing *in vitro*. However, the short half-life of siRNA makes *in vivo* use problematic; siRNAs are rapidly degraded by nucleases and quickly eliminated by renal glomeruli.¹⁹⁹ To solve this delivery conundrum, shRNA has been developed as an alternative which can be delivered via a viral delivery vector. The delivered vector bearing the short DNA sequence enters the nucleus and is transcribed to a hairpin loop structure by the endogenous RNA polymerase machinery. As a result, shRNA is constantly synthesized, leading to enduring gene silencing (lasting weeks) in

host cells, as compared with onetime transient siRNA complementarity. This process offers the advantage of stable prolonged silencing over the long-term, which is advantageous for chronic diseases such as heart failure. Furthermore, optimized delivery systems also demonstrate the superior silencing efficacy of shRNA over siRNA.²⁰⁰ These delivery systems also offer additional control at the level of the promoter; organotropic vectors with cardiac specific promoters can be used for transcriptional confinement to reduce off-target effects.²⁰¹

1.14.3 Long non-coding RNA

The lncRNAs comprise the largest portion of the non-coding transcriptome, with more than twice the number of protein-coding genes in the human.¹⁹⁵ lncRNAs are suggested to comprise 6.5% of transcripts in the human transcriptome, as compared to mRNA which accounts for less than 2%.^{202, 203} These endogenous transcripts have been reported to be involved in a diverse range of regulatory roles, including remodeling of chromatin, shaping of nuclear structure, and transcriptional, translational, and post-translational processing. For example, the lncRNA *XIST* is required for histone trimethylation and gene silencing of the inactive X chromosome.^{204, 205} lncRNAs can compete for the binding of miRNAs, inhibiting miRNA induced mRNA destabilization.¹⁹⁵ Other lncRNAs, such as *NEAT1*, possess the capacity to bind both DNA and protein, and thus aid in the concentration of both in nuclear bodies (paraspeckles) within the nucleus.²⁰⁶ lncRNA can interact with and modulate protein activity and protein-interactions, by competing with protein DNA-binding domains and providing a scaffold binding surface to assemble proteins.²⁰⁷ Several lncRNAs have been reported to interact with transcription factors, regulating their binding and activity,

thereby amplifying or attenuating transcription. For example, the dihydrofolate reductase pre-initiation complex assembly is controlled by a lncRNA transcript from an up-stream promoter.²⁰⁸ Others indirectly affect transcription factors by modulating their shuttling into the nucleus.²⁰⁹ The versatility of mechanisms by which lncRNA regulate biological processes is continuing to be defined; while the mechanisms of many lncRNAs have been uncovered,^{206, 207} the functions of the vast majority of lncRNAs are still unknown, leaving a great mystery of growing scientific interest.

1.14.4 Non-coding RNA in cardiovascular disease

ncRNA has been used to alter mRNA to affect cardiac disease in numerous pre-clinical studies. For example, shRNA has been used to augment activity of HIF-1 α for angiogenesis in ischemic heart disease by inhibiting translation of its regulator, prolyl hydroxylase-2.²¹⁰ The sarcoplasmic reticulum Ca²⁺ ATPase pump (SERCA2a) is often dysfunctional in the progression of heart failure, and typical pharmacological approaches have failed to modulate this target. In 2009, *Suckau* et al. demonstrated that adenoviral shRNA mediated-inhibition of SERCA2a regulator phospholamban normalized cardiac hypertrophy and restored cardiac function in a rat model of heart failure.²¹¹ Clinical trials using RNAi have demonstrated some efficacy in other disease settings (including targeting angiogenesis in ocular disease),²¹² however to the best of our knowledge, there has yet to be a clinical trial using RNAi therapy for cardiovascular disease of a non-genetic cause.

While RNA interference may revolutionize treatments, endogenous ncRNAs that play a significant role in cardiovascular disease have also come under the spotlight as both biomarkers which may be used in screening for disease, as well as therapeutic

targets to regulate pro-regenerative events post-cardiac injury. Many miRNA levels are significantly altered after MI and changes correlate with the progression of cardiac hypertrophy and fibrosis.^{196, 213}

Although many studies have been conducted on the activity of inhibitory RNAs in cardiovascular disease, the role of lncRNAs has been less well explored. In early 2015, *Ounzain* et al. identified hundreds of lncRNAs with potential roles in cardiogenesis and pathological remodeling after MI that could be used as candidate biomarkers in cardiovascular diseases.²¹⁴ Several lncRNAs are required for proper cardiogenesis, such as *H19*, which regulates cell proliferation and apoptosis during development.²¹⁵ More recently, analysis of cardiac progenitor cells from human fetal hearts supports the role for lncRNAs such as *CARMEN* (Cardiac Mesoderm Enhancer-associated Non-coding RNA) in cardiac differentiation.²¹⁶ Additionally, *He* et al. used RNA sequencing to report the differential lncRNA expression profiles of fetal and adult hearts, indicating lncRNA may be a candidate target for recapitulation of fetal gene expression post-MI.²¹⁷

Yang et al. have further suggested that lncRNA expression profiles more accurately discriminate failing hearts of different etiologies as compared to miRNAs.²¹⁸ Circulating lncRNA *LIPCAR*, for example, is indicated as a novel predicting biomarker of heart failure and death post-MI.²¹⁹ An association study identifying myocardial infarction associated transcript (*MIAT*) found single nucleotide polymorphisms (SNP) in lncRNAs that are associated with increased risk of cardiac disease.²²⁰ Other candidate lncRNAs include cardiac hypertrophy related factor (*CHRF*), which regulates cardiac hypertrophy, and cardiac apoptosis-related lncRNA (*CARL*) which suppresses cardiac apoptosis.^{221, 222} As this is a relatively new area of study, the first step towards clinical

application using lncRNA is to identify lncRNAs that are dysregulated in disease, and determine which are appropriate targets for therapeutic action. To this regard, *Viereck et al.* demonstrated that *Chast* (cardiac hypertrophy-associated transcript) is upregulated in cardiac hypertrophy; upon inhibition of *Chast* using antisense oligonucleotides, TAC-induced cardiac hypertrophy is prevented.²²³ The authors also discovered a human homolog, *CHAST*, which caused hypertrophy in human cells *in vitro*.

1.15 MALAT1

The lncRNA metastasis-associated lung adenocarcinoma transcript 1 (*MALAT1*) has been described as a regulator of EMT, apoptosis, cell cycle progression, and angiogenesis.²²⁴⁻²²⁶ *MALAT1* (also known as nuclear enriched abundant transcript 2; *NEAT2*), is a highly conserved lncRNA with a length of about 8000 nucleotides (two splice variants of 8352nt and 8110nt) transcribed from human chromosome 11q13.²²⁷ *Malat1* is also found in the mouse, with a length of about 6700 nucleotides located on chromosome 19A.²²⁸ Like *NEAT1* (described above), *MALAT1* has been shown to localize to nuclear bodies (nuclear speckles) within the nucleus, where it is suggested to regulate alternative splicing of several pre-mRNAs.²²⁹ *MALAT1* is highly expressed in many tissues, including those of the respiratory system, liver and biliary system, visual system, and importantly, the cardiovascular system.

1.15.1 A role for *MALAT1* in EMT and angiogenesis

While murine knockout mouse models demonstrate that loss of *Malat1* is compatible with normal development, its requirement becomes apparent under conditions of stress or disease.^{230, 231} Indeed, *MALAT1* was originally identified as a marker for non-

small cell lung cancers with metastatic propensity.²²⁷ *MALAT1* transcripts have also been found to be upregulated in numerous cancer types and it is thought to contribute to the maintenance of EMT for cell migration and invasion.^{232, 233} Inhibition of *MALAT1* in both *in vivo* and *in vitro* models of squamous cell carcinoma reduced cell migration and invasion, expression of EMT makers Slug and β -catenin, and the appearance of mesenchymal markers N-cadherin and Vimentin.²³³ Furthermore, Yang et al. demonstrated a direct link between *MALAT1* and TGF- β -induced EMT in human cell cultures in which knockdown of *MALAT1* suppressed TGF- β -mediated morphological changes, α -SMA expression, as well as the down-regulation of E-cadherin.²³⁴

MALAT1 also plays a role in tumor driven angiogenesis, and siRNA for *MALAT1* *in vitro* reduces pro-angiogenic factor expression in tumour cells.²³⁵ *In vivo*, *Malat1* plays a role in hypoxia related responses in the kidney, and genetic ablation of *Malat1* reduces neonatal retinal vascularization and post-ischemic angiogenesis in the hindlimb.^{226, 236} Similarly, evidence from ocular membranes from diabetic retinopathy patients (involving abnormal blood vessel proliferation) and mouse diabetic retinopathy models indicate augmented expression of *Malat1*.²³⁷ Furthermore, *MALAT1* expression is responsive to HIF-1 α in pulmonary artery smooth muscle cells, and GapmeR (antisense oligonucleotide) mediated reduction of *Malat1* reduced smooth muscle cell proliferation and ameliorated heart hypertrophy in mice with pulmonary hypertension.²³⁸

1.15.2 Effects of *MALAT1* on cell proliferation, and cell death

MALAT1 is also a known regulator of cell proliferation and cell death. Along with EMT, *MALAT1* contributes to cancer progression by promoting cell cycle advancement

and inhibiting p53 activation.²³⁹ *MALATI* has been shown to mediate progression through the G1/S phase of the cell cycle by interacting with unmethylated chromatin and relocating repressive complexes to support a gene activation milieu.²²⁴ Furthermore, siRNA mediated knockdown of *MALATI* promotes apoptosis of glioma cells and increases caspase-3 and Bax expression while attenuating Bcl-2 expression in human cervical cancer cells.^{225, 240} In human non-small-cell lung cancer, Bcl-2 expression depended on *MALATI* status.²⁴¹ Silencing *MALATI* also modulated cell proliferation in esophageal squamous cell carcinoma cells.²⁴² In more direct relation to the cardiovascular system, *MALATI* has been shown to protect endothelial cells from oxidative injury by up-regulating CXCR2 and AKT, which in turn promote cell proliferation, protect from apoptosis, and enhance angiogenesis.²⁴³ *Malat1* is thought to play a protective role in ischemic stroke; its expression is increased after ischemic stroke in mice, and *Malat1*^{-/-} mice experience larger brain infarct sizes, augmented cell death and enhanced caspase-3 activity.²⁴⁴ Importantly, plasma *MALATI* levels are increased in human MI patients.²⁴⁵ However, the role of *MALATI* in MI has not been elucidated.

1.16 Rationale and hypothesis

MI and subsequent heart failure are both life threatening and extremely costly ailments. Despite scientific advances and optimized current treatment, this is still a deadly disease, and breakthroughs in innovative disease treatment are needed. It has now been demonstrated that mammalian neonates possess the capacity to completely regenerate their hearts, turning treatment innovation towards augmenting strategies employed by neonatal hearts for regenerative repair. The recent developments in and understanding of ncRNA and RNAi technology has led to the study of their potential in

promoting or inhibiting tissue repair, however these methods have yet to show development in clinical trials, likely due to direction towards unsuitable targets. Ideal candidates to direct treatment strategies would enhance the endogenous repair processes that are demonstrated by neonates, such as EMT, and attenuate factors associated with adverse outcomes, such as cardiac damage and heart failure. Indeed, we and others have demonstrated that augmenting EMT mediated angiogenesis improves cardiac function and attenuates hypertrophy.¹³³ A new target which may affect the EMT capacity is the primary cilium, a small microtubule based organelle on the cell surface which is thought to play a role in regulating EMT processes.

Although hypertrophy, angiogenesis, and cytokine expression post-MI are important mediators in cardiac repair, the magnitude of the acute infarct is perhaps the most critical determinant of the development of contractile dysfunction.²⁴⁶ It is important to preserve existing cardiac mass given the hearts' limited capacity for regeneration. This is vital since current pharmacologic treatments can attenuate remodeling and preserve function post-MI, but have limited effects on the size of the initial infarct. Research directed at limiting infarct size by reduction of apoptosis has yielded positive results in animal models. Indeed, *Yaoita* et al. and others were able to attenuate infarct size and improve cardiac function using caspase inhibitors in rat models of ischemia.^{247, 248} However, no caspase inhibitors have advanced to clinical trials for cardiac disease because of poor pharmacologic properties.²⁴⁹ Among other mediators of cell death are the lncRNAs. Specifically, *Malat1* is a lncRNA implicated in both augmenting EMT and mitigating apoptosis. **The overall aim of this thesis was to assess the capacity for**

cardiac regeneration in neonatal mice and study the role of the primary cilium in EMT and the lncRNA *Malat1* in cell death post-myocardial infarction.

1.16.1 Aim 1: Cardiac regeneration in neonatal mice

Unlike adult mammals which undergo minimal regeneration after cardiac injury, the capacity for cardiac regeneration is transiently retained in the mammalian heart in early neonatal life. The regenerative capacity is critically dependent on a vascular supply. Coronary artery development during embryogenesis and neovascularization post-MI in the adult are dependent upon epicardial EMT for both a source of cells and cytokines for growth.¹²¹ *Wt1* and *MALAT1* are both known to support the EMT process.^{136, 234} However, the importance of *Wt1* and *Malat1* in the neonatal regenerative response have not been clarified. Thus, the first aim of this thesis was to develop a reproducible model of cardiac regeneration in neonatal mice with which to test the importance of both *Wt1* and *Malat1* in cardiac regeneration. **We hypothesized that a reproducible model of cardiac regeneration would be developed in neonates, and deficiency of *Wt1* and *Malat1* would abolish the regenerative capacity of the neonatal mouse.**

1.16.2 Aim 2: The primary cilium and EMT

It has been demonstrated that EMT genes are upregulated in the regenerating neonatal heart.¹¹⁰ EMT is a critical regulator of coronary artery development and neovascularization post-MI.¹²¹ To the best of our knowledge, the primary cilium has never before been targeted for healing post-MI, however its role in EMT has been demonstrated in numerous cancer metastases.¹⁶⁵ Furthermore, several important EMT signaling mediators are known to be harbored within the primary cilium.¹⁸⁶ Thus, the second aim of this thesis was to determine the role of the primary cilium in EMT and

cardiac repair post-MI. **We hypothesized that downregulation of *Ift88* using adenoviral shRNA would potentiate primary cilium disassembly and promote epicardial EMT leading to neovascularization and cardiac repair post-MI.**

1.16.3 Aim 3: *Malat1* and ischemic cell death

Finally, the exploration of lncRNA in the modulation of recovery from myocardial infarction has only recently begun. The lncRNA *MALAT1* has been shown to promote EMT, prevent cell apoptosis and support tissue repair. The role of *MALAT1* in EMT for metastasis has been demonstrated in several different types of cancer.²³² Similarly, *MALAT1* has been shown to play a role in ischemic angiogenesis.²²⁶ The role of *MALAT1* in cardiac ischemia, however, has been less well explored. The third aim of this thesis was to assess the role of *Malat1* in cardiac damage using a *Malat1*^{-/-} mouse. **We hypothesized that silencing of the lncRNA *Malat1* would result in augmented cardiac injury post-MI.**

1.17 References

1. Statistics Canada. The 10 leading causes of death, 2011. *Health Fact Sheets*. 2011.
2. World Health Organization. The top 10 causes of death. Fact sheet 310. 2015:937-52.
3. Frangogiannis NG. The immune system and cardiac repair. *Pharmacol Res*. 2008;58:88-111.
4. de Vreede JJ, et al. Did prognosis after acute myocardial infarction change during the past 30 years? A meta-analysis. *J Am Coll Cardiol*. 1991;18:698-706.
5. Rouleau JL, et al. Myocardial infarction patients in the 1990s--their risk factors, stratification and survival in Canada: the Canadian Assessment of Myocardial Infarction (CAMI) Study. *J Am Coll Cardiol*. 1996;27:1119-27.
6. Wang JY, et al. Cardiovascular Risk Factors and In-hospital Mortality in Acute Coronary Syndromes: Insights From the Canadian Global Registry of Acute Coronary Events. *Can J Cardiol*. 2015;31:1455-61.
7. Dai S, et al. Report Summary. Tracking heart disease and stroke in Canada 2009. *ARCHIVED - Chronic Diseases in Canada*. 2009;29.
8. Setayeshgar S, et al. Prevalence of 10-year risk of cardiovascular diseases and associated risks in Canadian adults: the contribution of cardiometabolic risk assessment introduction. *Int J Hypertens*. 2013;2013:276564.
9. Gerber Y, et al. Mortality Associated With Heart Failure After Myocardial Infarction: A Contemporary Community Perspective. *Circ Heart Fail*. 2016;9:e002460.
10. Banerjee I, et al. Determination of cell types and numbers during cardiac development in the neonatal and adult rat and mouse. *Am J Physiol Heart Circ Physiol*. 2007;293:H1883-91.
11. Vliegen HW, et al. Myocardial changes in pressure overload-induced left ventricular hypertrophy. A study on tissue composition, polyploidization and multinucleation. *Eur Heart J*. 1991;12:488-94.
12. Stott WT, et al. Blood-flow distribution in the mouse. *J Appl Toxicol*. 1983;3:310-2.
13. Baron T, et al. Type 2 myocardial infarction in clinical practice. *Heart*. 2015;101:101-6.

14. Wang JC, et al. Coronary artery spatial distribution of acute myocardial infarction occlusions. *Circulation*. 2004;110:278-84.
15. Doenst T, et al. Cardiac metabolism in heart failure: implications beyond ATP production. *Circ Res*. 2013;113:709-24.
16. Bouchardy B and Majno G. Histopathology of early myocardial infarcts. A new approach. *Am J Pathol*. 1974;74:301-30.
17. Anversa P, et al. Apoptosis and myocardial infarction. *Basic Res Cardiol*. 1998;93 Suppl 3:8-12.
18. Konstantinidis K, et al. Mechanisms of cell death in heart disease. *Arterioscler Thromb Vasc Biol*. 2012;32:1552-62.
19. Krijnen PA, et al. Apoptosis in myocardial ischaemia and infarction. *J Clin Pathol*. 2002;55:801-11.
20. McCully JD, et al. Differential contribution of necrosis and apoptosis in myocardial ischemia-reperfusion injury. *Am J Physiol Heart Circ Physiol*. 2004;286:H1923-35.
21. Teringova E and Tousek P. Apoptosis in ischemic heart disease. *J Transl Med*. 2017;15:87.
22. Festjens N, et al. RIP1, a kinase on the crossroads of a cell's decision to live or die. *Cell Death Differ*. 2007;14:400-10.
23. Gomez L, et al. Fas-independent mitochondrial damage triggers cardiomyocyte death after ischemia-reperfusion. *Am J Physiol Heart Circ Physiol*. 2005;289:H2153-8.
24. Kinnally KW, et al. Is mPTP the gatekeeper for necrosis, apoptosis, or both? *Biochim Biophys Acta*. 2011;1813:616-22.
25. Li P, et al. Cytochrome c and dATP-dependent formation of Apaf-1/caspase-9 complex initiates an apoptotic protease cascade. *Cell*. 1997;91:479-89.
26. Zou H, et al. An APAF-1.cytochrome c multimeric complex is a functional apoptosome that activates procaspase-9. *J Biol Chem*. 1999;274:11549-56.
27. Shamas-Din A, et al. BH3-only proteins: Orchestrators of apoptosis. *Biochim Biophys Acta*. 2011;1813:508-20.
28. Gustafsson AB and Gottlieb RA. Bcl-2 family members and apoptosis, taken to heart. *Am J Physiol Cell Physiol*. 2007;292:C45-51.

29. Jung F, et al. Chronic hypoxia induces apoptosis in cardiac myocytes: a possible role for Bcl-2-like proteins. *Biochem Biophys Res Commun.* 2001;286:419-25.
30. Latif N, et al. Upregulation of the Bcl-2 family of proteins in end stage heart failure. *J Am Coll Cardiol.* 2000;35:1769-77.
31. Mezzaroma E, et al. The inflammasome promotes adverse cardiac remodeling following acute myocardial infarction in the mouse. *Proc Natl Acad Sci U S A.* 2011;108:19725-30.
32. Sun M, et al. Excessive tumor necrosis factor activation after infarction contributes to susceptibility of myocardial rupture and left ventricular dysfunction. *Circulation.* 2004;110:3221-8.
33. He S, et al. Receptor interacting protein kinase-3 determines cellular necrotic response to TNF-alpha. *Cell.* 2009;137:1100-11.
34. Cho YS, et al. Phosphorylation-driven assembly of the RIP1-RIP3 complex regulates programmed necrosis and virus-induced inflammation. *Cell.* 2009;137:1112-23.
35. Chan FK, et al. A role for tumor necrosis factor receptor-2 and receptor-interacting protein in programmed necrosis and antiviral responses. *J Biol Chem.* 2003;278:51613-21.
36. Sun L, et al. Mixed lineage kinase domain-like protein mediates necrosis signaling downstream of RIP3 kinase. *Cell.* 2012;148:213-27.
37. Wang H, et al. Mixed lineage kinase domain-like protein MLKL causes necrotic membrane disruption upon phosphorylation by RIP3. *Mol Cell.* 2014;54:133-46.
38. Holler N, et al. Fas triggers an alternative, caspase-8-independent cell death pathway using the kinase RIP as effector molecule. *Nat Immunol.* 2000;1:489-95.
39. Moriwaki K and Chan FK. RIP3: a molecular switch for necrosis and inflammation. *Genes Dev.* 2013;27:1640-9.
40. Wu XN, et al. Distinct roles of RIP1-RIP3 hetero- and RIP3-RIP3 homo-interaction in mediating necroptosis. *Cell Death Differ.* 2014;21:1709-20.
41. Vandenabeele P, et al. The role of the kinases RIP1 and RIP3 in TNF-induced necrosis. *Sci Signal.* 2010;3:re4.
42. Kim SJ, et al. In vivo gene delivery of XIAP protects against myocardial apoptosis and infarction following ischemia/reperfusion in conscious rabbits. *Life Sci.* 2011;88:572-7.

43. Okamura T, et al. Effect of caspase inhibitors on myocardial infarct size and myocyte DNA fragmentation in the ischemia-reperfused rat heart. *Cardiovasc Res.* 2000;45:642-50.
44. Hochhauser E, et al. Bax deficiency reduces infarct size and improves long-term function after myocardial infarction. *Cell Biochem Biophys.* 2007;47:11-20.
45. Chen Z, et al. Overexpression of Bcl-2 attenuates apoptosis and protects against myocardial I/R injury in transgenic mice. *Am J Physiol Heart Circ Physiol.* 2001;280:H2313-20.
46. Lee P, et al. Fas pathway is a critical mediator of cardiac myocyte death and MI during ischemia-reperfusion in vivo. *Am J Physiol Heart Circ Physiol.* 2003;284:H456-63.
47. Nakagawa T, et al. Cyclophilin D-dependent mitochondrial permeability transition regulates some necrotic but not apoptotic cell death. *Nature.* 2005;434:652-8.
48. Smith CC, et al. Necrostatin: a potentially novel cardioprotective agent? *Cardiovasc Drugs Ther.* 2007;21:227-33.
49. Luedde M, et al. RIP3, a kinase promoting necroptotic cell death, mediates adverse remodelling after myocardial infarction. *Cardiovasc Res.* 2014;103:206-16.
50. Frangogiannis NG, et al. The inflammatory response in myocardial infarction. *Cardiovasc Res.* 2002;53:31-47.
51. Ma Y, et al. Neutrophil roles in left ventricular remodeling following myocardial infarction. *Fibrogenesis Tissue Repair.* 2013;6:11.
52. Weisman HF, et al. Cellular mechanisms of myocardial infarct expansion. *Circulation.* 1988;78:186-201.
53. Abbate A, et al. Acute myocardial infarction and heart failure: role of apoptosis. *Int J Biochem Cell Biol.* 2006;38:1834-40.
54. Palojoki E, et al. Cardiomyocyte apoptosis and ventricular remodeling after myocardial infarction in rats. *Am J Physiol Heart Circ Physiol.* 2001;280:H2726-31.
55. Gajarsa JJ and Kloner RA. Left ventricular remodeling in the post-infarction heart: a review of cellular, molecular mechanisms, and therapeutic modalities. *Heart Fail Rev.* 2011;16:13-21.

56. Loennechen JP, et al. Regional expression of endothelin-1, ANP, IGF-1, and LV wall stress in the infarcted rat heart. *Am J Physiol Heart Circ Physiol*. 2001;280:H2902-10.
57. Schomig A, et al. Catecholamine release and arrhythmias in acute myocardial ischaemia. *Eur Heart J*. 1991;12 Suppl F:38-47.
58. Sadoshima J, et al. Autocrine release of angiotensin II mediates stretch-induced hypertrophy of cardiac myocytes in vitro. *Cell*. 1993;75:977-84.
59. Miyata S, et al. Myosin heavy chain isoform expression in the failing and nonfailing human heart. *Circ Res*. 2000;86:386-90.
60. Yamazaki T, et al. Angiotensin II partly mediates mechanical stress-induced cardiac hypertrophy. *Circ Res*. 1995;77:258-65.
61. Ware JA and Simons M. Angiogenesis in ischemic heart disease. *Nat Med*. 1997;3:158-64.
62. Dobaczewski M, et al. Extracellular matrix remodeling in canine and mouse myocardial infarcts. *Cell Tissue Res*. 2006;324:475-88.
63. Brilla CG, et al. Role of angiotensin II and prostaglandin E2 in regulating cardiac fibroblast collagen turnover. *Am J Cardiol*. 1995;76:8D-13D.
64. Cleutjens JP, et al. Collagen remodeling after myocardial infarction in the rat heart. *Am J Pathol*. 1995;147:325-38.
65. Velagaleti RS, et al. Long-term trends in the incidence of heart failure after myocardial infarction. *Circulation*. 2008;118:2057-62.
66. Sam F, et al. Progressive left ventricular remodeling and apoptosis late after myocardial infarction in mouse heart. *Am J Physiol Heart Circ Physiol*. 2000;279:H422-8.
67. Chiong M, et al. Cardiomyocyte death: mechanisms and translational implications. *Cell Death Dis*. 2011;2:e244.
68. Bristow MR, et al. Decreased catecholamine sensitivity and beta-adrenergic-receptor density in failing human hearts. *N Engl J Med*. 1982;307:205-11.
69. Communal C, et al. Norepinephrine stimulates apoptosis in adult rat ventricular myocytes by activation of the beta-adrenergic pathway. *Circulation*. 1998;98:1329-34.
70. Kobirumaki-Shimozawa F, et al. Cardiac thin filament regulation and the Frank-Starling mechanism. *J Physiol Sci*. 2014;64:221-32.

71. Cohn JN, et al. Plasma norepinephrine as a guide to prognosis in patients with chronic congestive heart failure. *N Engl J Med*. 1984;311:819-23.
72. Kajstura J, et al. Angiotensin II induces apoptosis of adult ventricular myocytes in vitro. *J Mol Cell Cardiol*. 1997;29:859-70.
73. Cheung BM and Kumana CR. Natriuretic peptides--relevance in cardiovascular disease. *JAMA*. 1998;280:1983-4.
74. Lefer AM, et al. Mechanism of the cardioprotective effect of transforming growth factor beta 1 in feline myocardial ischemia and reperfusion. *Proc Natl Acad Sci U S A*. 1993;90:1018-22.
75. Li TS, et al. Regeneration of infarcted myocardium by intramyocardial implantation of ex vivo transforming growth factor-beta-preprogrammed bone marrow stem cells. *Circulation*. 2005;111:2438-45.
76. Wang Z, et al. bFGF inhibits ER stress induced by ischemic oxidative injury via activation of the PI3K/Akt and ERK1/2 pathways. *Toxicol Lett*. 2012;212:137-46.
77. Virag JA, et al. Fibroblast growth factor-2 regulates myocardial infarct repair: effects on cell proliferation, scar contraction, and ventricular function. *Am J Pathol*. 2007;171:1431-40.
78. Nakamura T, et al. Myocardial protection from ischemia/reperfusion injury by endogenous and exogenous HGF. *J Clin Invest*. 2000;106:1511-9.
79. Li Q, et al. Overexpression of insulin-like growth factor-1 in mice protects from myocyte death after infarction, attenuating ventricular dilation, wall stress, and cardiac hypertrophy. *J Clin Invest*. 1997;100:1991-9.
80. Saxena A, et al. Stromal cell-derived factor-1alpha is cardioprotective after myocardial infarction. *Circulation*. 2008;117:2224-31.
81. Petretta M, et al. NT-proBNP, IGF-I and survival in patients with chronic heart failure. *Growth Horm IGF Res*. 2007;17:288-96.
82. O'Gara PT, et al. 2013 ACCF/AHA guideline for the management of ST-elevation myocardial infarction: executive summary: a report of the American College of Cardiology Foundation/American Heart Association Task Force on Practice Guidelines: developed in collaboration with the American College of Emergency Physicians and Society for Cardiovascular Angiography and Interventions. *Catheter Cardiovasc Interv*. 2013;82:E1-27.
83. An international randomized trial comparing four thrombolytic strategies for acute myocardial infarction. The GUSTO investigators. *N Engl J Med*. 1993;329:673-82.

84. Johansen H, et al. Thirty-day in-hospital revascularization and mortality rates after acute myocardial infarction in seven Canadian provinces. *Can J Cardiol*. 2010;26:e243-8.
85. O'Gara PT, et al. 2013 ACCF/AHA guideline for the management of ST-elevation myocardial infarction: executive summary: a report of the American College of Cardiology Foundation/American Heart Association Task Force on Practice Guidelines. *Circulation*. 2013;127:529-55.
86. Effects of enalapril on mortality in severe congestive heart failure. Results of the Cooperative North Scandinavian Enalapril Survival Study (CONSENSUS). The CONSENSUS Trial Study Group. *N Engl J Med*. 1987;316:1429-35.
87. Bristow MR, et al. Carvedilol produces dose-related improvements in left ventricular function and survival in subjects with chronic heart failure. MOCHA Investigators. *Circulation*. 1996;94:2807-16.
88. Pitt B, et al. The effect of spironolactone on morbidity and mortality in patients with severe heart failure. Randomized Aldactone Evaluation Study Investigators. *N Engl J Med*. 1999;341:709-17.
89. Polanczyk CA, et al. Ten-year trends in hospital care for congestive heart failure: improved outcomes and increased use of resources. *Arch Intern Med*. 2000;160:325-32.
90. Roger VL, et al. Trends in heart failure incidence and survival in a community-based population. *JAMA*. 2004;292:344-50.
91. Christia P and Frangogiannis NG. Targeting inflammatory pathways in myocardial infarction. *Eur J Clin Invest*. 2013.
92. Engel FB, et al. FGF1/p38 MAP kinase inhibitor therapy induces cardiomyocyte mitosis, reduces scarring, and rescues function after myocardial infarction. *Proc Natl Acad Sci U S A*. 2006;103:15546-51.
93. Ptaszek LM, et al. Towards regenerative therapy for cardiac disease. *Lancet*. 2012;379:933-42.
94. Loffredo FS, et al. Bone marrow-derived cell therapy stimulates endogenous cardiomyocyte progenitors and promotes cardiac repair. *Cell Stem Cell*. 2011;8:389-98.
95. Murry CE, et al. Haematopoietic stem cells do not transdifferentiate into cardiac myocytes in myocardial infarcts. *Nature*. 2004;428:664-8.
96. Kurdi M and Booz GW. G-CSF-based stem cell therapy for the heart-unresolved issues part A: paracrine actions, mobilization, and delivery. *Congest Heart Fail*. 2007;13:221-7.

97. Waltenberger J. Modulation of growth factor action: implications for the treatment of cardiovascular diseases. *Circulation*. 1997;96:4083-94.
98. Cochain C, et al. Angiogenesis in the infarcted myocardium. *Antioxid Redox Signal*. 2013;18:1100-13.
99. Soonpaa MH and Field LJ. Assessment of cardiomyocyte DNA synthesis in normal and injured adult mouse hearts. *Am J Physiol*. 1997;272:H220-6.
100. D'Uva G, et al. ERBB2 triggers mammalian heart regeneration by promoting cardiomyocyte dedifferentiation and proliferation. *Nat Cell Biol*. 2015;17:627-38.
101. Bergmann O, et al. Evidence for cardiomyocyte renewal in humans. *Science*. 2009;324:98-102.
102. Tallini YN, et al. c-kit expression identifies cardiovascular precursors in the neonatal heart. *Proc Natl Acad Sci U S A*. 2009;106:1808-13.
103. Dawn B, et al. Cardiac stem cells delivered intravascularly traverse the vessel barrier, regenerate infarcted myocardium, and improve cardiac function. *Proc Natl Acad Sci U S A*. 2005;102:3766-71.
104. Mollmann H, et al. Stem cells in myocardial infarction: from bench to bedside. *Heart*. 2009;95:508-14.
105. Garbern JC, et al. Model systems for cardiovascular regenerative biology. *Cold Spring Harb Perspect Med*. 2013;3:a014019.
106. Feng Q, et al. Elevation of an endogenous inhibitor of nitric oxide synthesis in experimental congestive heart failure. *Cardiovasc Res*. 1998;37:667-75.
107. van Kats JP, et al. Angiotensin-converting enzyme inhibition and angiotensin II type 1 receptor blockade prevent cardiac remodeling in pigs after myocardial infarction: role of tissue angiotensin II. *Circulation*. 2000;102:1556-63.
108. Johns TN and Olson BJ. Experimental myocardial infarction. I. A method of coronary occlusion in small animals. *Ann Surg*. 1954;140:675-82.
109. Jopling C, et al. Zebrafish heart regeneration occurs by cardiomyocyte dedifferentiation and proliferation. *Nature*. 2010;464:606-9.
110. Porrello ER, et al. Transient regenerative potential of the neonatal mouse heart. *Science*. 2011;331:1078-80.
111. Haubner BJ, et al. Complete cardiac regeneration in a mouse model of myocardial infarction. *Aging (Albany NY)*. 2012;4:966-77.

112. Li F, et al. Rapid transition of cardiac myocytes from hyperplasia to hypertrophy during postnatal development. *J Mol Cell Cardiol.* 1996;28:1737-46.
113. Hanahan D and Weinberg RA. Hallmarks of cancer: the next generation. *Cell.* 2011;144:646-74.
114. Aurora AB, et al. Macrophages are required for neonatal heart regeneration. *J Clin Invest.* 2014;124:1382-92.
115. Jesty SA, et al. c-kit⁺ precursors support postinfarction myogenesis in the neonatal, but not adult, heart. *Proc Natl Acad Sci U S A.* 2012;109:13380-5.
116. Kikuchi K, et al. tcf21⁺ epicardial cells adopt non-myocardial fates during zebrafish heart development and regeneration. *Development.* 2011;138:2895-902.
117. Smart N, et al. Epicardial progenitor cells in cardiac regeneration and neovascularisation. *Vascul Pharmacol.* 2013;58:164-73.
118. Zhou B, et al. Adult mouse epicardium modulates myocardial injury by secreting paracrine factors. *J Clin Invest.* 2011;121:1894-904.
119. Chen T, et al. Epicardial induction of fetal cardiomyocyte proliferation via a retinoic acid-inducible trophic factor. *Dev Biol.* 2002;250:198-207.
120. Vicente-Steijn R, et al. Regional differences in WT-1 and Tcf21 expression during ventricular development: implications for myocardial compaction. *PLoS One.* 2015;10:e0136025.
121. von Gise A and Pu WT. Endocardial and epicardial epithelial to mesenchymal transitions in heart development and disease. *Circ Res.* 2012;110:1628-45.
122. Sadoshima J, et al. Molecular characterization of the stretch-induced adaptation of cultured cardiac cells. An in vitro model of load-induced cardiac hypertrophy. *J Biol Chem.* 1992;267:10551-60.
123. Yao HC, et al. Effect of basic fibroblast growth factor on the myocardial expression of hypoxia-inducible factor-1 α and vascular endothelial growth factor following acute myocardial infarction. *Heart Lung Circ.* 2013;22:946-951.
124. Kalluri R and Neilson EG. Epithelial-mesenchymal transition and its implications for fibrosis. *J Clin Invest.* 2003;112:1776-84.
125. Lamouille S, et al. Molecular mechanisms of epithelial-mesenchymal transition. *Nat Rev Mol Cell Biol.* 2014;15:178-96.
126. Moore AW, et al. YAC complementation shows a requirement for Wt1 in the development of epicardium, adrenal gland and throughout nephrogenesis. *Development.* 1999;126:1845-57.

127. Vinals F and Pouyssegur J. Transforming growth factor beta1 (TGF-beta1) promotes endothelial cell survival during in vitro angiogenesis via an autocrine mechanism implicating TGF-alpha signaling. *Mol Cell Biol.* 2001;21:7218-30.
128. Smith CL, et al. Epicardial-derived cell epithelial-to-mesenchymal transition and fate specification require PDGF receptor signaling. *Circ Res.* 2011;108:e15-26.
129. Langley RR, et al. Activation of the platelet-derived growth factor-receptor enhances survival of murine bone endothelial cells. *Cancer Res.* 2004;64:3727-30.
130. Strutz F, et al. Role of basic fibroblast growth factor-2 in epithelial-mesenchymal transformation. *Kidney Int.* 2002;61:1714-28.
131. Karsan A, et al. Fibroblast growth factor-2 inhibits endothelial cell apoptosis by Bcl-2-dependent and independent mechanisms. *Am J Pathol.* 1997;151:1775-84.
132. O'Connor DS, et al. Control of apoptosis during angiogenesis by survivin expression in endothelial cells. *Am J Pathol.* 2000;156:393-8.
133. Xiang FL, et al. Cardiac-specific overexpression of human stem cell factor promotes epicardial activation and arteriogenesis after myocardial infarction. *Circ Heart Fail.* 2014;7:831-42.
134. Carmona R, et al. Localization of the Wilm's tumour protein WT1 in avian embryos. *Cell Tissue Res.* 2001;303:173-86.
135. Rauscher FJ, 3rd. The WT1 Wilms tumor gene product: a developmentally regulated transcription factor in the kidney that functions as a tumor suppressor. *FASEB J.* 1993;7:896-903.
136. Martinez-Estrada OM, et al. Wt1 is required for cardiovascular progenitor cell formation through transcriptional control of Snail and E-cadherin. *Nat Genet.* 2010;42:89-93.
137. Wagner KD, et al. The Wilms' tumor suppressor Wt1 is expressed in the coronary vasculature after myocardial infarction. *FASEB J.* 2002;16:1117-9.
138. Koefoed K, et al. Cilia and coordination of signaling networks during heart development. *Organogenesis.* 2014;10:108-25.
139. Davenport JR and Yoder BK. An incredible decade for the primary cilium: a look at a once-forgotten organelle. *Am J Physiol Renal Physiol.* 2005;289:F1159-69.
140. Delling M, et al. Primary cilia are not calcium-responsive mechanosensors. *Nature.* 2016;531:656-60.

141. Pan J and Snell W. The primary cilium: keeper of the key to cell division. *Cell*. 2007;129:1255-7.
142. Boisvieux-Ulrich E, et al. The orientation of ciliary basal bodies in quail oviduct is related to the ciliary beating cycle commencement. *Biol Cell*. 1985;55:147-50.
143. Szymanska K and Johnson CA. The transition zone: an essential functional compartment of cilia. *Cilia*. 2012;1:10.
144. Kobayashi T and Dynlacht BD. Regulating the transition from centriole to basal body. *J Cell Biol*. 2011;193:435-44.
145. Kovacs JJ, et al. Beta-arrestin-mediated localization of smoothened to the primary cilium. *Science*. 2008;320:1777-81.
146. Berbari NF, et al. Identification of ciliary localization sequences within the third intracellular loop of G protein-coupled receptors. *Mol Biol Cell*. 2008;19:1540-7.
147. Kozminski KG, et al. A motility in the eukaryotic flagellum unrelated to flagellar beating. *Proc Natl Acad Sci U S A*. 1993;90:5519-23.
148. Snow JJ, et al. Two anterograde intraflagellar transport motors cooperate to build sensory cilia on *C. elegans* neurons. *Nat Cell Biol*. 2004;6:1109-13.
149. Schafer JC, et al. XB1-1 encodes a dynein light intermediate chain required for retrograde intraflagellar transport and cilia assembly in *Caenorhabditis elegans*. *Mol Biol Cell*. 2003;14:2057-70.
150. Cole DG, et al. *Chlamydomonas* kinesin-II-dependent intraflagellar transport (IFT): IFT particles contain proteins required for ciliary assembly in *Caenorhabditis elegans* sensory neurons. *J Cell Biol*. 1998;141:993-1008.
151. Pazour GJ, et al. *Chlamydomonas* IFT88 and its mouse homologue, polycystic kidney disease gene *tg737*, are required for assembly of cilia and flagella. *J Cell Biol*. 2000;151:709-18.
152. Christensen ST, et al. Sensory cilia and integration of signal transduction in human health and disease. *Traffic*. 2007;8:97-109.
153. Taulman PD, et al. Polaris, a protein involved in left-right axis patterning, localizes to basal bodies and cilia. *Mol Biol Cell*. 2001;12:589-99.
154. Murcia NS, et al. The Oak Ridge Polycystic Kidney (*orpk*) disease gene is required for left-right axis determination. *Development*. 2000;127:2347-55.
155. Huangfu D, et al. Hedgehog signalling in the mouse requires intraflagellar transport proteins. *Nature*. 2003;426:83-7.

156. Schneider L, et al. PDGFR α signaling is regulated through the primary cilium in fibroblasts. *Curr Biol*. 2005;15:1861-6.
157. Lancaster MA, et al. Subcellular spatial regulation of canonical Wnt signalling at the primary cilium. *Nat Cell Biol*. 2011;13:700-7.
158. Hirokawa N, et al. Nodal flow and the generation of left-right asymmetry. *Cell*. 2006;125:33-45.
159. Carpenter D, et al. Characterization of two patched receptors for the vertebrate hedgehog protein family. *Proc Natl Acad Sci U S A*. 1998;95:13630-4.
160. Gianakopoulos PJ and Skerjanc IS. Hedgehog signaling induces cardiomyogenesis in P19 cells. *J Biol Chem*. 2005;280:21022-8.
161. Clement CA, et al. The primary cilium coordinates early cardiogenesis and hedgehog signaling in cardiomyocyte differentiation. *J Cell Sci*. 2009;122:3070-82.
162. Haycraft CJ, et al. Gli2 and Gli3 localize to cilia and require the intraflagellar transport protein polaris for processing and function. *PLoS Genet*. 2005;1:e53.
163. Rohatgi R, et al. Patched1 regulates hedgehog signaling at the primary cilium. *Science*. 2007;317:372-6.
164. Caspary T, et al. The graded response to Sonic Hedgehog depends on cilia architecture. *Dev Cell*. 2007;12:767-78.
165. Hassounah NB, et al. Molecular pathways: the role of primary cilia in cancer progression and therapeutics with a focus on Hedgehog signaling. *Clin Cancer Res*. 2012;18:2429-35.
166. Rimkus TK, et al. Targeting the sonic hedgehog signaling pathway: Review of smoothed and GLI inhibitors. *Cancers (Basel)*. 2016;8.
167. Gao C and Chen YG. Dishevelled: The hub of Wnt signaling. *Cell Signal*. 2010;22:717-27.
168. Gitler AD, et al. Molecular markers of cardiac endocardial cushion development. *Dev Dyn*. 2003;228:643-50.
169. Corbit KC, et al. Kif3a constrains β -catenin-dependent Wnt signalling through dual ciliary and non-ciliary mechanisms. *Nat Cell Biol*. 2008;10:70-6.
170. Yang X, et al. Wnt signaling through Snail1 and Zeb1 regulates bone metastasis in lung cancer. *Am J Cancer Res*. 2015;5:748-55.

171. Niehrs C. The complex world of WNT receptor signalling. *Nat Rev Mol Cell Biol.* 2012;13:767-79.
172. Cao Y, et al. Intraflagellar transport proteins are essential for cilia formation and for planar cell polarity. *J Am Soc Nephrol.* 2010;21:1326-33.
173. Jones C, et al. Ciliary proteins link basal body polarization to planar cell polarity regulation. *Nat Genet.* 2008;40:69-77.
174. Borovina A, et al. Vangl2 directs the posterior tilting and asymmetric localization of motile primary cilia. *Nat Cell Biol.* 2010;12:407-12.
175. May-Simera HL, et al. Bbs8, together with the planar cell polarity protein Vangl2, is required to establish left-right asymmetry in zebrafish. *Dev Biol.* 2010;345:215-25.
176. Oishi I, et al. Regulation of primary cilia formation and left-right patterning in zebrafish by a noncanonical Wnt signaling mediator, duboraya. *Nat Genet.* 2006;38:1316-22.
177. Tallquist M and Kazlauskas A. PDGF signaling in cells and mice. *Cytokine Growth Factor Rev.* 2004;15:205-13.
178. Andrae J, et al. Role of platelet-derived growth factors in physiology and medicine. *Genes Dev.* 2008;22:1276-312.
179. Schneider L, et al. Directional cell migration and chemotaxis in wound healing response to PDGF-AA are coordinated by the primary cilium in fibroblasts. *Cell Physiol Biochem.* 2010;25:279-92.
180. Jechlinger M, et al. Autocrine PDGFR signaling promotes mammary cancer metastasis. *J Clin Invest.* 2006;116:1561-70.
181. Van Den Akker NM, et al. Platelet-derived growth factors in the developing avian heart and maturing coronary vasculature. *Dev Dyn.* 2005;233:1579-88.
182. Nielsen BS, et al. PDGFR β and oncogenic mutant PDGFR α D842V promote disassembly of primary cilia through a PLC γ - and AURKA-dependent mechanism. *J Cell Sci.* 2015;128:3543-9.
183. Menzl I, et al. Loss of primary cilia occurs early in breast cancer development. *Cilia.* 2014;3:7.
184. Hassounah NB, et al. Primary cilia are lost in preinvasive and invasive prostate cancer. *PLoS One.* 2013;8:e68521.
185. Plotnikova OV, et al. Cell cycle-dependent ciliogenesis and cancer. *Cancer Res.* 2008;68:2058-61.

186. Fliegauf M, et al. When cilia go bad: cilia defects and ciliopathies. *Nat Rev Mol Cell Biol.* 2007;8:880-93.
187. Afzelius BA. Situs inversus and ciliary abnormalities. What is the connection? *Int J Dev Biol.* 1995;39:839-44.
188. Li Y, et al. Global genetic analysis in mice unveils central role for cilia in congenital heart disease. *Nature.* 2015;521:520-4.
189. Elbedour K, et al. Cardiac abnormalities in the Bardet-Biedl syndrome: echocardiographic studies of 22 patients. *Am J Med Genet.* 1994;52:164-9.
190. Neugebauer JM, et al. FGF signalling during embryo development regulates cilia length in diverse epithelia. *Nature.* 2009;458:651-4.
191. Van der Heiden K, et al. Monocilia on chicken embryonic endocardium in low shear stress areas. *Dev Dyn.* 2006;235:19-28.
192. Rozycki M, et al. The fate of the primary cilium during myofibroblast transition. *Mol Biol Cell.* 2014;25:643-57.
193. Egorova AD, et al. Lack of primary cilia primes shear-induced endothelial-to-mesenchymal transition. *Circ Res.* 2011;108:1093-101.
194. Djebali S, et al. Landscape of transcription in human cells. *Nature.* 2012;489:101-8.
195. Uchida S and Dimmeler S. Long noncoding RNAs in cardiovascular diseases. *Circ Res.* 2015;116:737-50.
196. Samanta S, et al. MicroRNA: A new therapeutic strategy for cardiovascular diseases. *Trends Cardiovasc Med.* 2016;26:407-19.
197. Mercer TR, et al. Long non-coding RNAs: insights into functions. *Nat Rev Genet.* 2009;10:155-9.
198. Li Z and Rana TM. Therapeutic targeting of microRNAs: current status and future challenges. *Nat Rev Drug Discov.* 2014;13:622-38.
199. Sato A, et al. Polymer brush-stabilized polyplex for a siRNA carrier with long circulatory half-life. *J Control Release.* 2007;122:209-16.
200. Boudreau RL, et al. Minimizing variables among hairpin-based RNAi vectors reveals the potency of shRNAs. *RNA.* 2008;14:1834-44.
201. Poller W, et al. Cardiac-targeted delivery of regulatory RNA molecules and genes for the treatment of heart failure. *Cardiovasc Res.* 2010;86:353-64.

202. Imanishi T, et al. Integrative annotation of 21,037 human genes validated by full-length cDNA clones. *PLoS Biol.* 2004;2:e162.
203. Frith MC, et al. The amazing complexity of the human transcriptome. *Eur J Hum Genet.* 2005;13:894-7.
204. Plath K, et al. Role of histone H3 lysine 27 methylation in X inactivation. *Science.* 2003;300:131-5.
205. McHugh CA, et al. The Xist lncRNA interacts directly with SHARP to silence transcription through HDAC3. *Nature.* 2015;521:232-6.
206. Engreitz JM, et al. Long non-coding RNAs: spatial amplifiers that control nuclear structure and gene expression. *Nat Rev Mol Cell Biol.* 2016;17:756-770.
207. Geisler S and Collier J. RNA in unexpected places: long non-coding RNA functions in diverse cellular contexts. *Nat Rev Mol Cell Biol.* 2013;14:699-712.
208. Martianov I, et al. Repression of the human dihydrofolate reductase gene by a non-coding interfering transcript. *Nature.* 2007;445:666-70.
209. Willingham AT, et al. A strategy for probing the function of noncoding RNAs finds a repressor of NFAT. *Science.* 2005;309:1570-3.
210. Huang M, et al. Short hairpin RNA interference therapy for ischemic heart disease. *Circulation.* 2008;118:S226-33.
211. Suckau L, et al. Long-term cardiac-targeted RNA interference for the treatment of heart failure restores cardiac function and reduces pathological hypertrophy. *Circulation.* 2009;119:1241-52.
212. Guzman-Aranguez A, et al. Small-interfering RNAs (siRNAs) as a promising tool for ocular therapy. *Br J Pharmacol.* 2013;170:730-47.
213. Schulte C and Zeller T. microRNA-based diagnostics and therapy in cardiovascular disease-Summing up the facts. *Cardiovasc Diagn Ther.* 2015;5:17-36.
214. Ounzain S, et al. Genome-wide profiling of the cardiac transcriptome after myocardial infarction identifies novel heart-specific long non-coding RNAs. *Eur Heart J.* 2015;36:353-68a.
215. Han Y, et al. Downregulation of long non-coding RNA H19 promotes P19CL6 cells proliferation and inhibits apoptosis during late-stage cardiac differentiation via miR-19b-modulated Sox6. *Cell Biosci.* 2016;6:58.

216. Ounzain S, et al. CARMEN, a human super enhancer-associated long noncoding RNA controlling cardiac specification, differentiation and homeostasis. *J Mol Cell Cardiol.* 2015;89:98-112.
217. He C, et al. Systematic Characterization of Long Noncoding RNAs Reveals the Contrasting Coordination of Cis- and Trans-Molecular Regulation in Human Fetal and Adult Hearts. *Circ Cardiovasc Genet.* 2016;9:110-8.
218. Yang KC, et al. Deep RNA sequencing reveals dynamic regulation of myocardial noncoding RNAs in failing human heart and remodeling with mechanical circulatory support. *Circulation.* 2014;129:1009-21.
219. Kumarswamy R, et al. Circulating long noncoding RNA, LIPCAR, predicts survival in patients with heart failure. *Circ Res.* 2014;114:1569-75.
220. Ishii N, et al. Identification of a novel non-coding RNA, MIAT, that confers risk of myocardial infarction. *J Hum Genet.* 2006;51:1087-99.
221. Wang K, et al. The long noncoding RNA CHRF regulates cardiac hypertrophy by targeting miR-489. *Circ Res.* 2014;114:1377-88.
222. Wang K, et al. CARL lncRNA inhibits anoxia-induced mitochondrial fission and apoptosis in cardiomyocytes by impairing miR-539-dependent PHB2 downregulation. *Nat Commun.* 2014;5:3596.
223. Viereck J, et al. Long noncoding RNA Chast promotes cardiac remodeling. *Sci Transl Med.* 2016;8:326ra22.
224. Yang L, et al. ncRNA- and Pc2 methylation-dependent gene relocation between nuclear structures mediates gene activation programs. *Cell.* 2011;147:773-88.
225. Xiang J, et al. Silencing of long non-coding rna MALAT1 promotes apoptosis of glioma cells. *J Korean Med Sci.* 2016;31:688-94.
226. Michalik KM, et al. Long noncoding RNA MALAT1 regulates endothelial cell function and vessel growth. *Circ Res.* 2014;114:1389-97.
227. Ji P, et al. MALAT-1, a novel noncoding RNA, and thymosin β 4 predict metastasis and survival in early-stage non-small cell lung cancer. *Oncogene.* 2003;22:8031-41.
228. Zhang B, et al. The lncRNA Malat1 is dispensable for mouse development but its transcription plays a cis-regulatory role in the adult. *Cell Rep.* 2012;2:111-23.
229. Tripathi V, et al. The nuclear-retained noncoding RNA MALAT1 regulates alternative splicing by modulating SR splicing factor phosphorylation. *Mol Cell.* 2010;39:925-38.

230. Eissmann M, et al. Loss of the abundant nuclear non-coding RNA MALAT1 is compatible with life and development. *RNA Biol.* 2012;9:1076-87.
231. Gutschner T, et al. The noncoding RNA MALAT1 is a critical regulator of the metastasis phenotype of lung cancer cells. *Cancer Res.* 2013;73:1180-9.
232. Gutschner T, et al. MALAT1 -- a paradigm for long noncoding RNA function in cancer. *J Mol Med (Berl).* 2013;91:791-801.
233. Zhou X, et al. Long non coding rna MALAT1 promotes tumor growth and metastasis by inducing epithelial-mesenchymal transition in oral squamous cell carcinoma. *Sci Rep.* 2015;5:15972.
234. Yang S, et al. Long non-coding rna malat1 mediates transforming growth factor beta1-induced epithelial-mesenchymal transition of retinal pigment epithelial cells. *PLoS One.* 2016;11:e0152687.
235. Tee AE, et al. The long noncoding RNA MALAT1 promotes tumor-driven angiogenesis by up-regulating pro-angiogenic gene expression. *Oncotarget.* 2016;7:8663-75.
236. Lelli A, et al. Induction of long noncoding RNA MALAT1 in hypoxic mice. *Hypoxia.* 2015;3:45-52.
237. Liu JY, et al. Pathogenic role of lncRNA-MALAT1 in endothelial cell dysfunction in diabetes mellitus. *Cell Death Dis.* 2014;5:e1506.
238. Brock M, et al. Analysis of hypoxia-induced noncoding RNAs reveals metastasis-associated lung adenocarcinoma transcript 1 as an important regulator of vascular smooth muscle cell proliferation. *Exp Biol Med (Maywood).* 2017;242:487-496.
239. Tripathi V, et al. Long noncoding RNA MALAT1 controls cell cycle progression by regulating the expression of oncogenic transcription factor B-MYB. *PLoS Genet.* 2013;9:e1003368.
240. Guo F, et al. Inhibition of metastasis-associated lung adenocarcinoma transcript 1 in CaSki human cervical cancer cells suppresses cell proliferation and invasion. *Acta Biochim Biophys Sin (Shanghai).* 2010;42:224-9.
241. Schmidt LH, et al. Prognostic impact of Bcl-2 depends on tumor histology and expression of MALAT-1 lncRNA in non-small-cell lung cancer. *J Thorac Oncol.* 2014;9:1294-304.
242. Wang X, et al. Silencing of long noncoding RNA MALAT1 by miR-101 and miR-217 inhibits proliferation, migration, and invasion of esophageal squamous cell carcinoma cells. *J Biol Chem.* 2015;290:3925-35.

243. Tang Y, et al. The lncRNA MALAT1 protects the endothelium against ox-LDL-induced dysfunction via upregulating the expression of the miR-22-3p target genes CXCR2 and AKT. *FEBS Lett.* 2015;589:3189-96.
244. Zhang X, et al. Long noncoding rna malat1 regulates cerebrovascular pathologies in ischemic stroke. *J Neurosci.* 2017;37:1797-1806.
245. Vausort M, et al. Long noncoding RNAs in patients with acute myocardial infarction. *Circ Res.* 2014;115:668-77.
246. Choi KM, et al. Transmural extent of acute myocardial infarction predicts long-term improvement in contractile function. *Circulation.* 2001;104:1101-7.
247. Yaoita H, et al. Attenuation of ischemia/reperfusion injury in rats by a caspase inhibitor. *Circulation.* 1998;97:276-81.
248. Kovacs P, et al. Non-specific caspase inhibition reduces infarct size and improves post-ischaemic recovery in isolated ischaemic/reperfused rat hearts. *Naunyn Schmiedebergs Arch Pharmacol.* 2001;364:501-7.
249. MacKenzie SH, et al. The potential for caspases in drug discovery. *Curr Opin Drug Discov Devel.* 2010;13:568-76.

Chapter 2

Complete cardiac regeneration occurs in neonatal mice after myocardial infarction

A version of this chapter has been published in *Journal of Visualized Experiments* 2016;111:e54100. <http://www.jove.com/video/5410>

Blom JN, Lu X, Arnold P, Feng Q.

“Myocardial infarction in neonatal mice, a model of cardiac regeneration”

2 Chapter 2

2.1 Chapter Summary

Myocardial infarction induced by coronary artery ligation has been used in many animal models as a tool to study the mechanisms of cardiac repair, and to define new targets for therapeutics. For decades, models of complete heart regeneration existed in amphibians and fish, but a mammalian counterpart was not available. The recent discovery of a postnatal window during which mice possess regenerative capabilities has led to the establishment of a mammalian model of cardiac regeneration. A surgical model of mammalian cardiac regeneration in the neonatal mouse is presented herein. Briefly, postnatal day 1 (P1) mice were anesthetized by isoflurane and placed on an ice pad to induce hypothermia. After the chest was opened, and the left anterior descending coronary artery (LAD) was visualized, a suture was placed around the LAD to inflict myocardial ischemia in the left ventricle. The surgical procedure took 10-15 minutes. Visualization of the coronary artery is crucial for accurate suture placement and reproducibility. This protocol can be used to as a tool to elucidate mechanisms of mammalian cardiac regeneration after myocardial infarction. Using this model, the role of *Wt1* and *Malat1* in cardiac regeneration after myocardial infarction was investigated with *Wt1*^{CreER} knock-in (or *Wt1*^{+/-}) and *Malat1*^{-/-} mice. Our data indicate that indeed the neonatal mouse possesses a robust capacity for cardiac regeneration and this was not affected by changes in gene expression of *Wt1* or *Malat1*.

2.2 Introduction

Myocardial infarction (MI) is a leading cause of death worldwide, and remains responsible for about one third of heart failure cases.¹ While the advent of percutaneous intervention and continuous optimization of the use of thrombolytics has increased reperfusion following MI, cardiomyocyte death and loss of contractile myocardium nevertheless occurs. There also remain large numbers of “no-option” patients who are not candidates for or do not see benefit from these interventions. These patients continue to experience disabling ischemia leading to scar formation and deleterious ventricular remodeling as a mechanism of infarct healing. This process ultimately results in heart failure, for which prognosis remains poor despite best available pharmacologic management with angiotensin-converting enzyme inhibitors (ACEi) and beta blockers. Unfortunately, the one-year mortality rate for patients with severely impaired left ventricular function still remains as high as 26%.² Heart transplant is the final treatment option for patients with heart failure. However, the limited donor pool for heart transplantation does not make this a viable option for most patients. Thus, the discovery of novel therapeutic agents to restore the damaged myocardium remains paramount to solving the cardiac disease problem. Reliable animal models of cardiac injury are therefore required as a critical component of this process.

Traditional dogma has dictated that adult cardiomyocytes are post-mitotic, terminally differentiated cells, incapable of dividing or de-differentiating to replace the damaged myocardium.³ As such, an adult mammalian heart could never completely recover from injury, and lost cardiomyocytes would be replaced with fibrous tissue. Thus, research has focused primarily on therapeutic agents to minimize infarct expansion

and reduce scar formation. More recently however, a paradigm shift has occurred from promoting cardiac healing to focusing on the potential for cardiac regeneration.⁴

2.2.1 Models of cardiac repair

Until recently, *in vivo* study of cardiac regeneration was restricted to non-vertebrate models, such as those in urodele amphibians and teleost fish.⁵⁻⁷ However, the discovery of the capacity for cardiac regeneration in the neonatal mouse has led to the development of two surgical models of mammalian cardiac regeneration: resection of the cardiac apex and coronary artery occlusion to induce myocardial infarction.^{8, 9} In 2011, a mouse apex resection model was used to demonstrate that complete cardiac regeneration is possible at postnatal day 1 (P1). However, this capacity declines rapidly after the initial neonatal period. The mammalian heart loses its regenerative potential shortly after birth at P7 as progenitor cell numbers decline, and cardiomyocytes become binucleated, lose their proliferative competency, and permanently exit the cell cycle.^{10, 11} Understanding the fundamental differences between the neonatal and adult mammalian heart may lead to novel insights into cardiac regeneration.

While apex resection indeed offers insight into re-growth of contractile tissue, the model does not simulate typical human cardiac injury, and thus does not lend itself as well to extrapolation for the development of therapeutics. The coronary artery occlusion model, however, more directly simulates the pathophysiologic aspects of MI pathology, and thus may provide more useful insights into mechanisms that may be applicable to therapeutic advancement for human use.

Surgical coronary ligation has been used as a useful experimental technique in many animal models.¹²⁻¹⁴ In the adult coronary artery ligation model, animals are anesthetized and intubated to allow opening of the chest cavity while maintaining respiration. The heart continues to beat regularly, permitting visualization of the coronary vasculature and allowing for accurate suture placement. Furthermore, the heart remains pink as perfusion continues, and after ligation the ischemic myocardium appears pale, indicating successful coronary artery ligation. The protocol described for neonatal mice, however, is less reliable as the coronary artery is not visualized and the surgeon must estimate where to place the suture.¹⁵ Although the general anatomy of the coronary vasculature is the same, individual animal variability in the direction and branching of the LAD exists.¹⁶ Thus, when “going in blind,” the artery could be easily missed. Other techniques such as echocardiography are then required to confirm successful induction of MI, and to ensure all surgeries result in a similar infarct size. Described here is an improvement on the recently published method where the position of the LAD can be established and thus the LAD may be ligated to reproducibly induce MI.

As described previously, this technique does not require endotracheal intubation or mechanical ventilation, as thoracotomy in a hypothermic state in the neonatal mouse does not result in lung collapse.¹⁵ However, in the method described previously, severe hypothermia must be induced to the point of both complete apnea and cessation of the cardiac rhythm. The major limitation of this approach is that the coronary artery is no longer perfused and the heart appears pale even before LAD ligation.¹⁵ In the approach described herein, coronary artery visualization is possible at a point of torpor before deep

hypothermia and cardiac rhythm cessation, with full recovery of the neonatal mouse after the surgery. This method offers a major advantage of 100% reproducibility.

2.2.2 Angiogenesis in the regenerating myocardium

The protocol described above can be used to as a tool to elucidate mechanisms of mammalian cardiac regeneration after myocardial infarction. Mechanisms which support tissue repair are similar across tissue types. These include reducing the magnitude of cell death upon tissue injury, polarizing the inflammatory response to a more M2 type pro-regenerative response, increasing cell proliferation to replace damaged tissue, recruiting resident and bone marrow stem cells, and supporting neovascularization in the wounded region.¹⁷ Several studies indicate that like regeneration in the zebrafish, cardiomyocyte proliferation is vital to the mammalian neonatal regenerative response. Specifically, fate mapping indicates that the majority of new cardiomyocytes come from pre-existing cardiomyocytes, and this can be altered by regulators of the ERBB2 and Hippo families which support dedifferentiation and proliferation.^{4, 8, 18} However, the ability of cardiomyocytes to replace damaged tissue is intimately linked with the formation of new supportive blood vessels. Indeed, numerous studies indicate that neovascularization is required for wound repair, and impaired angiogenesis results in delayed or defective wound healing.^{19, 20} While evidence from coronary corrosion casts indicates that a vascular response does restore perfusion during neonatal heart regeneration, the source of this regenerative vasculature is unknown.²¹

In lower vertebrates, such as the zebrafish, regeneration primarily occurs through cardiomyocyte proliferation. However, a crucial component of zebrafish regeneration is activation of the epicardium as it acts as a multipotent cardiac progenitor cell, both

providing a cellular source of the regenerated perivascular cells, and acting as a paracrine mediator of cell proliferation.²² During cardiac development, the coronary arteries arise from an epicardial cell source; epicardium derived cells (EPDCs) contribute to coronary vascular smooth muscle cells, perivascular fibroblasts, and potentially vascular endothelial cells.²³ Beyond direct cellular contributions, the epicardium is also a critical signaling source during cardiac formation, secreting retinoic acid (RA), fibroblast growth factor (FGF), and other pro-mitogenic and angiogenic paracrine signals.²⁴ The epicardium becomes quiescent in the adult mammal, but it re-adapts its embryonic phenotype following myocardial injury contributing to myocardial healing, albeit this contribution is not enough to support full regeneration.²⁵ As in the zebrafish, epicardial cells are activated post-injury in the neonatal mouse heart, evidenced by upregulation of embryonic epicardial gene expression.^{8,9}

2.2.3 Modulators of epithelial-to-mesenchymal transition

Wilm's tumor 1 (Wt1) is a transcription factor expressed in the epicardium during development.²⁶ Specifically, it marks EPDCs which undergo EMT during embryonic coronary artery formation. Wt1 knockout is embryonic lethal, partially due to impaired coronary plexus formation.²⁷ Interestingly, not only is Wt1 expressed in endothelial cells in development, it is also up-regulated in the infarct and peri-infarct area after MI.²⁸ Several of the major mediators of EMT are controlled by Wt1 including, Snail (*Snail*), E-cadherin (*Cdh1*), β -catenin (*Ctnnb1*), and RALDH2 (*Raldh2*).^{27, 29} Specifically, after MI Wt1 marks the activation of the epicardium and is expressed in the coronary vasculature.³⁰ It is thought that post-MI hypoxia triggers Wt1 expression and activates EMT and angiogenesis. The importance of Wt1 for angiogenesis has been confirmed in

matrigel plugs and aortic rings from *Wt1* knockout mice which displayed reduced sprouting capacity.³¹ To date however, the role of *Wt1* in the neonatal mouse cardiac regenerative response has not been elucidated.

Transcriptome analysis of human tissue indicates that long non-coding RNA (lncRNA) accounts for more than double the number of protein coding transcripts in the human transcriptome, and plays numerous diverse regulatory roles in transcription, translation, and post-translational processing.^{32, 33} Metastasis-associated lung adenocarcinoma transcript 1 (*MALAT1*; aka nuclear enriched abundant transcript 2, *NEAT2*) is a highly conserved lncRNA associated with poor progression, and metastasis of numerous cancers.³⁴ In fact, increasing levels of *MALAT1* are associated with worse prognosis.³⁵ Molecularly, *MALAT1* is suggested to promote EMT, owing to its ability to support Slug and β -catenin expression, and TGF- β -mediated mesenchymal change.^{36, 37} Downstream, *Malat1* also causes tumor angiogenesis and post-ischemic angiogenesis, as demonstrated in a hindlimb ischemia model.^{38, 39} The role of *Malat1* in myocardial angiogenesis has not been elucidated. Specifically, the role of *Malat1* in neonatal cardiac regeneration has never been studied.

In the zebrafish, disruption of epicardial signaling abates regeneration,⁴⁰ thus, we hypothesized that disruption of epicardial EMT in the neonatal mouse would diminish its regenerative capacity. Specifically, we hypothesized that a reproducible model of cardiac regeneration would be developed in neonates, and deficiency of *Wt1* and *Malat1* would attenuate murine neonatal cardiac regeneration.

2.3 Methods

2.3.1 Animals

2.3.1.1 Animal Care

Animals used in this study were handled in accordance with the guidelines of the Canadian Council on Animal Care, and study protocols were approved by the Animal Use Subcommittee at Western University, London, Canada.

2.3.1.2 Mouse Strains

Breeding pairs of C57BL/6 (wild type; WT) and CD-1 IG-S mice were purchased from Charles River. To investigate the role of *Wt1* in the cardiac regenerative response, a mouse heterozygous for *Wt1* expression was used to emulate *Wt1* knockdown. The $Wt1^{CreER}$ mouse was designed using a “knock-in” allele strategy, which abolishes *Wt1* homologous gene function. Homozygous *Wt1* deletion is embryonic lethal by E13.5 due to numerous developmental abnormalities, including those of the heart.²⁷ However, heterozygous $Wt1^{CreER}$ are viable, fertile and phenotypically normal.⁴¹ $Wt1^{CreER}$ mice were generated by crossing $Wt1^{CreER}$ males with WT females, to ensure heterozygosity. To investigate the role of *Malat1* in the cardiac regenerative response, a *Malat1* knockout mouse line ($Malat1^{-/-}$)⁴² was obtained from Dr. David L. Spector, Cold Spring Harbor Laboratory, New York. This mouse was generated via homologous recombination in ESCs, and shown to be both viable and fertile.⁴²

2.3.1.3 Genotyping

Genotyping was carried out to identify $Wt1^{CreER}$ positive and $Malat1^{-/-}$ by PCR using genomic DNA from tail biopsies. Primer sequences can be found in **Table 2.1**.

Table 2.1. Genotyping PCR primer sequences.

Gene	Forward	Reverse
<i>Wt1^{CreER}</i>	tgccacgaccaagtgacagc	ccaggttacggatatagttcatg
<i>Malat1-WT</i>	gggaggcaatggtctaactggacctcca	tcgcacacggcctggcggcaccgtcctgct
<i>Malat1^{-/-}</i>	gggaggcaatggtctaactggacctcca	cattcttcttctgggccttggcagtcagc

2.3.1.4 Foster Care of Neonates

After birthing was complete and pups were initially breast-fed by their mother for a few hours, they were placed in a different cage with a CD-1 foster mother. CD-1 mothers display a calmer phenotype with a strong fostering instinct, and have a lower tendency to cannibalize injured pups.¹⁵

2.3.2 Surgery

The following surgical protocol was used to reproducibly cause myocardial infarction (MI) in neonatal mice.

1. Anesthesia was induced by placing the pup in a sealed isoflurane chamber (approximately 500 μ l of 100% v/v isoflurane allowed to dissipate over 1300 cm^3 chamber). The mouse was kept in the chamber until cessation of movement (about 30 sec).
2. The mouse was removed from the isoflurane chamber and hypothermic anesthesia induced by placing mouse on wet ice.
3. To avoid frostbite, ice was placed inside a sterile surgical glove, the mouse was wrapped within the glove and the glove covered with ice OR the mouse was

wrapped in sterile wet gauze and placed on ice.

NOTE: Mice cool faster when contact with ice is over a larger surface area, and as such melted ice can shorten hypothermia induction time.

4. Anesthesia was confirmed by lack of movement response to toe and tail pinch.

NOTE: Cessation of provoked movement occurs at a body temperature between 15 °C and 8 °C. (Cooling time to this temperature approximately 1 minute). Complete apnea and asystole is **NOT** required for LAD ligation.

5. The ice bed was moved to the surgical area equipped with an operating microscope. The mouse pup remained on ice during the whole surgical procedure.

NOTE: The surgical area, gauze and surgical instruments were sterilized. The sterile field was maintained throughout the procedure, and single use, sterile surgical gloves were worn. Ophthalmic ointment is not required as mice are born with their eyes closed.⁴³

6. The mouse pup was placed in the right lateral decubitus position.
7. The chest was disinfected by gently wiping with betadine solution followed by an ethanol swab.

8. A skin incision was performed on the left chest along the mid-axillary line by cutting the skin between the xyphoid and left axilla a few millimeters below the left foreleg. Scissors were also used to cut through the underlying pectoral muscle layer.
9. A left thoracotomy was performed in the 4th intercostal space by separating the ribs and intercostal muscles with forceps.

NOTE: Neonatal ribs are very fragile and can be easily broken. To avoid this, ribs were gently separated by opening forceps along the intercostal muscle (rather than grasping ribs).

10. The left anterior descending coronary artery (LAD) was visualized emerging from the left auricle behind the pulmonary vein and descending beyond the great cardiac vein.

NOTE: In this early neonatal window, the thymus is often visualized and may cover part of the cardiac base. The LAD can be seen emerging beside the position of the thymus, depending on the angle of thoracic incision.

11. The LAD was ligated by passing a 11-0 nylon suture (0.007 mm diameter needle) below the artery through the mid ventricle below the left auricle (**Figure 2.1C**). Ischemia was confirmed with blanching of the myocardium below the suture site

(Figure 2.1G).

12. The thoracic incision was closed using 8-0 nylon sutures (0.15 mm diameter needle). Two sutures were used to close the ribs. Both rib sutures were placed before ligating to ensure the needle did not puncture the lungs when passing through the body cavity.
13. After closing the ribs, the mouse was removed from the ice bed. The mouse was kept within the surgical area and placed directly on the sterile surgical towel over a warm heating pad at 37 °C to begin warming.
14. Once on the sterile heated area, the muscle and skin layers were closed using 8-0 nylon sutures (0.15 mm diameter needle). One suture for the muscle layer and two sutures for the skin incision were used.

NOTE: Muscle and skin layers may be closed on a heating pad to reduce hypothermia exposure time. Mouse temperature begins to rise once placed on the heating pad, but remains sufficiently low enough for anesthesia maintenance during muscle and skin closure.

2.3.2.1 Surgical Recovery

1. Rapid warming on a warm heating pad was continued until return of spontaneous movement. Animals were not left unattended until they had regained sufficient consciousness to maintain sternal recumbency.
2. Betadine and blood were removed by gently wiping injury site with an ethanol swab.

3. After sufficient recovery from anesthesia, neonates were removed from the sterile surgical area, smeared with bedding from foster mother's cage, and returned to the foster mother. This helped prevent maternal rejection or cannibalization. Mice recovered from surgery with no apparent complications and were breast fed alongside their littermates with no observable difficulty.

NOTE: Pups were not returned to a cage with other animals until fully recovered. If an entire litter was not used, and littermates remained with the foster mother, recovered pups were placed in the middle of the litter. If performing more than one surgery, all surgeries required for an individual litter were completed before returning mice to their foster mother.

4. Behavior of foster mother toward the pup was observed every 10-15 minutes for 2-3 hours to ensure acceptance of the pup. If the mother displayed aggression towards the injured pup, the pup was removed and euthanized by isoflurane overdose (>5%; until cessation of breathing), followed by decapitation.

NOTE: Perioperative analgesia medications are not required as the centralized pain reflexes are not fully developed at this early age.¹⁵

5. Surgical instruments were wiped clean with water and then ethanol followed by sterilization in a bead sterilizer before the next procedure.

To study the role of *Wt1*, two entire *Wt1*^{CreER}/WT litters were subject to MI at P1, and neonates were genotyped for the Cre allele after the procedure (to ensure blinding to the surgeon). Mice from each group (4 Cre positive and 7 WT) were collected 21-days post-MI for tissue analysis. To investigate the role of *Malat1* in cardiac regeneration, three litters of *Malat1*^{-/-} and two litters of WT mice were subjected to CAL. Tissues from 12 *Malat1*^{-/-} and 12 WT mice were collected 21-days post-MI for analysis.

2.3.3 Measurement of Myocardial Infarct Size 4-6 hours Post-MI

To ensure induction of an infarction event, the following protocol was used to determine myocardial infarct size in 13 WT neonatal mice.

1. Pups were allowed to recover in the care of a CD-1 foster mother for a period of 4-6 hours. The pup was removed from the cage with the mother and euthanized by isoflurane overdose followed by decapitation with large scissors.
2. The heart was excised under a dissecting microscope, with care not to rip the myocardium.
 - i. The skin from the xyphoid process to the top of the thorax was cut.
 - ii. The abdominal wall was opened below the ribcage.
 - iii. The lower rib cage was grasped and cut through the ribs and musculature longitudinally along the left mid-axillary line from the diaphragm to the axilla.
 - iv. Scissors were held in the transverse plane and carefully cut through the diaphragm from the left to the right side. ** Scissors were placed below the level of the heart so as to avoid any damage to the apex.
 - v. The rib cage was grasped and cut on the right side of the ribs and the

musculature along the right mid-axillary line.

- vi. All vascular connections to heart were removed with scissors.
 - vii. The heart was removed from the chest cavity by grasping the base.
3. The heart was sectioned into three pieces using a surgical carbon steel razor blade. The first cut was made along the short-axis of the heart at the midpoint between the suture and the cardiac apex. The second cut was made at the level of the suture (**Figure 2.5A**).

NOTE: This left an apex section approximately 0.75 mm diameter, weighing 0.0018 g; a mid-base section approximately 1mm diameter, weighing 0.0065 g; and the base of the heart.

4. The heart sections were placed in 1% 2,3,5-triphenyltetrazolium chloride (TTC) at room temperature for 10-15 minutes. The specimen was carefully watched to avoid over-staining.
5. To increase contrast, stained heart slices were fixed with 4% paraformaldehyde overnight at 4 °C.
6. To calculate % infarct area, heart sections were photographed and infarct area measured on imaging software. The viable myocardium stains red while the infarct area is demarcated as white.⁴⁴

2.3.4 Measurement of Cardiac Function Post-MI

To ensure MI resulted in reduced cardiac function, the following protocol was used to assess cardiac function in 25 WT neonatal mice.

1. Pups were allowed to recover in the care of a CD-1 foster mother for a period of 24 – 48 hours. Anesthesia was induced by placing the pup in a sealed isoflurane chamber (approximately 5% isoflurane). The mouse was kept in the chamber until cessation of movement (about 30 seconds).
2. The pup was secured in the supine position on a heated dock (temperature 37 °C) with its nose in a cone to deliver 0.5-1% isoflurane (for anesthesia maintenance).
3. Pre-warmed echo gel was placed on the left thoracic area.
4. A parasternal long-axis view of the left ventricle (LV) was obtained, and M-mode echocardiography images were recorded using Vevo 2100 system with a MS 400 transducer. The images were obtained below the level of the suture in the LV. Once the correct position was acquired, the echocardiography probe was turned 90° to obtain a parasternal short-axis view, and record M-mode echocardiography images.
5. The end diastolic left ventricular internal diameter and end systolic left ventricular internal diameter were measured from the short-axis M-mode images. Ejection fraction and fractional shortening were calculated.

2.3.5 Measurement of Myocardial Infarct Size 24 hours Post-MI

To ensure induction of a reproducible infarct size, the following protocol was used to determine myocardial infarct size per area at risk in 4 WT neonatal mice.

1. Pups were allowed to recover in the care of a CD-1 foster mother for a period of 24 hours. The pup was removed from the cage with the mother and euthanized by isoflurane overdose followed by decapitation with a large scissors.
2. The chest cavity was opened as in steps 2.2.4 1 - 5. Before excising the heart, the

thoracic aorta was carefully grasped just above the diaphragm with fine forceps. Fine scissors were held in the coronal plane, flat against the thoracic wall, and the thoracic aorta was cut off the posterior thoracic wall moving scissors in the cranial direction. The aorta was cut free from the thoracic wall and any other connections until it reached the heart. The heart was excised by grasping the superior vena cava and removing all other vascular connections to the body.

3. The heart was rinsed (with aorta attached) in saline.
4. The thoracic aorta was carefully cannulated with a 30 gauge needle and the aorta tied to the cannula with 8-0 nylon suture thread. The heart was perfused with 1 mL of saline through the aorta via a 30 gauge needle at a rate of 1 mL/min.
5. The heart was perfused with 150 μ L of 2% Evans-Blue solution at a rate of 1 mL/min.
6. The heart was removed from the cannula, sectioned into three pieces and stained with TTC as described in 2.2.4 3 – 4.
7. To calculate infarct size, heart sections were photographed and infarct area measured on imaging software. The viable myocardium stains blue, the area at risk stains red, and the infarct area is demarcated as white.

2.4 Results

The myocardial infarction procedure can be completed in 10-15 minutes and has a mortality rate of 7%. After surgery, mice recover from hypothermic anesthesia within the next 5-20 minutes (time of recovery depends on body temperature reached during anesthesia and speed of surgeon). When using P7 pups (for comparison with a non-regenerative myocardium), a longer period of cooling is required to reach torpor. P7 pups

are much larger and have more difficulty recovering from both cardiac injury and hypothermia, resulting in a much higher mortality rate of 30%.

Results from previous studies are confirmed herein, indicating induction of hypothermic anesthesia at close to 10 °C (between 8 °C and 15 °C).⁴⁵ Within this temperature window, heart rate is slow, but rhythm continues at rates of between 24 bpm and 11 bpm. The low heart rate at this level of cooling significantly reduces intraoperative bleeding. The LAD can be easily visualized and ligated at these temperatures (**Figure 2.1**). The LAD remains visible until body temperatures reach between 9.6 °C and 4.9 °C, causing lowering of heart rate to 2 bpm or asystole.

Post-MI, pups recover fully and grow to a body size comparable to that of littermate controls. Once placed back with their foster mother, pups regain awareness and feeding capabilities comparable to littermates within 5-10 minutes. Upon histological examination 3 days post-MI, there is evidence of a pale infarct area, with infiltrating inflammatory cells, a typical post-infarction response (**Figure 2.2**). At day 7 post-MI, there is evidence of regeneration with left ventricular tissue appearing normal. By day 21 post-MI, complete cardiac regeneration has occurred.

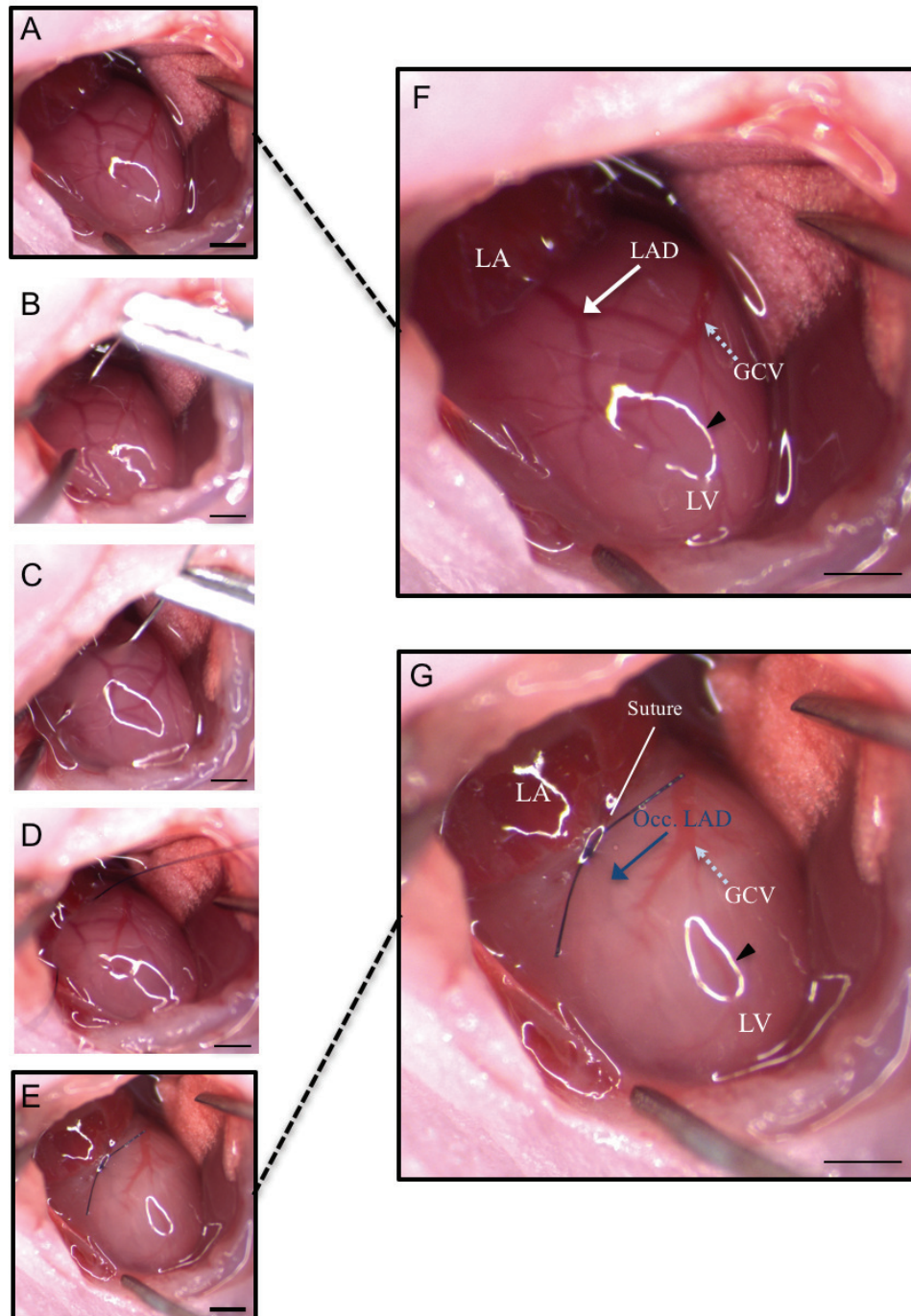


Figure 2.1. Coronary artery is visible during neonatal CAL procedure.

P1 neonatal mouse after hypothermic anesthesia, skin incision, muscle incision and lateral thoracotomy in the fourth intercostal space. A) Left anterior descending coronary artery (LAD) is visible. B-D) 11-0 nylon suture is passed through the mid ventricle. E) LAD is ligated and blanching observed below the suture site. F) and G) are magnifications of A) and E) respectively. Occ. LAD, occluded left anterior descending artery. LA, left atrium. LV, left ventricle. GCV, great coronary vein. White arrow, LAD. Black arrow head, glare from lighting. Scale bars are 1 mm.

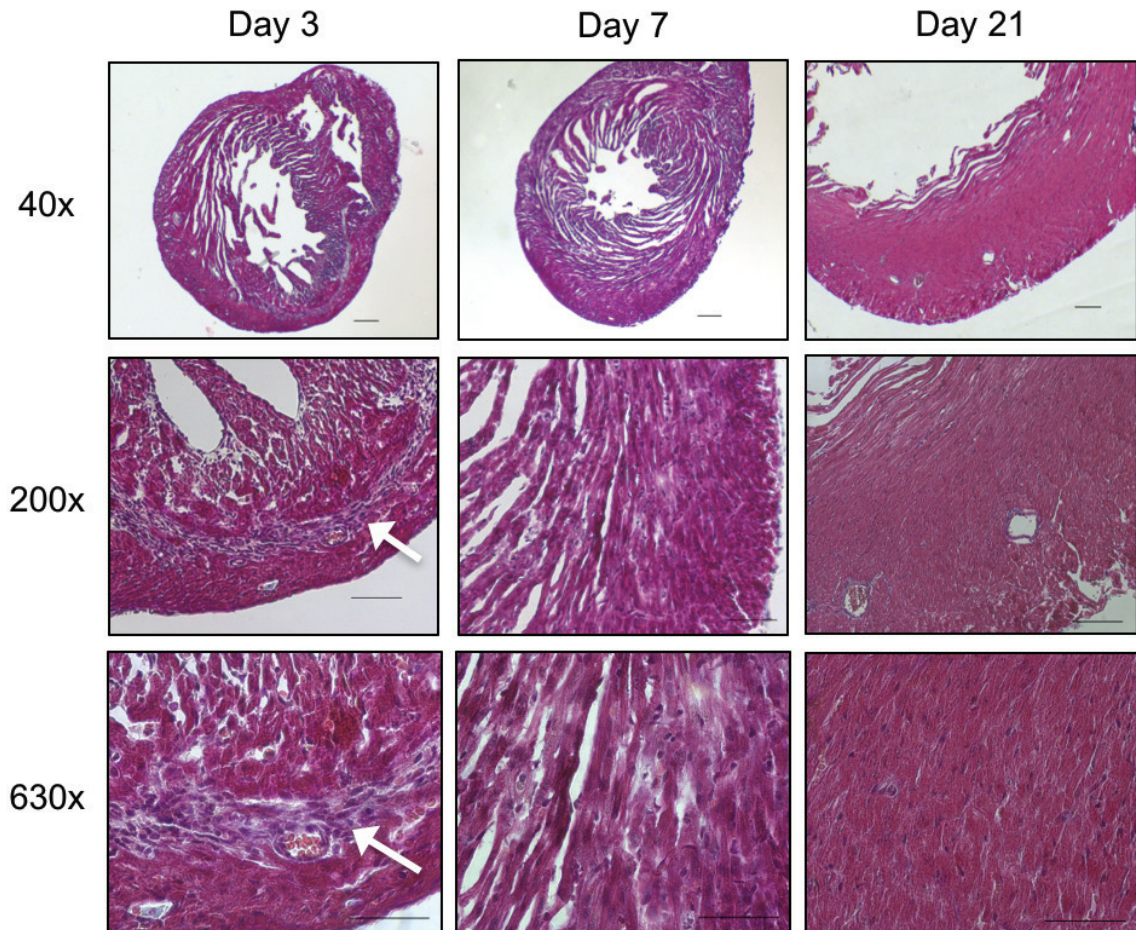


Figure 2.2 Evidence of complete cardiac regeneration after neonatal LAD ligation.

Masson's trichrome staining after LAD ligation in P1 neonatal mice. Whole hearts and magnifications at the infarction areas are shown on day 3, 7 and 21 post-LAD ligation. Note myocyte loss and inflammatory cell infiltrate in infarct region at day 3 post-MI (white arrow). Complete infarct zone regeneration beginning at day 7 post-MI. Little evidence of fibrosis noted at day 21 post-MI. Scale bars are 200 μm , 100 μm and 50 μm for 40x, 200x, and 400x magnification respectively.

There are multiple methods that can be used to confirm infarct induction and determine myocardial infarct size. These include echocardiography, troponin T level measurement, and 2,3,5-triphenyltetrazolium chloride (TTC) staining. Assessing troponin T levels requires a significant blood volume and with present techniques would not be possible for individual neonatal mice without sacrificing them. Instead, echocardiography was performed at both 24 hours and 48 hours post-infarction to confirm successful LAD ligation (**Figures 2.3** and **2.4** respectively). At 24 hours post-MI, ejection fraction (EF) was significantly reduced from 84% to 74%, and fractional shortening (FS) significantly reduced from 50% to 40% (**Figure 2.3**). By 48 hours post-infarction, EF was further reduced to 46%, as compared to 80% in controls. At 48 hours FS was also reduced significantly to 25%, as compared to 50% in controls. Furthermore, there was a significant increase in systolic left ventricular internal diameter at 24 and 48 hours.

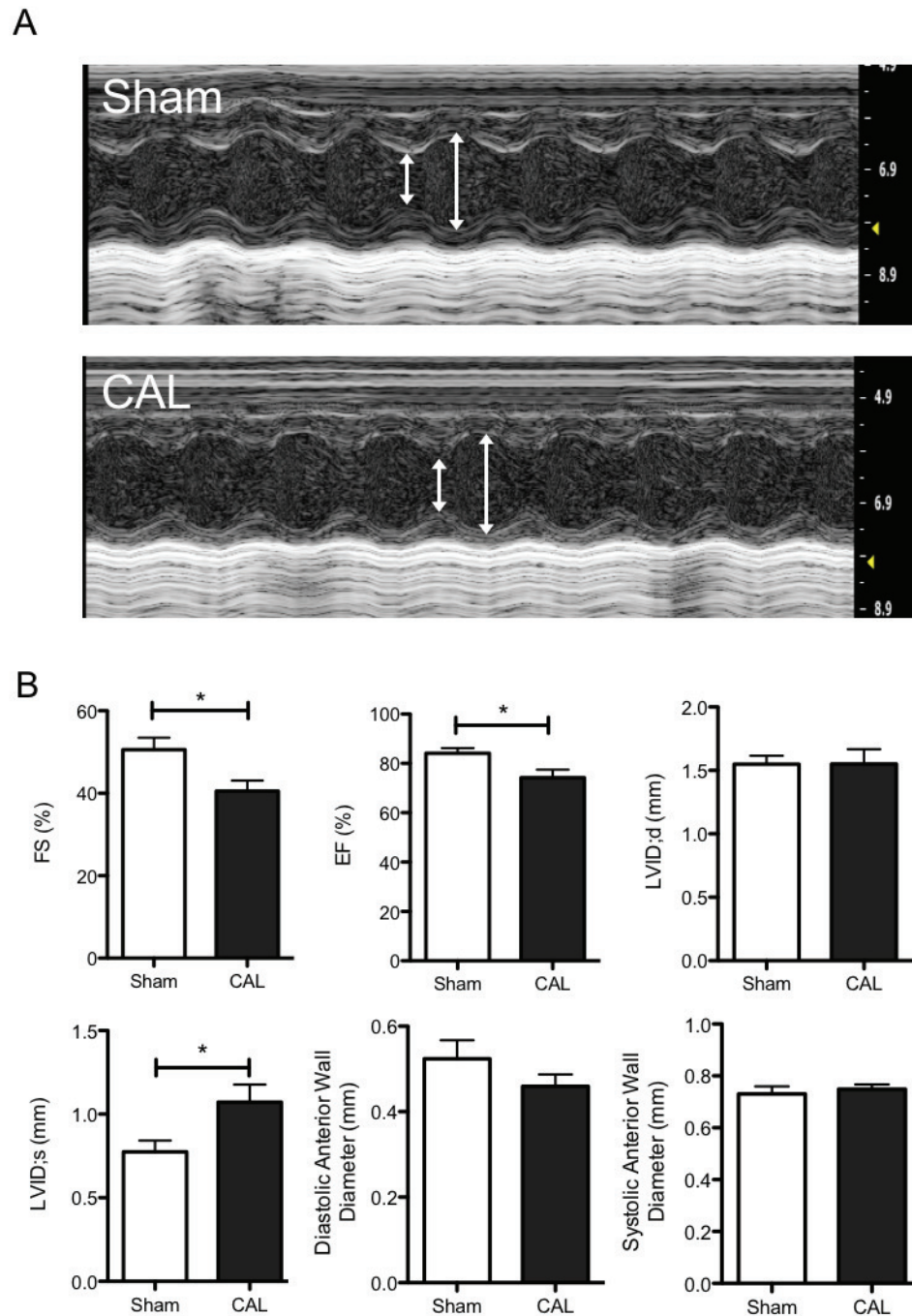


Figure 2.3. Neonatal LAD ligation results in cardiac damage at 24 hours post-MI.

Assessment of cardiac function by echocardiography at 24 hours post-infarction. A) Representative cine-loop images at end-diastole and end-systole for both SHAM operated and LAD ligated mice. B) Cardiac functional measurements by echocardiography including fractional shortening (FS), ejection fraction (EF), left ventricular internal diameter (LVID) at both diastole and systole, and anterior wall thickness at both diastole and systole. Data are mean ± SEM. n = 8 & 7 mice for SHAM and coronary artery ligation (CAL) respectively. * $P < 0.05$.

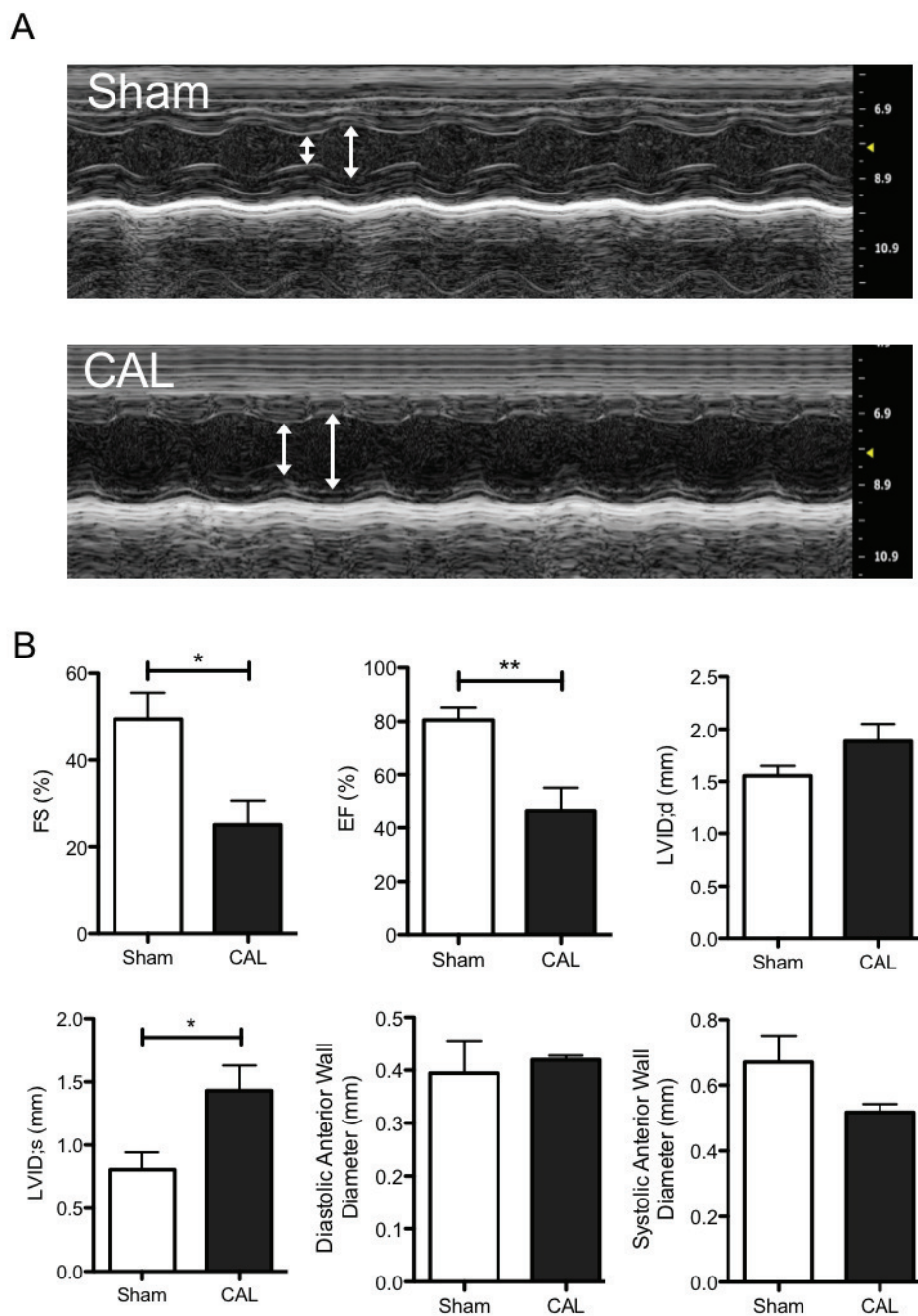


Figure 2.4. Neonatal LAD ligation results in cardiac damage at 48 hours post-MI.

Assessment of cardiac function by echocardiography at 48 hours post-infarction. A) Representative cine-loop images at end-diastole and end-systole for both SHAM operated and LAD ligated mice. B) Cardiac functional measurements by echocardiography including fractional shortening (FS), ejection fraction (EF), left ventricular internal diameter (LVID) at both diastole and systole, and anterior wall thickness at both diastole and systole. Data are mean \pm SEM. $n = 4$ & 6 mice for SHAM and coronary artery ligation (CAL) respectively. * $P < 0.05$, ** $P < 0.01$.

TTC staining is low cost, reproducible and reliable, and easily performed with high throughput. For these reasons, TTC staining 4-6 hours post-infarction was used as a confirmation of consistent induction of MI. The red area represents viable myocardium and the white area represents ischemic dead tissue. In a total of 13 LAD ligation surgeries, 100% of the hearts were infarcted, with an average infarct size of 36% (**Figure 2.5**). TTC staining with Evans blue was also performed at 48 hours post-infarction to demonstrate persistence of infarcted tissue and measure infarct size based on area at risk (**Figure 2.6**). In these hearts, viable myocardium stains blue, the area at risk stains red, and the infarct area is demarcated as white. Infarct size was calculated as a percent of the area at risk. In 4 LAD ligation surgeries, 100% of the hearts were infarcted, with an average infarct size of 49% of the area at risk (**Figure 2.6**).

To determine the capacity of cardiac regeneration in $Wt1^{CreER}$ and $Malat1^{-/-}$ neonatal mice, these mice were subjected to MI at P1. Hearts collected 21 days post-MI (P22) were sectioned and stained with Masson's trichrome staining to detect the presence of any residual scarring. $Wt1$ heterozygosity did not affect the cardiac regenerative capacity, as indicated by robust regeneration and lack of scarring in hearts day 21 post-MI (**Figure 2.7A**). Similarly, there was no evidence of scarring in any of the 12 $Malat1^{-/-}$ hearts at P22 (**Figure 2.7B**), suggesting *Malat1* is not required for the neonatal cardiac regenerative response.

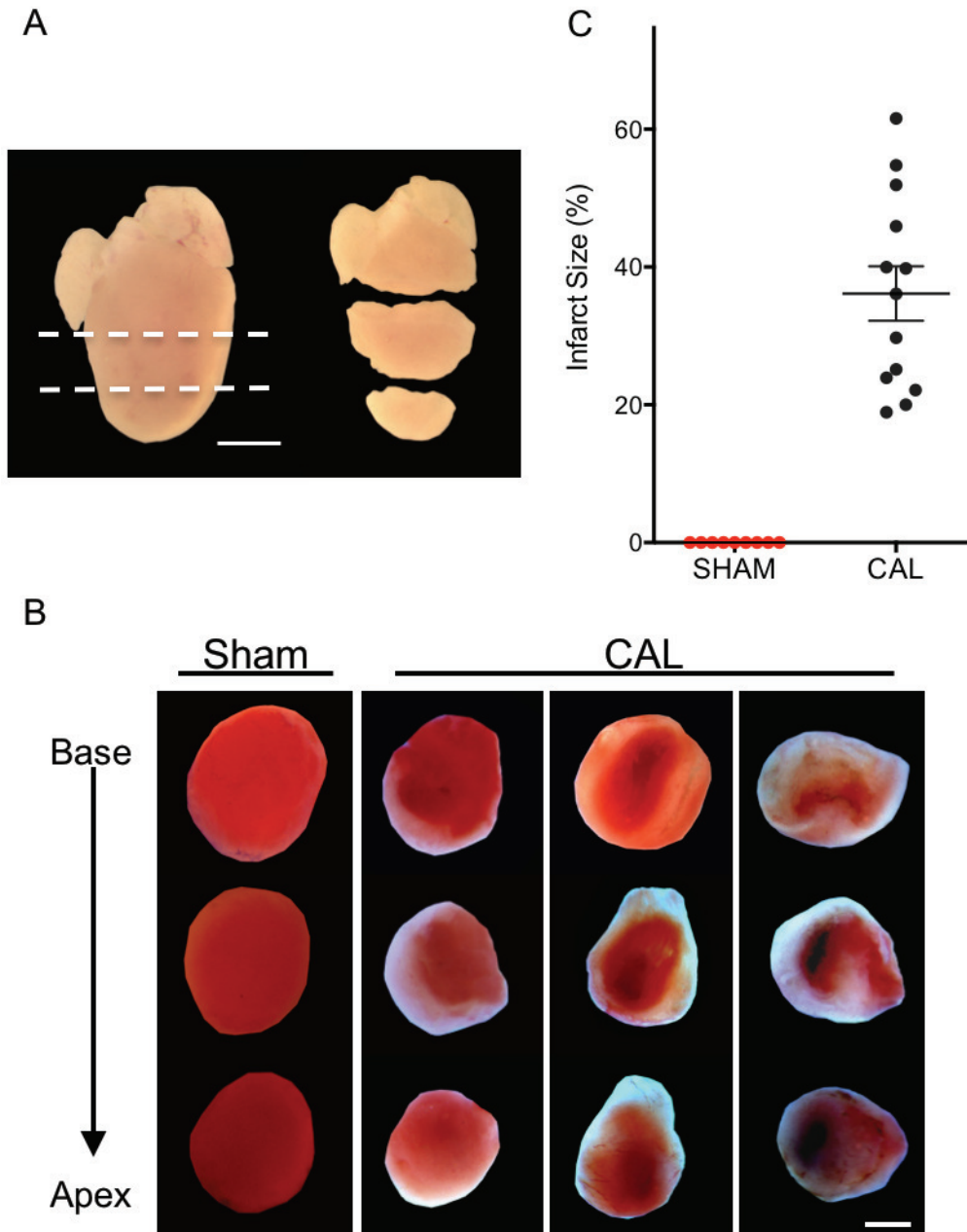


Figure 2.5. Neonatal LAD ligation is 100% reproducible.

A) Lines of sectioning of whole heart to create a 0.75 mm apex piece and a 1 mm mid-base piece for TTC staining. B) Representative images of TTC stained SHAM control and LAD ligated hearts. Scale bars are 1 mm. C) Infarct size in 13 LAD ligations in P1 neonatal mice. Hearts collected 4-6 hours post-infarction and infarct size measured after TTC staining. Red indicates viable myocardium; white indicates necrosis. Data are mean \pm SEM.

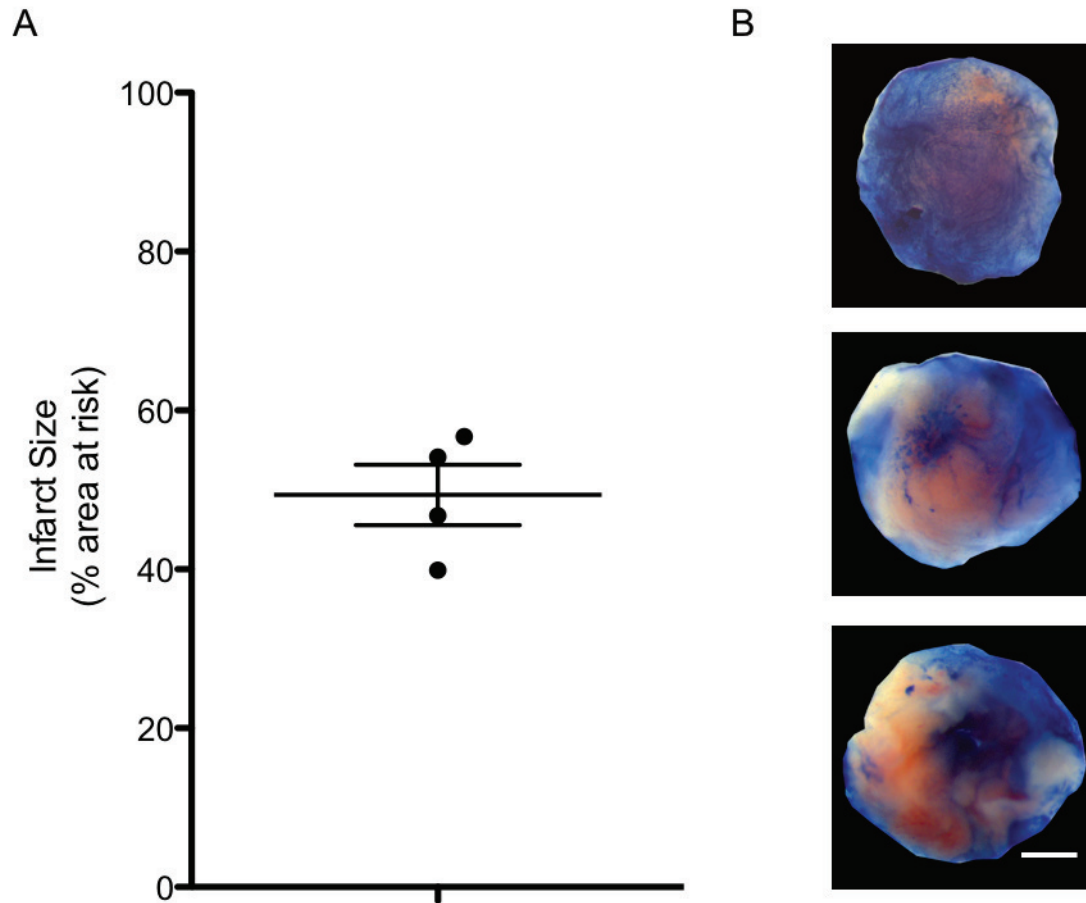


Figure 2.6. Neonatal LAD ligation results in reliable infarct area percentage.

A) Infarct size as % of ischemic area in 4 LAD ligations in P1 neonatal mice. Hearts collected 48 hours post-infarction and infarct size measured after Evans blue and TTC staining. Blue indicates viable myocardium; red indicates area at risk; white indicates necrosis. Data are mean \pm SEM. B) Representative images of Evans blue and TTC stained LAD ligated hearts. Scale bar is 1 mm.

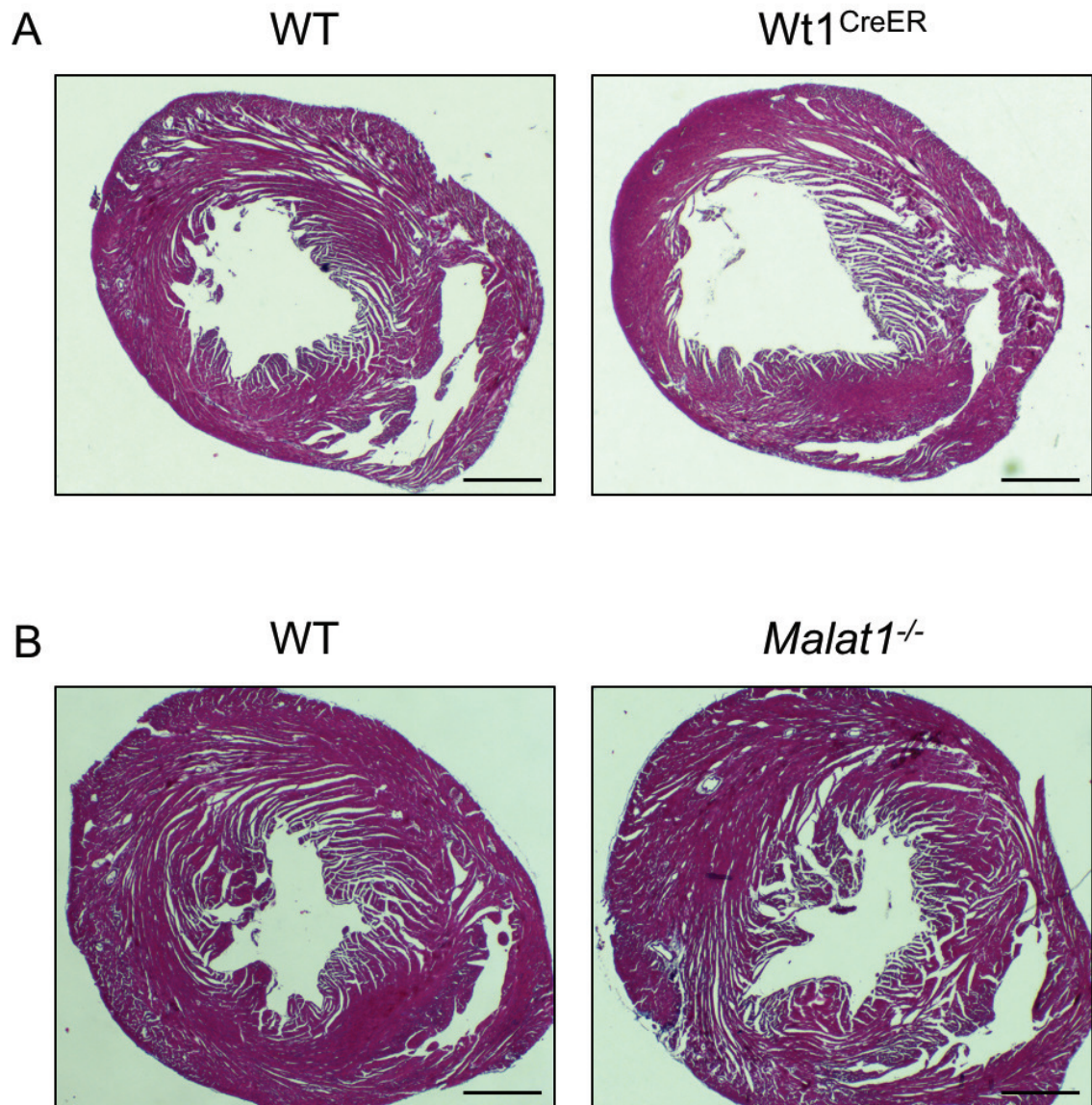


Figure 2.7. The neonatal mouse maintains a robust propensity for cardiac regeneration.

$Wt1^{CreER}$ mice and WT littermate controls underwent coronary artery ligation (CAL) at P1. Similarly, $Malat1^{-/-}$ and corresponding WT mice received CAL at P1. Hearts from all mice were collected 21 days post-MI (P22), sectioned and stained with Masson's trichrome staining. As with WT controls, both $Wt1^{CreER}$ (A) and $Malat1^{-/-}$ (B) mouse hearts were completely regenerated 21 days post-MI (indicated by lack of blue scar). Shown are representative images from $n = 4$ for $Wt1^{CreER}$ and $n = 12$ for $Malat1^{-/-}$ mice. Scale bars are 0.5 mm.

2.5 Discussion

The surgical LAD ligation demonstrated herein is a reliable method to produce MI in neonatal mice. This model provides researchers with a reproducible model with which to study mammalian heart regeneration. Visualization of the coronary vasculature is a key component of this method, ensuring correct suture placement and thus guaranteeing reproducibility. While adult mice do not possess capabilities of poikilotherms, the body temperature and metabolic rate of neonatal mice is closely associated with ambient temperature. Furthermore, the small size of neonatal mice makes them ideal for hypothermic induction by surface cooling. The timing of surgery and mouse body temperature are crucial for accuracy in replicating this procedure and thus must be monitored carefully. Ligation as soon as possible after torpor is reached provides the opportunity to visualize blanching of the myocardium post-ligation, confirming surgical success.

The reproducibility of this technique may be confirmed by functional analysis such as echocardiography, viability TTC staining, or immunohistochemistry. If the investigator is experiencing difficulty visualizing the LAD (likely due to deep hypothermia induction), the left auricle may be lifted slightly with forceps, as the main root of the LAD is larger than the more distal segments and may be more easily appreciated. If the LAD cannot be visualized, the investigator should not presume artery location. This pup should not be used for experimental ligation and could rather be used as a sham operated control. Difficulty may arise if entry into the chest cavity is not performed at the 4th intercostal space. This space is easily found by visualizing the lower edge of the left lung beneath the 4th intercostal space musculature. If a minor amount of

bleeding occurs during the procedure, remove blood with sterile gauze. If bleeding is significant, however, the surgeon has likely not cooled the mouse sufficiently before beginning the procedure, and further cooling is required. Due to the small size of neonatal mice, obtaining clear images for echocardiographic analysis may prove difficult. For best results, ensure heart rate maintenance with light anesthesia (0.5-1% isoflurane inhalation) and maintenance of body temperature (heated dock and warmed echo gel). Images are best acquired if the body is tilted slightly downwards towards the right shoulder ($\sim 5^\circ$ cranially and 5° rightward). Ensure sufficient echo gel is applied to minimize noise.

Although this approach does offer 100% reproducibility, the size of the infarct may be somewhat variable depending on the coronary artery branching anatomy of the individual neonate (**Figure 2.2**). As a result, higher n numbers may be required to reach statistical significance in determining the effects of different treatments or genetic manipulations on cardiac regeneration.

From the time of this publication, cryoinjury has also been demonstrated to cause reproducible cardiac injury.⁴⁶ However, the approach presented here holds major advantages over both neonatal apex resection and cryoinjury as the pathophysiology of these mechanisms of injury may be entirely different from MI and thus may not accurately represent human MI.^{8, 47} This approach more directly mimics typical human injury, and may be used to study cardiac regeneration in the setting of mammalian MI.

This model is unique as it allows for the study of the differences in the mechanisms of recovery from cardiac injury between the non-regenerative (adult) and the regenerative (neonatal) mammalian myocardium. For example, the adult mouse MI

model results in permanent scar formation. Ventricular rupture often occurs as a result of infarct expansion. In our experience with this model (>100 surgeries), complete regeneration is evident 21 days post-infarction and ventricular rupture has not been observed.

The information accrued from use of this model may offer novel insights into mechanisms that may promote cardiac regeneration in the adult. For example, recent evidence indicates cardiomyocyte proliferation is a major contributor to cardiac regeneration.⁹ This is in contrast to previous thinking suggesting substantial contributions from progenitor cell pools. This has directed research efforts to determining methods of promoting cardiomyocyte proliferation rather than progenitor cell activation. For example, Meis1 and Neuregulin 1 signaling have already been identified as critical regulators of cardiomyocyte proliferation and neonatal cardiac regeneration.^{4, 48}

Our study indicates that neonatal mice retain a remarkable capacity for cardiac regeneration. The role of Wt1 in both coronary artery development and neovascularization post-MI has been confirmed by numerous groups.^{26, 30, 49} Here we show that, like their WT counterparts, Wt1^{CreER} mice heterozygous for the Wt1 allele are able to recover from myocardial infarction injury at P1 without scarring or phenotypic consequences three weeks after injury. These results suggest that high level Wt1 expression is not required for this regenerative response. The pitfall of using heterozygous mice is that the remaining allele may produce sufficient Wt1 to achieve cardiac regeneration in neonates. To test this, Wt1 protein expression levels can be measured by Western blotting. Other methods to achieve sufficient knockdown of Wt1 include conditional knockout mouse lines (homozygous deletion is embryonic fatal),²⁷

shRNA administration with a viral construct, or by targeted genome editing using the CRISPR/Cas 9 system.

Malat1 is a lncRNA known to promote hypoxia-mediated angiogenesis, and support EMT.^{37, 39} Similar to our neonatal *Wt1*^{CreER} mice, homozygous deletion of the lncRNA *Malat1* (*Malat1*^{-/-}) did not affect the regenerative capacity in the neonatal stage. This was surprising since *Malat1* has also been suggested to support cardiomyocyte proliferation, which is required for the neonatal regenerative response.⁵⁰ *Malat1* does not appear to be critical to embryonic development, since *Malat1*^{-/-} mice develop and reproduce normally.⁵¹ This lack of necessity for *Malat1* may apply to the neonatal transition period after birth, where some embryonic responses and expression of some embryonic genes are still present.^{52, 53} However, alterations in *Malat1* may become increasingly important in the adult during situations of stress or disease.⁵⁴ Thus, it may be important to test the effects of *Malat1* deficiency on cardiac injury in the adult heart.

Together, the results presented herein confirm the robust regenerative capacity of the neonatal mammalian heart, and that this regenerative response is not sensitive to perturbations in *Wt1* or *Malat1* expression. This intrinsic regenerative capacity has even recently been demonstrated in a newborn human child who spontaneously recovered normal cardiac function after massive cardiac damage from severe MI.⁵⁵ Although alterations in *Wt1* and *Malat1* in the early neonatal stage did not affect cardiac regeneration, this does not negate their importance in the adult healing response. Continued research in this field may elucidate the mechanisms supporting neonatal cardiac regeneration, an understanding of which may aid in the development of therapeutic targets for post-MI repair.

2.6 References

1. Benjamin EJ, et al. Heart disease and stroke statistics-2017 update: A report from the american heart association. *Circulation*. 2017;135:e146-e603.
2. Meta-analysis Global Group in Chronic Heart Failure. The survival of patients with heart failure with preserved or reduced left ventricular ejection fraction: an individual patient data meta-analysis. *Eur Heart J*. 2012;33:1750-7.
3. Soonpaa MH and Field LJ. Assessment of cardiomyocyte DNA synthesis in normal and injured adult mouse hearts. *Am J Physiol*. 1997;272:H220-6.
4. D'Uva G, et al. ERBB2 triggers mammalian heart regeneration by promoting cardiomyocyte dedifferentiation and proliferation. *Nat Cell Biol*. 2015;17:627-38.
5. Oberpriller JO and Oberpriller JC. Response of the adult newt ventricle to injury. *J Exp Zool*. 1974;187:249-53.
6. Poss KD, et al. Heart regeneration in zebrafish. *Science*. 2002;298:2188-90.
7. Jopling C, et al. Zebrafish heart regeneration occurs by cardiomyocyte dedifferentiation and proliferation. *Nature*. 2010;464:606-9.
8. Porrello ER, et al. Transient regenerative potential of the neonatal mouse heart. *Science*. 2011;331:1078-80.
9. Haubner BJ, et al. Complete cardiac regeneration in a mouse model of myocardial infarction. *Aging (Albany NY)*. 2012;4:966-77.
10. Soonpaa MH, et al. Cardiomyocyte DNA synthesis and binucleation during murine development. *Am J Physiol*. 1996;271:H2183-9.
11. Li F, et al. Rapid transition of cardiac myocytes from hyperplasia to hypertrophy during postnatal development. *J Mol Cell Cardiol*. 1996;28:1737-46.
12. Feng Q, et al. Elevation of an endogenous inhibitor of nitric oxide synthesis in experimental congestive heart failure. *Cardiovasc Res*. 1998;37:667-75.
13. Xiang FL, et al. Cardiomyocyte-specific overexpression of human stem cell factor improves cardiac function and survival after myocardial infarction in mice. *Circulation*. 2009;120:1065-74.
14. van Kats JP, et al. Angiotensin-converting enzyme inhibition and angiotensin II type 1 receptor blockade prevent cardiac remodeling in pigs after myocardial infarction: role of tissue angiotensin II. *Circulation*. 2000;102:1556-63.

15. Mahmoud AI, et al. Surgical models for cardiac regeneration in neonatal mice. *Nat Protoc.* 2014;9:305-11.
16. Ahn D, et al. Induction of myocardial infarcts of a predictable size and location by branch pattern probability-assisted coronary ligation in C57BL/6 mice. *Am J Physiol Heart Circ Physiol.* 2004;286:H1201-7.
17. Forbes SJ and Rosenthal N. Preparing the ground for tissue regeneration: from mechanism to therapy. *Nat Med.* 2014;20:857-69.
18. Xin M, et al. Hippo pathway effector Yap promotes cardiac regeneration. *Proc Natl Acad Sci U S A.* 2013;110:13839-44.
19. Zhou Z, et al. Impaired angiogenesis, delayed wound healing and retarded tumor growth in perlecan heparan sulfate-deficient mice. *Cancer Res.* 2004;64:4699-702.
20. Swift ME, et al. Impaired wound repair and delayed angiogenesis in aged mice. *Lab Invest.* 1999;79:1479-87.
21. Porrello ER, et al. Regulation of neonatal and adult mammalian heart regeneration by the miR-15 family. *Proc Natl Acad Sci U S A.* 2013;110:187-92.
22. Kikuchi K, et al. Primary contribution to zebrafish heart regeneration by gata4(+) cardiomyocytes. *Nature.* 2010;464:601-5.
23. Reese DE, et al. Development of the coronary vessel system. *Circ Res.* 2002;91:761-8.
24. Masters M and Riley PR. The epicardium signals the way towards heart regeneration. *Stem Cell Res.* 2014;13:683-92.
25. Zhou B, et al. Adult mouse epicardium modulates myocardial injury by secreting paracrine factors. *J Clin Invest.* 2011;121:1894-904.
26. Carmona R, et al. Localization of the Wilm's tumour protein WT1 in avian embryos. *Cell Tissue Res.* 2001;303:173-86.
27. von Gise A, et al. WT1 regulates epicardial epithelial to mesenchymal transition through beta-catenin and retinoic acid signaling pathways. *Developmental Biology.* 2011;356:421-431.
28. Duim SN, et al. Cardiac endothelial cells express Wilms' tumor-1: Wt1 expression in the developing, adult and infarcted heart. *J Mol Cell Cardiol.* 2015;81:127-35.
29. Martinez-Estrada OM, et al. Wt1 is required for cardiovascular progenitor cell formation through transcriptional control of Snail and E-cadherin. *Nat Genet.* 2010;42:89-93.

30. Wagner KD, et al. The Wilms' tumor suppressor Wt1 is expressed in the coronary vasculature after myocardial infarction. *FASEB J.* 2002;16:1117-9.
31. Wagner KD, et al. The Wilms' tumour suppressor Wt1 is a major regulator of tumour angiogenesis and progression. *Nat Commun.* 2014;5:5852.
32. Imanishi T, et al. Integrative annotation of 21,037 human genes validated by full-length cDNA clones. *PLoS Biol.* 2004;2:e162.
33. Frith MC, et al. The amazing complexity of the human transcriptome. *Eur J Hum Genet.* 2005;13:894-7.
34. Ji P, et al. MALAT-1, a novel noncoding RNA, and thymosin β 4 predict metastasis and survival in early-stage non-small cell lung cancer. *Oncogene.* 2003;22:8031-41.
35. Yang L, et al. High MALAT1 expression predicts a poor prognosis of cervical cancer and promotes cancer cell growth and invasion. *Eur Rev Med Pharmacol Sci.* 2015;19:3187-93.
36. Zhou X, et al. Long non coding rna MALAT1 promotes tumor growth and metastasis by inducing epithelial-mesenchymal transition in oral squamous cell carcinoma. *Sci Rep.* 2015;5:15972.
37. Yang S, et al. Long non-coding rna malat1 mediates transforming growth factor beta1-induced epithelial-mesenchymal transition of retinal pigment epithelial cells. *PLoS One.* 2016;11:e0152687.
38. Tee AE, et al. The long noncoding RNA MALAT1 promotes tumor-driven angiogenesis by up-regulating pro-angiogenic gene expression. *Oncotarget.* 2016;7:8663-75.
39. Michalik KM, et al. Long noncoding RNA MALAT1 regulates endothelial cell function and vessel growth. *Circ Res.* 2014;114:1389-97.
40. Lepilina A, et al. A dynamic epicardial injury response supports progenitor cell activity during zebrafish heart regeneration. *Cell.* 2006;127:607-19.
41. Xiang FL, et al. Cardiac-specific overexpression of human stem cell factor promotes epicardial activation and arteriogenesis after myocardial infarction. *Circ Heart Fail.* 2014;7:831-42.
42. Zhang B, et al. The lncRNA Malat1 is dispensable for mouse development but its transcription plays a cis-regulatory role in the adult. *Cell Rep.* 2012;2:111-23.
43. Kao WW, et al. Signaling pathways in morphogenesis of cornea and eyelid. *Ocul Surf.* 2008;6:9-23.

44. Redfors B, et al. Myocardial infarct size and area at risk assessment in mice. *Experimental & Clinical Cardiology*. 2012;17:268-272.
45. Phifer CB and Terry LM. Use of hypothermia for general anesthesia in preweanling rodents. *Physiol Behav*. 1986;38:887-90.
46. Polizzotti BD, et al. A cryoinjury model in neonatal mice for cardiac translational and regeneration research. *Nat Protoc*. 2016;11:542-52.
47. Jesty SA, et al. c-kit⁺ precursors support postinfarction myogenesis in the neonatal, but not adult, heart. *Proc Natl Acad Sci U S A*. 2012;109:13380-5.
48. Mahmoud AI, et al. Meis1 regulates postnatal cardiomyocyte cell cycle arrest. *Nature*. 2013;497:249-53.
49. Moore AW, et al. YAC complementation shows a requirement for Wt1 in the development of epicardium, adrenal gland and throughout nephrogenesis. *Development*. 1999;126:1845-57.
50. Zhao J, et al. MAPK1 up-regulates the expression of MALAT1 to promote the proliferation of cardiomyocytes through PI3K/AKT signaling pathway. *Int J Clin Exp Pathol*. 2015;8:15947-53.
51. Eissmann M, et al. Loss of the abundant nuclear non-coding RNA MALAT1 is compatible with life and development. *RNA Biol*. 2012;9:1076-87.
52. Ng WA, et al. Cardiac myosin heavy chain mRNA expression and myocardial function in the mouse heart. *Circ Res*. 1991;68:1742-50.
53. Takeuchi T. Regulation of cardiomyocyte proliferation during development and regeneration. *Dev Growth Differ*. 2014;56:402-9.
54. Gutschner T, et al. The noncoding RNA MALAT1 is a critical regulator of the metastasis phenotype of lung cancer cells. *Cancer Res*. 2013;73:1180-9.
55. Haubner BJ, et al. Functional recovery of a human neonatal heart after severe myocardial infarction. *Circ Res*. 2016;118:216-21.

Chapter 3

Primary cilia disassembly promotes epicardial epithelial-to-mesenchymal transition, neovascularization, and cardiac repair post-myocardial infarction

Blom JN, Lu X, Kim YK, Feng Q.

In preparation for submission.

3 Chapter 3

3.1 Chapter summary

Pathological ventricular remodeling following ischemic cardiac injury is a leading cause of death. Typical pharmaceutical approaches to treat this disease have extended life but have not improved mortality. Augmenting angiogenesis is considered a promising therapeutic target for supporting healing after ischemic cardiac injury. The epicardium is a potential source of vascular cells to support healing. Primary cilia are increasingly being recognized as hubs of cellular signaling, and their presence can alter traditional signaling pathways. Here, we report on the involvement of primary cilia as modulators of epicardial epithelial-to-mesenchymal transition (EMT) post-myocardial infarction (MI). We demonstrate that mouse epicardial cells are ciliated, and that inhibition of ciliary assembly using an adenoviral vector encoding short-hairpin RNA for the mouse intraflagellar transport protein-88 (Ad-shIft88) enhances epicardial EMT *in vitro*. Concomitantly, Ad-shIft88 treatment in the myocardium supports a regenerative response in a post-regenerative state in a mammalian neonatal mouse (postnatal day 7), demonstrated by reduced infarct size and improved cardiac function after MI. Finally, treatment with Ad-shIft88 promotes epicardial EMT and neovascularization in the peri-infarct area, which results in improved cardiac function three weeks post-MI in adult mice. This study suggests that the primary cilium may serve as a therapeutic target to improve cardiac repair and function post-MI.

3.2 Introduction

Ischemic heart disease is the leading global cause of death.¹ After surviving from acute myocardial infarction (MI), a deleterious remodeling process takes place whereby the infarct expands, a fibrous collagen scar replaces lost myocardium, and the remaining viable cardiomyocytes hypertrophy in effort to compensate for lost contractile tissue. This deleterious remodeling post-MI often causes heart failure, a debilitating and deadly disease with a 5 year mortality of 60-75%.² The current treatment options for heart failure can moderately extend life, however the end stage disease remains a major cause of death, and is associated with approximately one in eight deaths in the United States.³ Collectively, heart failure is a major economic burden, with a current global economic cost of about \$108 billion per annum.⁴

It has recently been demonstrated that the neonatal mouse possesses the capacity to completely regenerate its heart, however, this response is lost by postnatal day 7 (P7).⁵ Neovascularization in the infarct and peri-infarct area is critical to a cardiac regenerative response. Cardiac progenitor cells have been demonstrated to be involved in healing post-MI, and may contribute to angiogenesis and arteriogenesis for vascularization.⁶ Specifically, epicardium derived cells (EPDCs) are endogenous multipotent cardiac progenitors which support coronary artery development during embryogenesis. During cardiogenesis, these epicardial cells begin to express the transcription factor Wilms' tumour 1 (Wt1), and undergo the process of epithelial-to-mesenchymal transition (EMT) to invade the myocardium and contribute perivascular and interstitial fibroblasts, epithelial cells and smooth muscle cells for vascularization.⁷ Typically, the adult epicardium is dormant; however, after MI, many epicardial cells express markers of

embryonic progenitors (including *Wt1*, *Tbx18*, *c-kit* and *CD34*), and are activated to undergo EMT and form EPDCs to promote neovascularization.^{8, 9} Unfortunately, this endogenous EPDC response is insufficient, and does not support adequate vascularization necessary for recovery post-MI. However, EMT genes are upregulated post-cardiac apex resection in the neonate, implicating epicardial EMT in neovascularization contributing to regeneration.¹⁰

The primary cilium is an immotile specialized organelle protruding from the apical surface of most vertebrate cells. It is thought to integrate numerous sensory signaling pathways from extracellular signals, affectionately earning the name the cellular “antenna.” Included in the signaling pathways associated with the cilium are sonic hedgehog (Shh), wingless-type integration site (Wnt; canonical & non-canonical), and platelet-derived growth factor (PDGF), which are all integrated in the network related to EMT activation.¹¹ Shh, Wnt and PDGF pathways support the loss of E-cadherin, gain of N-cadherin, and induce expression of other pro-EMT mediators such as TGF- β .¹² Interestingly, it has been proposed that primary ciliary disassembly primes endothelial cells to shear-stress induced EMT during heart development.¹³ Loss of the primary cilium is also suggested to be responsible for EMT based metastatic invasion in numerous cancer cell types.¹⁴ Finally, in association with tissue wounding, TGF- β provokes deciliation along the wound edge, which incites EMT-type transitions.¹⁵ However, the effects of primary ciliary disassembly on epicardial EMT and post-MI angiogenesis are not known. Intraflagellar transport protein 88 (*Ift88*) is a transport protein required for both the assembly and structural maintenance of the primary cilium.¹⁶ In the present study, we hypothesized that knockdown of *Ift88* using an

adenoviral construct encoding a short hairpin RNA against Ift88 (Ad-shIf88) would potentiate primary cilia disassembly and promote epicardial EMT, myocardial neovascularization, and cardiac repair post-MI.

3.3 Methods

3.3.1 Animals

All protocols were approved by the Animal Use Subcommittee at the University of Western Ontario, London, Ontario Canada, and animals were handled in accordance with the guidelines of the Canadian Council on Animal Care.

3.3.2 Adenoviruses

To inhibit ciliary signalling, an adenoviral construct (Type 5 dE1E3) encoding short-hairpin RNA for the mouse intraflagellar transport protein-88 (Ad-shIf88) (shRNA sequence: ccgg-gcaggaagactgaaagtgaatctcgagattcacttcagtcttctgc-ttttg),¹⁷ driven by the human RNA polymerase III U6 promoter, and tagged with eGFP (cytomegalovirus promoter driven; CMV), was obtained from Vector Biolabs (Malvern, PA). An adenoviral construct containing CMV-driven green fluorescent protein (GFP) was used as control. Adenoviruses were propagated using HEK 293 cells, purified, and titered using an AdEasy viral titer kit according to the manufacturer's instructions (Agilent Technologies, Santa Clara, CA).

3.3.3 Coronary artery ligation and *in vivo* adenoviral injection

Coronary artery ligation (CAL) to induce MI in postnatal day 7 mice (P7) was performed as previously described.¹⁸ Briefly, mice were anesthetized using isoflurane and then cooling on an ice bed. A left thoracotomy was performed at the 4th intercostal space,

and an 11-0 suture was used to ligate the left anterior descending coronary artery (LAD). The thoracic cavity was closed using 8-0 sutures and mice were warmed to 37 °C on a heating pad. For sham operations, a left thoracotomy was performed without ligation of the LAD. Similarly, adult LAD coronary occlusion was performed as described previously.¹⁹ Mice were anesthetized with an IP injection of a ketamine (50 mg/kg) and xylazine (12.5 mg/kg) mixture, intubated endotracheally, and ventilated with positive pressure by a respirator (Model SAR-830, CWE Inc, Ardmore, PA) at a rate of 90 breaths/min. A left thoracotomy was performed, and the coronary artery was ligated with an 8-0 suture. Both neonatal and adult mice were randomly assigned to injection of either Ad-GFP or Ad-shIfit88 (10^9 PFU in 3 μ L saline for neonates, and 10^{10} PFU in 5 μ L saline for adults). Immediately after CAL, viruses were injected intramyocardially into 3 sites of the peri-infarct area, just below the epicardium using a 29 Gauge needle connected to a 25 μ L Hamilton gastight syringe. The surgeon was blinded to the virus group. Hearts were collected 3, 5 and 21 days post-MI. Adenoviral infection was confirmed by visualization of GFP fluorescence in heart sections; only those mice whose hearts expressed GFP upon visualization, indicating adenoviral infection, were used for subsequent analysis.

Neonatal hearts were serially sectioned, and fibrosis was detected by Masson's trichrome staining as per the manufacturer's instructions (Sigma-Aldrich, St. Louis, MO). The fibrotic area was expressed as a percentage of left ventricular surface area, averaged from 5 sections across the heart, evenly spaced from the suture site to the apex.²⁰ Adult heart weight and body weight was recorded at the time of euthanasia. Infarct size of the adult heart was measured and expressed as a fraction of the total cross-sectional

endocardial circumference.¹⁹ Finally, LV thickness, evaluated at the ventricular septum at the level of the suture was determined.

3.3.4 Echocardiography

Neonatal heart function was measured at P28 (21 days post-MI or sham surgery) using Vevo 2100 system with a MS 400 transducer (VisualSonics, Toronto, Ontario).^{21, 22} For adult mice, echocardiographic imaging was performed prior to surgery, as well as 5 and 21 days post-MI. Mice were anesthetized by inhalation of isoflurane, and fur was removed from the chest using hair-removal cream (Nair). Two-dimensional images were obtained in both the long-axis and short-axis views. M-mode image recordings on short axis were used to measure the left ventricular internal diameter (LVID) at systole and diastole.

3.3.5 Cell culture and adenovirus infection *in vitro*

Primary epicardium derived cells (EPDCs) were cultured as described previously.²³ Briefly, fetal hearts at embryonic day 13.5 (E13.5) were dissected and ventricles were cut into four pieces. After brief washing in warm PBS, ventricle pieces were plated onto 1% gelatin-coated dishes in Dulbecco's Modified Eagle Medium (DMEM) containing 10% fetal bovine serum (FBS), 1% penicillin and streptomycin (Wisent Inc, Canada), and covered with a glass coverslip to promote adherence. Epicardial cells migrated outward from the cardiac explant, forming a monolayer across the gelatin surface. After EPDCs were allowed to grow outward for a period of 7 days, ventricle explants were removed using sterile forceps and epicardial cells were trypsinized and re-plated for further experiments. To avoid inclusion of non-EPDC cell

types from the culture, only cells from an initial (approx. 4 minute) wash with trypsin were used. To test purity of EPDCs in culture, first passage EPDCs were plated onto 1% gelatin-covered glass coverslips, fixed, and stained with rabbit anti-mouse Wt1 (1:800, Calbiochem, San Diego, CA), goat anti-rabbit Cy3 conjugated secondary antibody (Jackson ImmunoResearch, PA, USA), and Hoechst 33342 (Invitrogen, Carlsbad CA) to mark nuclei. For validation of Ift88 knockdown, first passage EPDCs were plated onto either 1% gelatin-covered glass coverslips or 24-well plates (approx. 10^5 EPDCs per well). Cells were grown to confluence and treated with 10^7 PFU (approx. 100 MOI) Ad-shIft88 or Ad-GFP. After 48 hours, medium containing virus was replaced with fresh serum-free medium for 24 hours (serum starvation has been shown to induce cilia formation and elongation in culture).^{24, 25} Cells grown on coverslips were then fixed in 80% methanol and 20% acetone mixture at -20 °C for 10 minutes and air dried. Cells grown in 24-well plates were used for analysis of mRNA levels by RT-qPCR. Immunocytochemistry was performed on cells fixed on coverslips. Cells were rinsed with PBS, and permeabilized with 0.1% Triton for 12 minutes. After blocking with 2% BSA for 30 minutes, cells were stained with acetylated α -tubulin primary antibody (1:2000, Sigma-Aldrich, St. Louis, MO) in 2% BSA for 90 minutes, followed by 45 minute incubation with Cy3 conjugated anti-mouse secondary antibody (1:600, Jackson ImmunoResearch, PA, USA). Nuclei were stained with Hoechst 33342. A minimum of 30 cells were examined for each culture using a fluorescent microscope (Observer D1, Zeiss, Germany) at 630x magnification to quantify the cells containing a cilium, and to measure the length of cilia. To quantify the percentage of cells containing a cilium, cells containing a cilium equal to or greater than 1.5 μm were considered ciliated.

3.3.6 EPDC EMT assay *in vitro*

When embryonic day 12.5-13.5 hearts are explanted on a collagen gel, epicardial cells grow outward and by about 12 hours, they begin to undergo epithelial-to-mesenchymal transition (EMT).²⁶ Collagen (1 mg/ml, type I rat tail collagen, VWR CanLab) was solidified to a gel in 24-well plates and hydrated with OPTI-MEM media containing 1% FBS and insulin-transferrin-selenium (ITS) for 30 minutes at 37 °C. To determine the effect of ciliary disassembly on EMT, ventricles of E13.5 embryos were harvested as described above and plated on the hydrated collagen gel.^{23,26} M199 medium (Sigma-Aldrich, St. Louis, MO) containing Ad-GFP or Ad-shIft88 (10^7 PFU) was then added to the culture. After three days, the number of spindle shaped cells grown outward from the explanted ventricles was quantified. Images were captured using phase contrast microscope (Observer D1, Zeiss, Germany).

3.3.7 Histological analysis

Both adult and neonatal samples were fixed in 4% paraformaldehyde at 4 °C overnight, dehydrated in ethanol, and paraffin embedded. Hearts were cut into 5 µm sections (Leica RM2255 microtome) and mounted on positively charged microslides. All images for histological analysis were obtained using a light microscope and Axiocam ICc 5 camera (Zeiss, Germany). Cardiac tissue sections from adult mice 21 days post-MI were stained with hematoxylin and eosin (H/E) for analysis of myocyte cell size.²⁷ Myocyte diameter was measured as shortest cross sectional diameter at nuclei level in a minimum of 5 sections and 50 cells per heart.

3.3.8 Immunohistochemical analysis

To assess the number of Wt1 positive cells, heart sections were immunostained using rabbit anti-mouse Wt1 antibody (1:800, Calbiochem, San Diego, CA) following antigen retrieval in citrate buffer 10 mM pH 6.0 for 12 minutes at 94 °C using a microwave oven (BP-111; Microwave Research & Applications, Inc., Carol Stream, IL).⁶ EMT is thought to result in coronary artery formation and neovascularization post-MI.²⁸ Thus, capillary and arteriole abundance was quantified in the peri-infarct area 5 days post-MI, the time when EPDCs begin to re-differentiate, and 21 days post-MI, to ensure a long-lasting effect on vascularization. To quantify capillary abundance, heart sections were stained with biotinylated *Griffonia (Bandeiraea) simplicifolia* lectin I (1:200, Vector Laboratory, CA). Arteriole abundance was analyzed by staining smooth muscle cells with α -smooth muscle actin antibody (α -SMA; 1:1000, Sigma-Aldrich, St. Louis, MO). Primary antibodies for Wt1 and α -SMA were followed by goat anti-rabbit IgG secondary antibody (1:500, Vector Laboratories) and rabbit anti-mouse IgG secondary antibody (1:500, Vector Laboratories) respectively. All signals were visualized using avidin and biotinylated HRP (Santa Cruz) followed by 3-3'diaminobenzidine tetrahydrochloride (Sigma-Aldrich St. Louis, MO). Nuclei were counterstained with modified Mayer's hematoxylin (Thermo Scientific, Waltham, MA). The abundance of positive signal was analyzed in at least 5 individual heart sections per sample, and at least 4 fields in each section. For quantification of Wt1 positive cells, arteriole abundance, and capillary abundance, the number of positive cells/vessels were quantified and normalized to the myocardial area in each section.⁶

3.3.9 Real-time qPCR

For analysis of expression of *Ift88* and *E-cadherin* in cells, EPDCs grown as discussed above were rinsed twice with PBS, and total RNA collected in 150 μ L of Trizol (Ambion, Foster City, CA). For *in vivo* expression analysis, the peri-infarct area of hearts was collected three days post-MI. Tissue was rinsed in PBS and homogenized (Pro Scientific homogenizer) in Trizol. Moloney murine leukemia virus (M-MLV) reverse transcriptase was used to synthesize cDNA (from a minimum total RNA of 0.35 μ g for cells and 0.55 μ g for tissue) in 20 μ L reactions. EvaGreen qPCR MasterMix (ABM, Vancouver, BC) was used for real-time PCR amplification with 2 μ L cDNA, as per the manufacturer's instructions. Samples were amplified for 35 cycles using an Eppendorf Realplex² Real-Time qPCR machine and analyzed using cycle threshold (Ct) analysis. Primer sequences for expression analysis are listed in **Table 3.1**. The mRNA levels in relation to murine glyceraldehyde 3-phosphate dehydrogenase (*GAPDH*) as an internal control were determined using a comparative C_T method.²⁷

Table 3.1 Real-time RT-PCR primer sequences

Gene	Accession #	Forward	Reverse
<i>Ift88</i>	NM_009376	gcgtttcttggttcgtctct	cactcccctctcgtttgct
<i>E-Cadherin (Cdh1)</i>	NM_009864	actgtgaagggacggtcaac	ggagcagcaggatcagaatc
<i>Snail1</i>	NM_011427.2	cacacgctgccttgtgtct	ggtcagcaaaagcacggtt
<i>Slug</i>	NM_011415.2	caacgcctccaagaagccca	gagctgccgacgatgtccat
<i>β-Catenin</i>	NM_001165902	cttggtgaacctcacagat	agcttccttttgaaagctg
<i>Wnt1</i>	NM_021279	ctggaactgccccactgct	gccaaagaggcgacccaaaat
<i>Tbx18</i>	NM_023814	gagcagcaaccgctctgtga	gggactgtgcaatcgggaagg
<i>HIF-1α</i>	NM_001313919	cagcctcaccagacagagca	gtgcacagtcacctggttgc
<i>bFGF</i>	NM_008006	caagggagtgtgtgccaacc	tgccagttcgtttcagtgc
<i>Aldh1a2</i>	NM_009022.4	ggcagcaatcgcttctcaca	cagcactggccttggtgaa
<i>Tgf-β1</i>	NM_011577	gcccgaagcggactactatg	cactgctcccgaatgtctg
<i>GAPDH</i>	NM_001289726	gatgggtgtgaaccacgaga	agtgatggcatggactgtgg

3.3.10 Statistical Analysis

Data are means \pm SEM. A one- or two-way ANOVA followed by a Bonferroni test was performed for multiple group comparisons (GraphPad Prism program, version 6.0). An unpaired Student's t-test was used to detect significance between two groups. All tests were two sided, using a significance level of $P < 0.05$.

3.4 Results

3.4.1 Outgrowth of cultured EPDCs

When grown in culture, EPDCs can grow outward from E13.5 heart explants to form a cobblestone monolayer of cells (**Figure 3.1A**). After passage 1 EPDCs were plated on gelatin coated coverslips, and EPDC purity was confirmed by detecting Wilms' Tumour 1 (Wt1) expression; 100% of cells outgrown from heart explants were Wt1 positive, indicating all cells exhibited traits of EPDCs (**Figure 3.1B**).

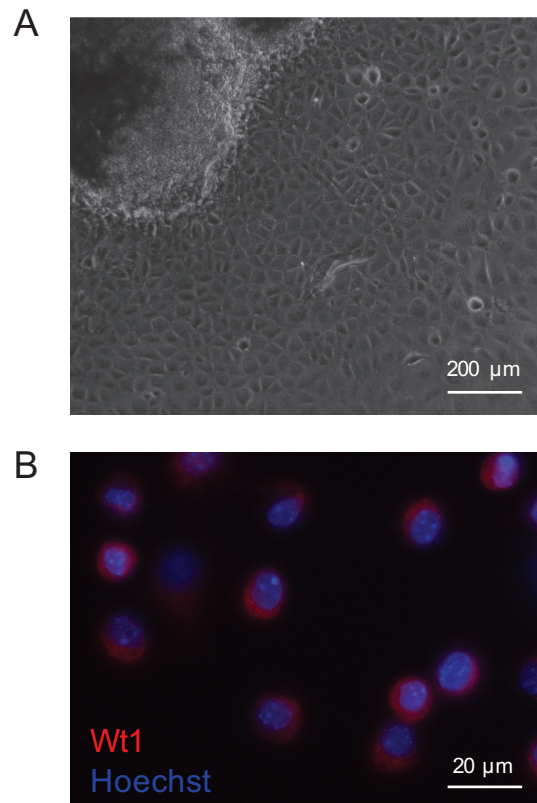


Figure 3.1 *In vitro* culture of EPDCs.

After heart explant culture, epicardium derived cells grow in a cobblestone shaped cell monolayer around the explant. A) Cobblestone cells observed three days after explant. Passage 1 EPDCs grown outward from heart explants can be used for future experiments.. B) Passage 1 EPDCs were 100% positive for Wt1 (red). Nuclear counterstain with Hoechst (blue).

To determine the direct effects of ciliary knockdown on EPDCs, two different *in vitro* assays were used. First, passage 1 EPDCs were grown on gelatin coated 24-well plates, and treated with 10^7 PFU of an adenoviral construct containing shRNA for Intraflagellar transport protein 88 (Ad-shIft88), a protein vital to ciliary assembly, or a green fluorescent protein adenovirus control (Ad-GFP). Two days after treatment, medium was changed to virus free, serum free medium to elucidate the presence of the cilium in culture. *Ift88* mRNA from these cells was quantified by real time RT-qPCR. Treatment with Ad-shIft88 significantly reduced *Ift88* transcript levels as compared to Ad-GFP treated cells ($P < 0.05$, **Figure 3.2C**). Additionally, a significant reduction in *E-cadherin* (*Cdh1*) mRNA levels, a characteristic of EMT, was observed ($P < 0.05$, **Figure 3.2C**). Notably, the primary cilium was revealed in cultured EPDCs using immunostaining of acetylated α -tubulin (with dense localization in the primary cilium) (**Figure 3.2A**). Ad-shIft88 treatment significantly reduced cilia length ($P < 0.01$) as well as the percent of ciliated cells ($P < 0.05$) (**Figure 3.2B**).

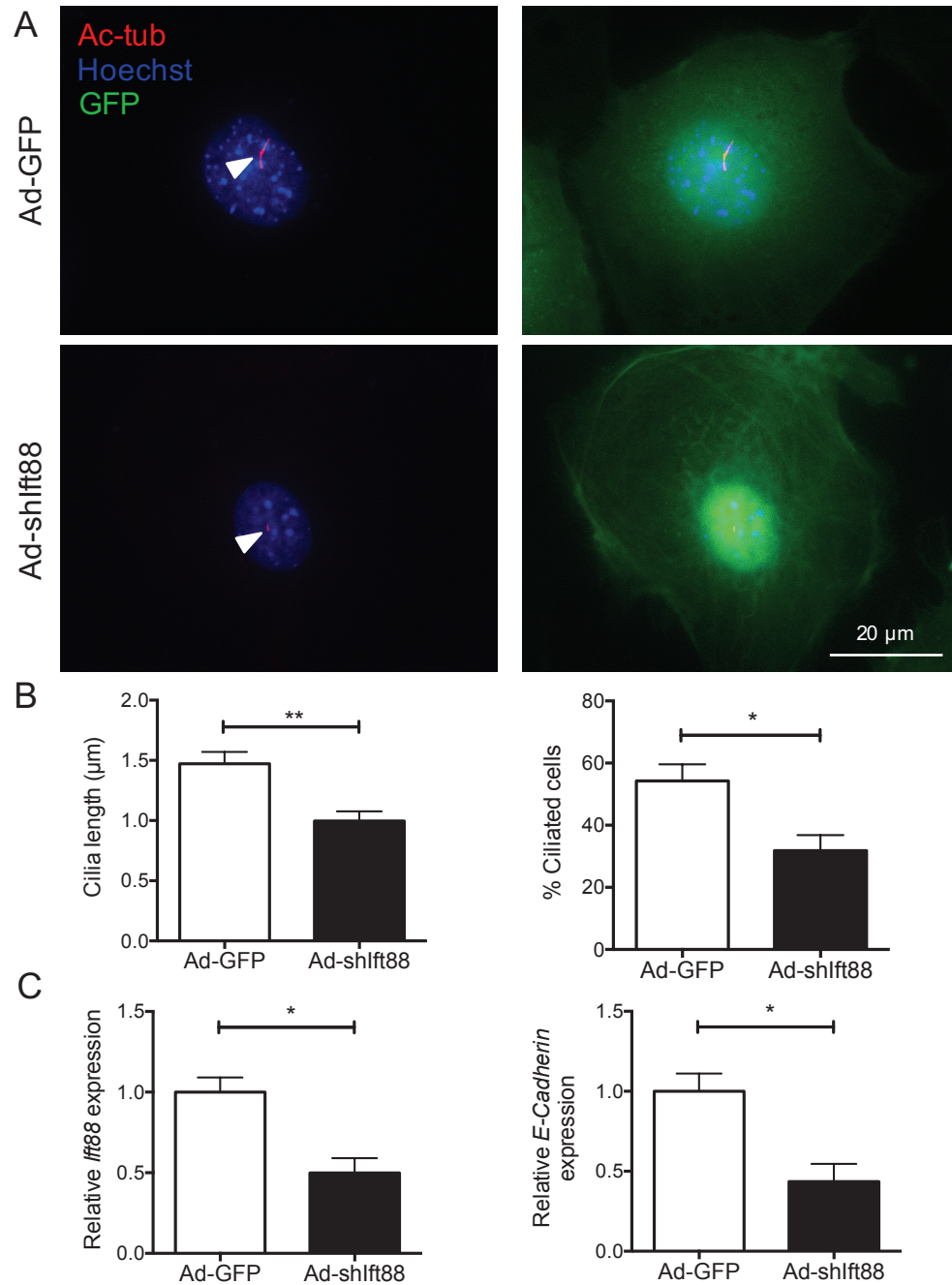


Figure 3.2. Ad-shIft88 reduces Ift88 expression, ciliary number, cilia length, and cellular E-cadherin mRNA in EPDCs.

Epicardium derived cells (EPDCs) isolated from E13.5 cardiac explants were grown on a gelatin coated dish. Cells were treated with 10^7 PFU Ad-GFP or Ad-shIft88 for 48 hours followed by 24 hours serum starvation. A) Representative image of EPDCs stained with acetylated α -tubulin (red; white arrow head). Control and treatment adenovirus infection indicated by GFP expression (green). Each image shows a single cell. B) Cilia length and percentage of cells with the primary cilium longer than 1.5 μ m. C) *Ift88* and *E-Cadherin* mRNA levels measured by real-time qPCR. Data are presented as mean \pm SEM from 3 independent experiments. * P <0.05, ** P <0.01.

3.4.2 Epicardial EMT *ex-vivo*

To investigate whether Ift88 knockdown supports epicardial EMT, E13.5 hearts were cultured on a collagen gel to allow epicardial cell outgrowth, and cell EMT to become spindle shaped cells.³⁰ The number of spindle shaped cells was quantified and normalized to heart explant area. Ad-shIft88 treated cultures had a significantly higher number of spindle shaped EPDCs as compared to Ad-GFP controls ($P < 0.05$, **Figure 3.3**). These data indicate that Ift88 knockdown supports EMT of epicardial cells.

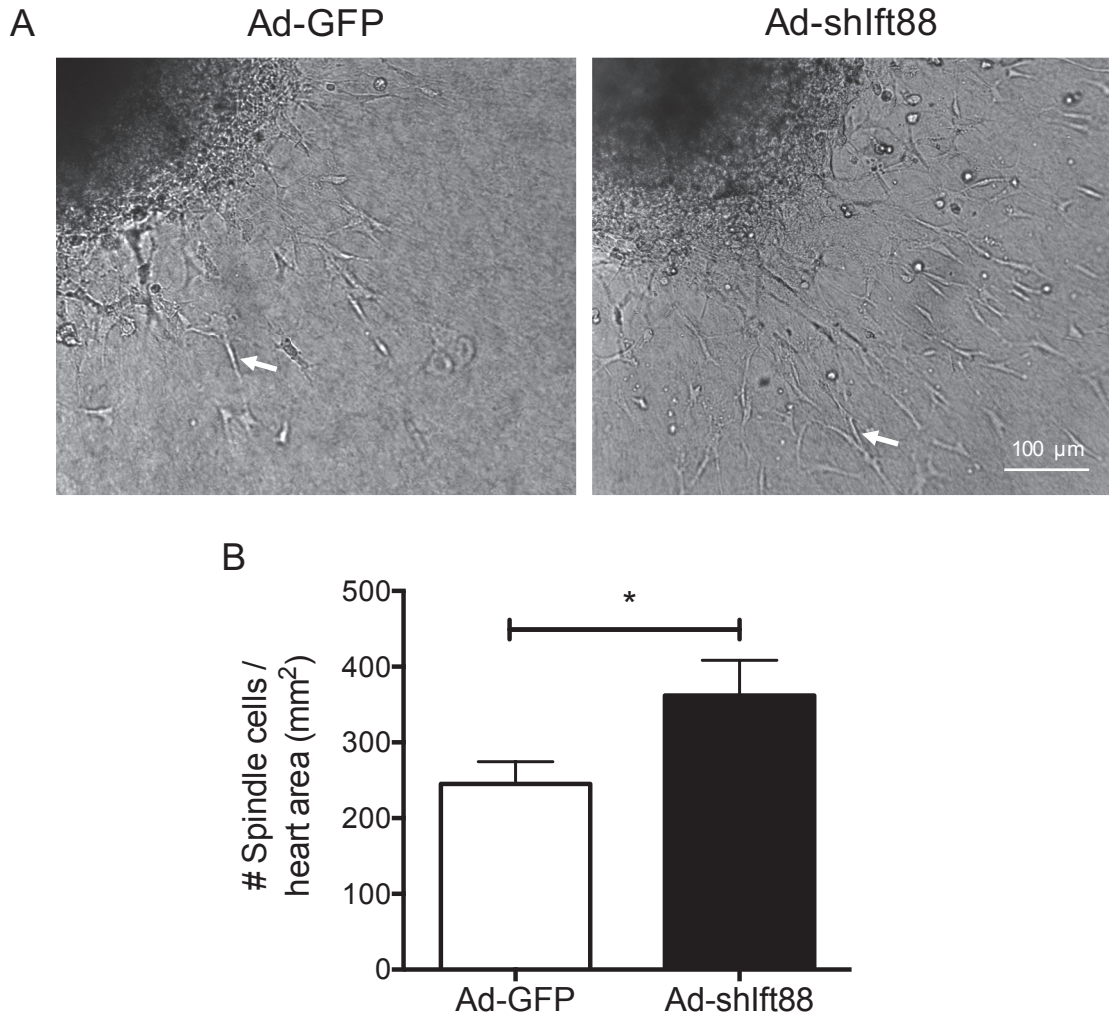


Figure 3.3. Inhibition of Ift88 promotes EPDC EMT.

Epicardial cells migrate from cardiac explant culture to become EPDCs and undergo EMT to become mesenchymal like (white arrow). A) E13.5 heart explants were cultured on collagen coated dishes with Ad-GFP or Ad-shIft88 (10^7 PFU) treatment. B) Three days post-treatment the number of spindle shaped cells (the cells that have undergone EMT) was quantified. Data are mean \pm SEM from 9 independent experiments. * $P < 0.05$.

3.4.3 Ift88 knockdown in a post-regenerative *in vivo* model

To investigate the effect of primary ciliary disassembly on cardiac function after injury in a post-regenerative state, myocardial infarction (MI) or sham surgery was performed on postnatal day 7 (P7) C57BL/6 mice, followed by intramyocardial injection of Ad-shIft88 or Ad-GFP (10^9 PFU). Cardiac function was assessed by echocardiography 21 days-post infarction (P28) (the time required for full cardiac regeneration in the neonatal mouse).¹⁸ Representative M-mode images of echocardiographic measurements are shown in **Figure 3.4A**. Measurements of ejection fraction (EF) and fractional shortening (FS) indicate that MI significantly reduced cardiac function as compared to aged matched sham operated animals ($P < 0.01$, **Figure 3.4B**). The left ventricular internal diameter during systole was also significantly increased after MI in the Ad-GFP group ($P < 0.05$). Notably, mice that received Ad-shIft88 treatment had a significantly higher EF and FS than the Ad-GFP treated group ($P < 0.05$ for both). Importantly, both EF and FS of mice treated with Ad-shIft88 were restored to similar levels as sham operated mice.

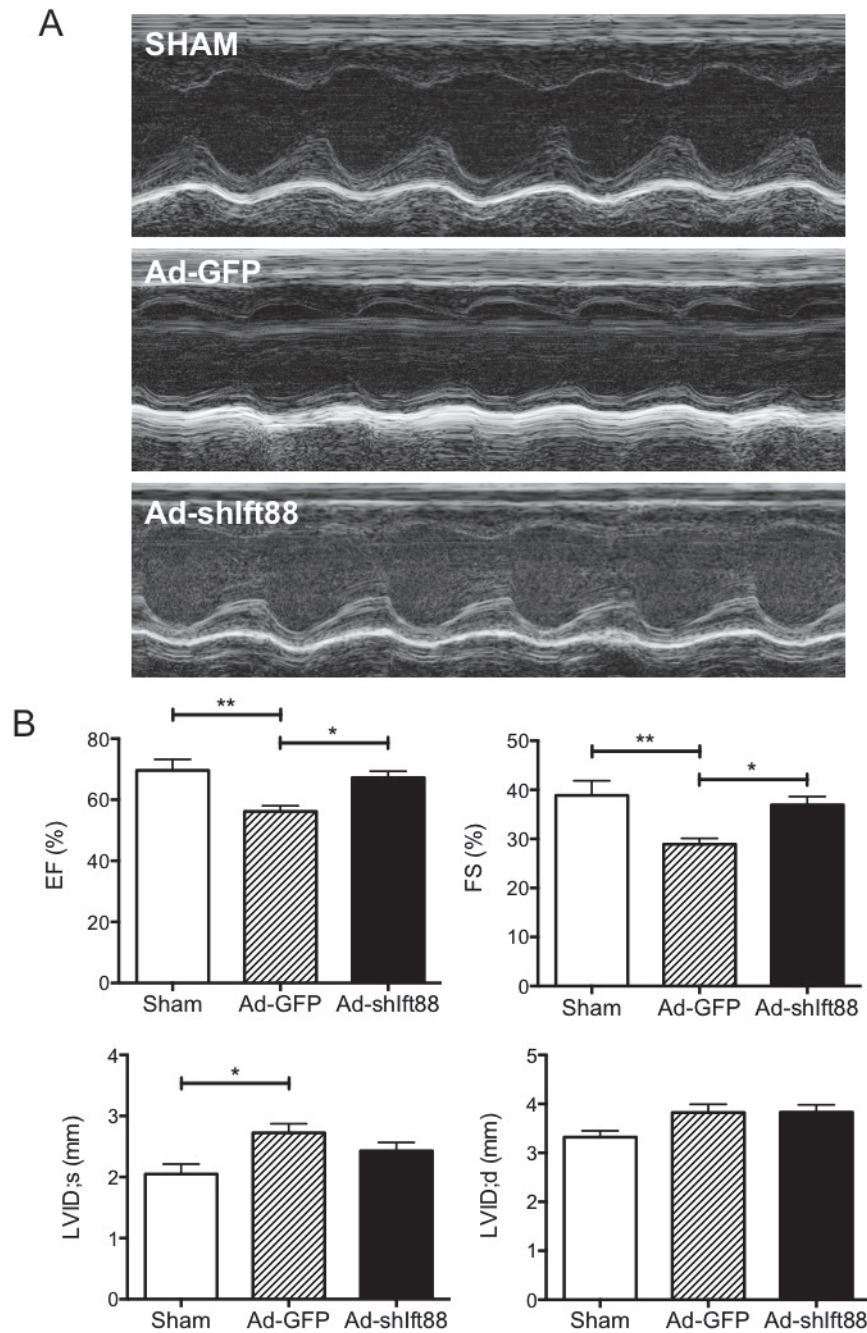


Figure 3.4. Inhibition of Ift88 attenuates cardiac functional impairment post-myocardial infarction in neonatal mice.

Postnatal day 7 (P7) mice were subjected to MI by coronary artery ligation, and hearts were injected with Ad-GFP or Ad-shIft88 (10^9 PFU) in the peri-infarct area. Echocardiography was performed 21 days post-MI (P28). A) Representative M-mode images. B) Measurements of ejection fraction (EF), fractional shortening (FS) and left ventricular internal diameter (LVID) at systole and diastole. Data are mean \pm SEM, n = 8-9 mice per group. * $P < 0.05$, ** $P < 0.01$.

Next, fibrotic scar development was assessed 21 days post-MI as an indicator of the propensity for contractile tissue regeneration. Masson's trichrome staining of heart sections revealed the formation of a significant scar post-P7 MI (**Figure 3.5A**). This data is in agreement with the published demonstration of loss of the regenerative phenotype by P7.⁵ Notably, there was a significantly smaller scar in Ad-shIft88 treated hearts as compared to Ad-GFP controls ($P < 0.05$, **Figure 3.5B**), indicative of enhanced cardiac repair post-MI.

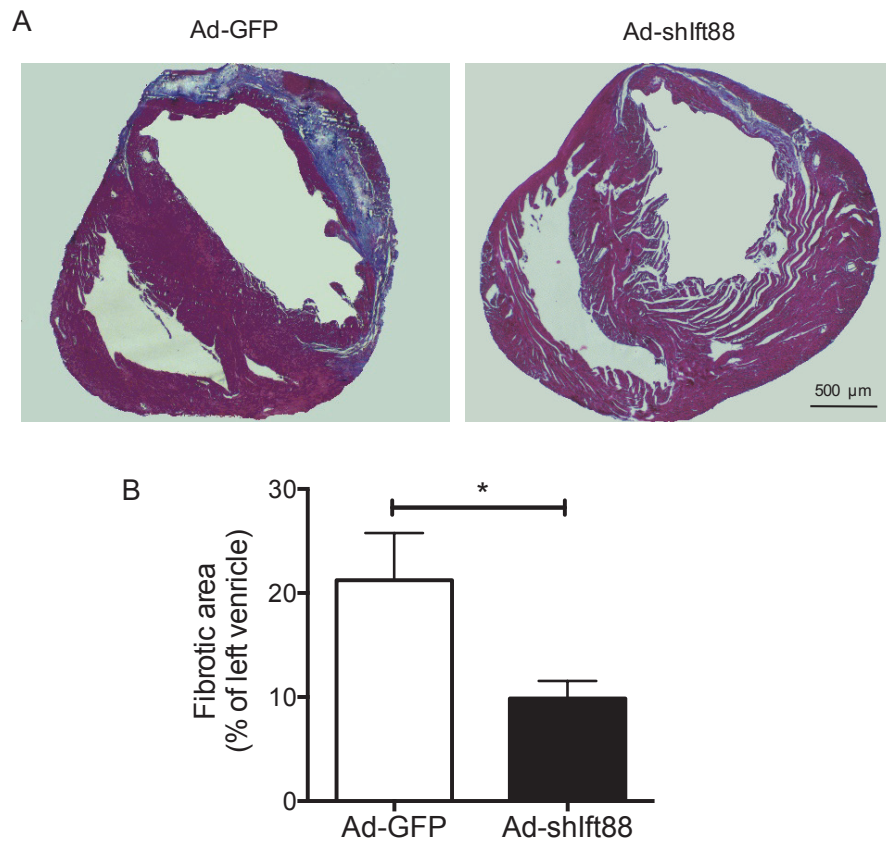


Figure 3.5. Inhibition of Ift88 attenuates infarct size post-myocardial infarction in neonatal mice.

Postnatal day 7 (P7) mice were subject to MI by coronary artery ligation, and hearts were injected with Ad-GFP or Ad-shIft88 (10^9 PFU) in the peri-infarct area. A) Hearts were collected 21 days post-MI (P28) and stained with Masson's trichrome stain. Red indicates cytoplasm & muscle; blue indicates collagen. B) The fibrotic area in the heart calculated as % of left ventricular myocardium area. Data are mean \pm SEM, $n = 13-15$ mice per group (6-7 litters). * $P < 0.05$.

3.4.4 Cardiac function post-MI in adult mice

To determine whether ciliary disassembly affects the capacity for cardiac repair post-MI in the adult, coronary artery ligation was performed in adult mice (2 – 4 months of age). Cardiac function was assessed by echocardiography before MI (baseline), and 5 and 21 days post-MI. Representative images are shown in **Figure 3.6**. MI significantly reduced EF and FS ($P < 0.01$, **Figure 3.7**), however this reduction was abrogated by Ad-shIft88 ($P < 0.01$). Furthermore, MI resulted in a significant increase in the left ventricular internal diameter (LVID) in both groups ($P < 0.001$ for Ad-GFP, $P < 0.05$ for Ad-shIft88), however this increase was significantly lower after Ad-shIft88 treatment ($P < 0.05$, **Figure 3.7C & D**).

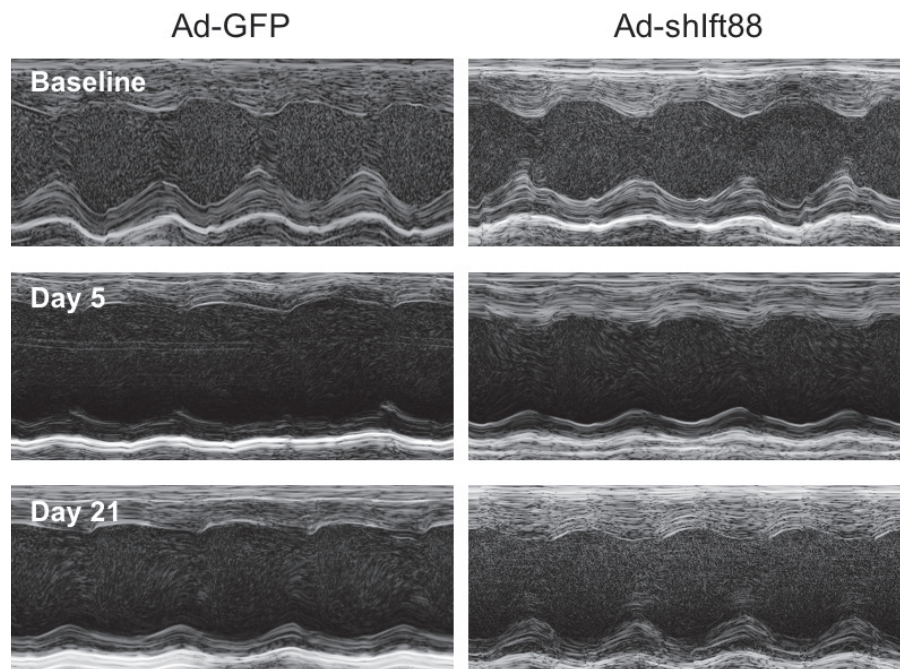


Figure 3.6. Inhibition of Ift88 attenuates cardiac functional impairment post-myocardial infarction in adult mice.

Mice were subjected to MI by coronary artery ligation and injected with Ad-GFP or Ad-shIft88 (10^{10} PFU) in the peri-infarct area. Shown are representative M-mode images of echocardiography performed before infarction (baseline), and at 5 days and 21 days post-MI.

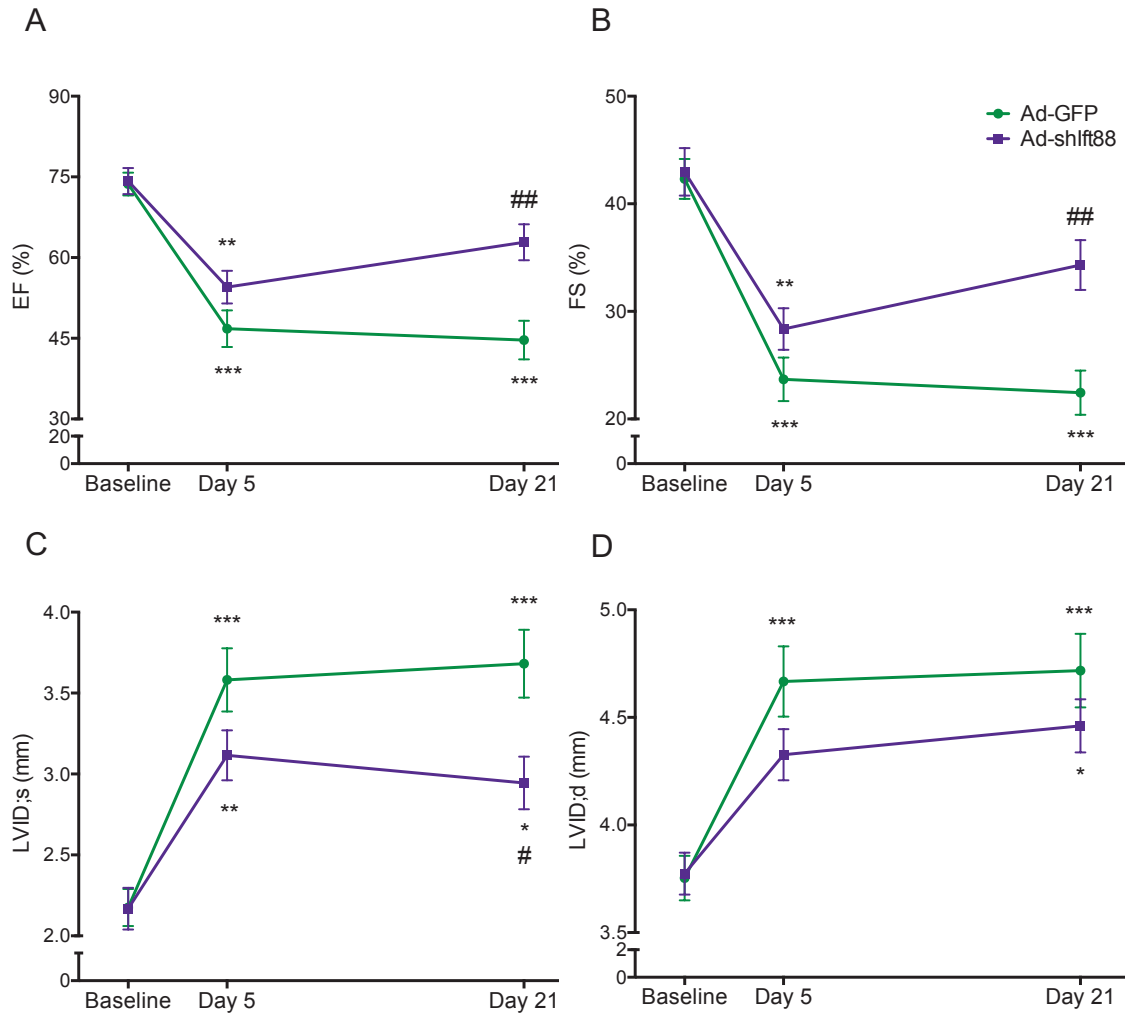


Figure 3.7. Inhibition of Ift88 attenuates cardiac functional impairment post-myocardial infarction in adult mice.

Mice were subjected to MI by coronary artery ligation and injected with of Ad-GFP or Ad-shIft88 (10^{10} PFU) in the peri-infarct area. Echocardiography was performed before infarction (baseline), and at 5 days and 21 days post-MI. Measurements of A) ejection fraction (EF), B) fractional shortening (FS), C) left ventricular internal diameter during systole (LVID;s) and D) left ventricular internal diameter during diastole (LVID;d). Data are mean \pm SEM, n = 10-11 mice per group. * P <0.05, ** P <0.01, *** P <0.001 vs. baseline. # P <0.05, ## P <0.01 vs. Ad-GFP group.

3.4.5 Epicardial activation and growth factor release 3 days post-MI in adult mice

To investigate the mechanisms responsible for preserved cardiac function in the Ad-shIft88 treated group, the involvement of EMT was evaluated 3 days post-MI. Both epicardial and myocardial Wt1 expression was assessed by immunohistochemistry (**Figure 3.8A**). Quantitative analysis demonstrated that there were significantly more Wt1 positive cells both on the epicardium in the peri-infarct area as well as in the myocardium of the peri-infarct area in Ad-shIft88 treated mice compared to Ad-GFP treated mice post-MI ($P < 0.05$, **Figure 3.8B**).

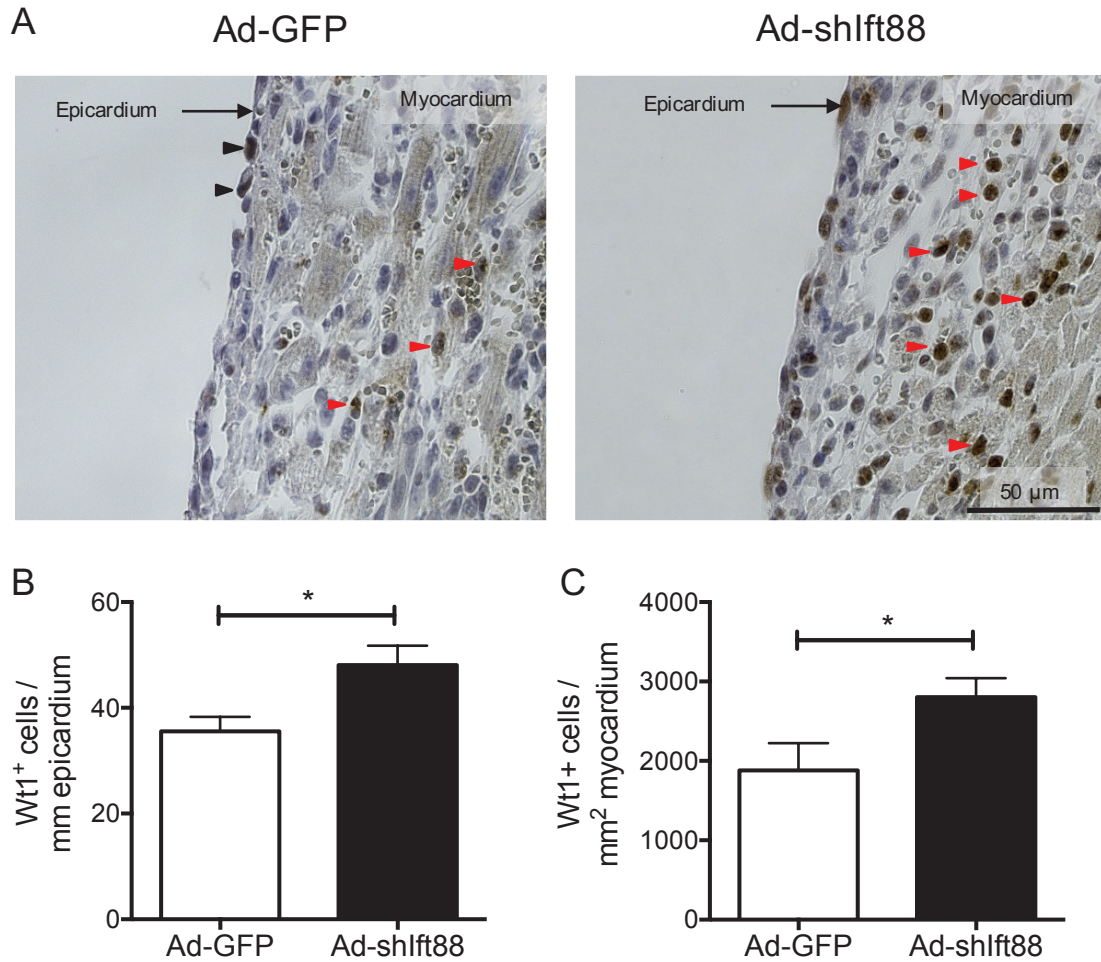


Figure 3.8. Inhibition of Ift88 augments Wt1 expression in the peri-infarct area post-MI.

Adult mice were subjected to MI by coronary artery ligation and injected with either Ad-GFP or Ad-shIft88 (10^{10} PFU) intramyocardially in the peri-infarct area. Hearts were collected 3 days post-MI. A) Representative images of Wt1 staining. Wt1 positive cells show dark brown nuclear staining. Black and red arrow heads point to Wt1 positive cells in the epicardium and myocardium, respectively. Quantification of Wt1 positive cells in B) epicardium and C) myocardium of the peri-infarct area. Data are mean \pm SEM, n = 8-9 mice per group. * $P < 0.05$ vs. Ad-GFP.

To further understand the effect of primary ciliary disassembly on EMT in the peri-infarct area post-MI, expression of key molecular regulators of EMT was measured by RT-qPCR. *Tbx18* is also a known epicardial transcription factor enriched in the embryonic heart, and marks epicardial activation after injury.^{31, 32} *Tbx18* has been shown to upregulate *Snail* and *Slug* expression, which are involved in EMT and critically modulate *E-cadherin* expression.^{33, 34} *Wnt1* and β -catenin are also critical to EMT and aid in epicardial activation via both canonical Wnt (β -catenin-dependent) and non-canonical Wnt signaling (β -catenin-independent).³⁵ There has also been a direct role established between *Wt1* expression and both β -catenin and retinoic acid signaling pathways (aldehyde dehydrogenase 2, *Aldh1a2* gene).³⁶ Importantly, *Tbx18*, *Snail*, *Slug*, *Wnt1*, β -catenin, and *Aldh1a2* are all known to be expressed by transitioning EPDCs. Ad-shIf88 treatment significantly increased the mRNA expression of *Tbx18*, *Snail*, *Slug*, *Wnt1*, and β -catenin in the peri-infarct area post-MI ($P < 0.05$, **Figure 3.9**). A trend also indicates an increase in *Aldh1a2* expression, however this was not statistically significant (**Figure 3.9F**). Additionally, hypoxia-inducible factor 1-alpha (HIF-1 α) is a master regulator of vasculogenesis, which induces growth factors to provoke both EMT and blood vessel development.³⁷ For example, HIF-1 α is increased in the peri-infarct region post-MI, and it promotes the expression of basic fibroblast growth factor (bFGF) and platelet derived growth factor -B (PDGFB), well known pro-angiogenic growth factors.³⁸⁻⁴⁰ Not only are bFGF and PDGFB suggested to play a role in activating EPDCs, they also support cardiomyocyte survival, function, and proliferation via a paracrine mechanism.^{41, 42} Expression of *HIF-1 α* , *bFGF*, and *PDGFB* were all significantly higher in the Ad-shIf88 treated group as compared to controls ($P < 0.05$, **Figure 3.10**). Finally, EMT of EPDCs is

regulated by TGF- β .⁴³ Although not significant, there was a trend of an increase in *TGF- β* mRNA expression in the Ad-shIft88 treated group ($P=0.059$, **Figure 3.10D**). Together, these results indicate that Ad-shIft88 enhances the expression of transcription and growth factors that promote epicardial EMT post-MI.

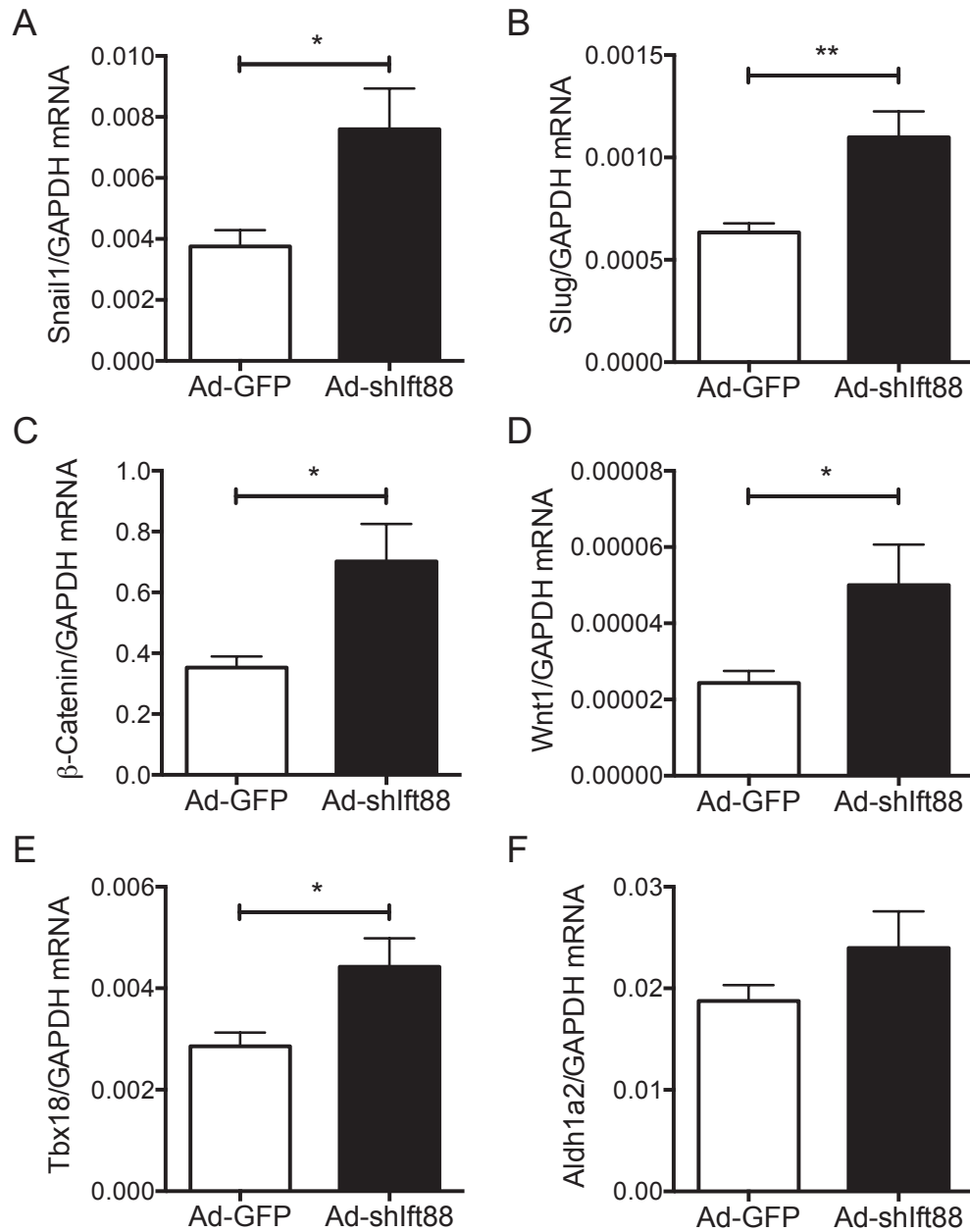


Figure 3.9. Expression of EMT markers is upregulated post-MI in hearts treated with Ad-shIft88.

Adult mice were subjected to MI by coronary artery ligation and injected with either Ad-GFP or Ad-shIft88 (10^{10} PFU) intramyocardially in the peri-infarct area. Tissues from peri-infarct area were collected 3 days post-MI. mRNA levels were analyzed by real-time qPCR for A) *Snail*, B) *Slug*, C) β -Catenin, D) *Wnt1*, E) *Tbx18*, and F) *Aldh1a2*. Data are mean \pm SEM, n = 6 mice per group. * $P < 0.05$ vs. Ad-GFP.

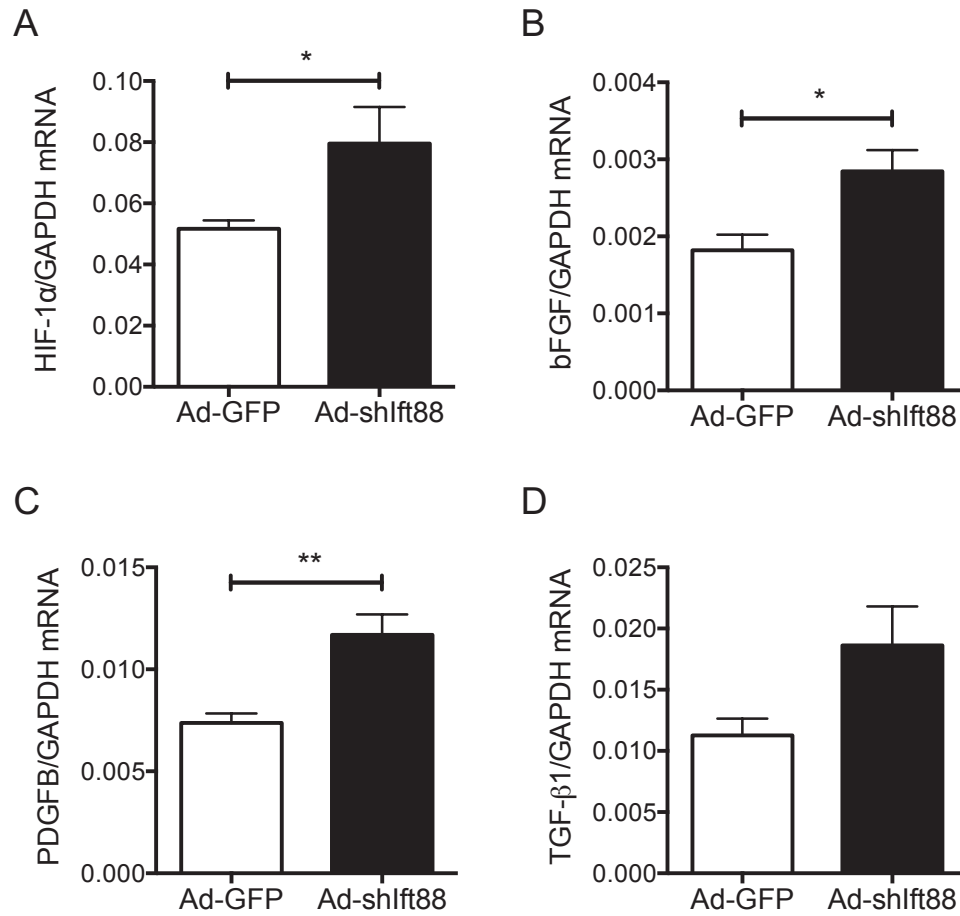


Figure 3.10. Ad-shIf88 treatment increases myocardial expression of HIF-1 α and its downstream targets that are implicated in neovascularization and EMT.

Adult mice were subjected to MI by coronary artery ligation and injected with either Ad-GFP or Ad-shIf88 (10^{10} PFU) intramyocardially in the peri-infarct area. Tissues from peri-infarct area were collected 3 days post-MI. mRNA levels were analyzed by real-time qPCR for A) *HIF-1 α* , B) *bFGF*, C) *PDGFB*, and D) *TGF β 1*. Data are mean \pm SEM, n = 6 mice per group. * P <0.05, ** P <0.01 vs. Ad-GFP.

3.4.6 Capillary and arteriole density 5 and 21 days post-MI

EPDCs are essential for the development of endothelial cells of the coronary vasculature.⁴⁴ Given the observed increase in EPDC activation post-MI, we hypothesized that Ad-shIft88 treatment would augment angiogenesis in the peri-infarct region. To investigate these effects, lectin staining was employed to specifically stain endothelial cells and quantify myocardial capillary density (**Figure 3.11A**). As early as 5 days post-MI, myocardial capillary density was significantly higher in the Ad-shIft88 treated group as compared to the Ad-GFP group ($P<0.05$, **Figure 3.11B**). This difference was maintained to day 21 post-MI ($P<0.05$, **Figure 3.11C**).

As with endothelial cells, EPDCs are thought to contribute to the development of the smooth muscle cell compartment of the coronary circulation.⁴⁴ To determine whether enhanced epicardial activation affected arteriogenesis in the peri-infarct region, α -SMA staining was employed to stain smooth muscle cells. The number of arterioles (between 10-150 μm in diameter) in the peri-infarct area 5 days post-MI was quantified. Arteriole density was significantly higher in Ad-shIft88 treated hearts as compared to Ad-GFP mice ($P<0.05$, **Figure 3.12B**). This difference was maintained in the long term to the 21 day time point post-MI ($P<0.05$, **Figure 3.12C**). These data suggest that knockdown of primary cilia function supports EMT and neovascularization post-MI.

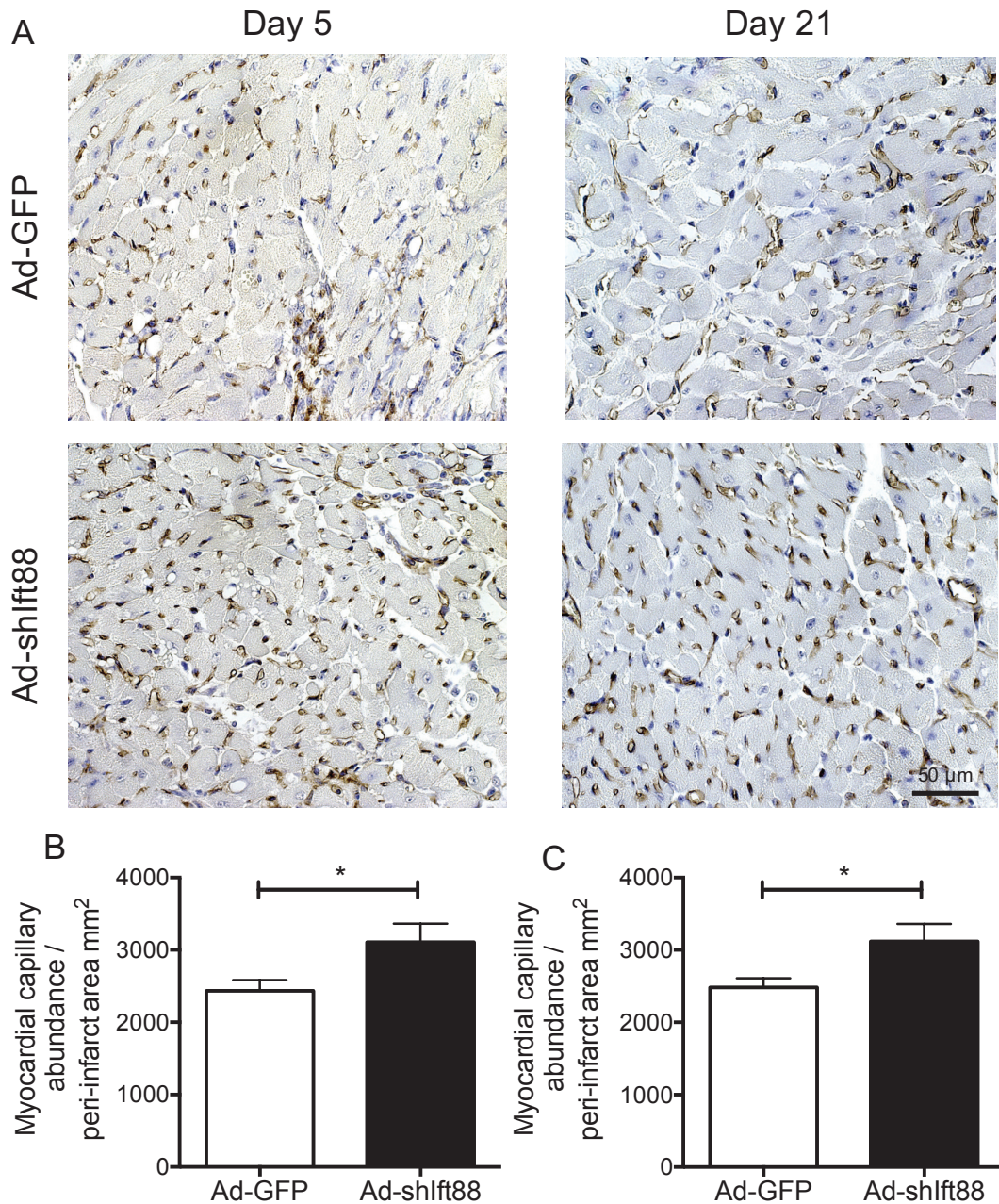


Figure 3.11. Inhibition of Ift88 improves myocardial capillary density in the peri-infarct area post-MI.

Adult mice were subjected to MI by coronary artery ligation and injected with either Ad-GFP or Ad-shIft88 (10^{10} PFU) in the peri-infarct area. A) Representative images of lectin staining (brown). Quantification of capillary density in the peri-infarct area B) 5 days and C) 21 days post-MI. Data are mean \pm SEM, $n = 5-6$ mice per group for day 5 and $8-9$ mice per group for day 21. * $P < 0.05$ vs. Ad-GFP.

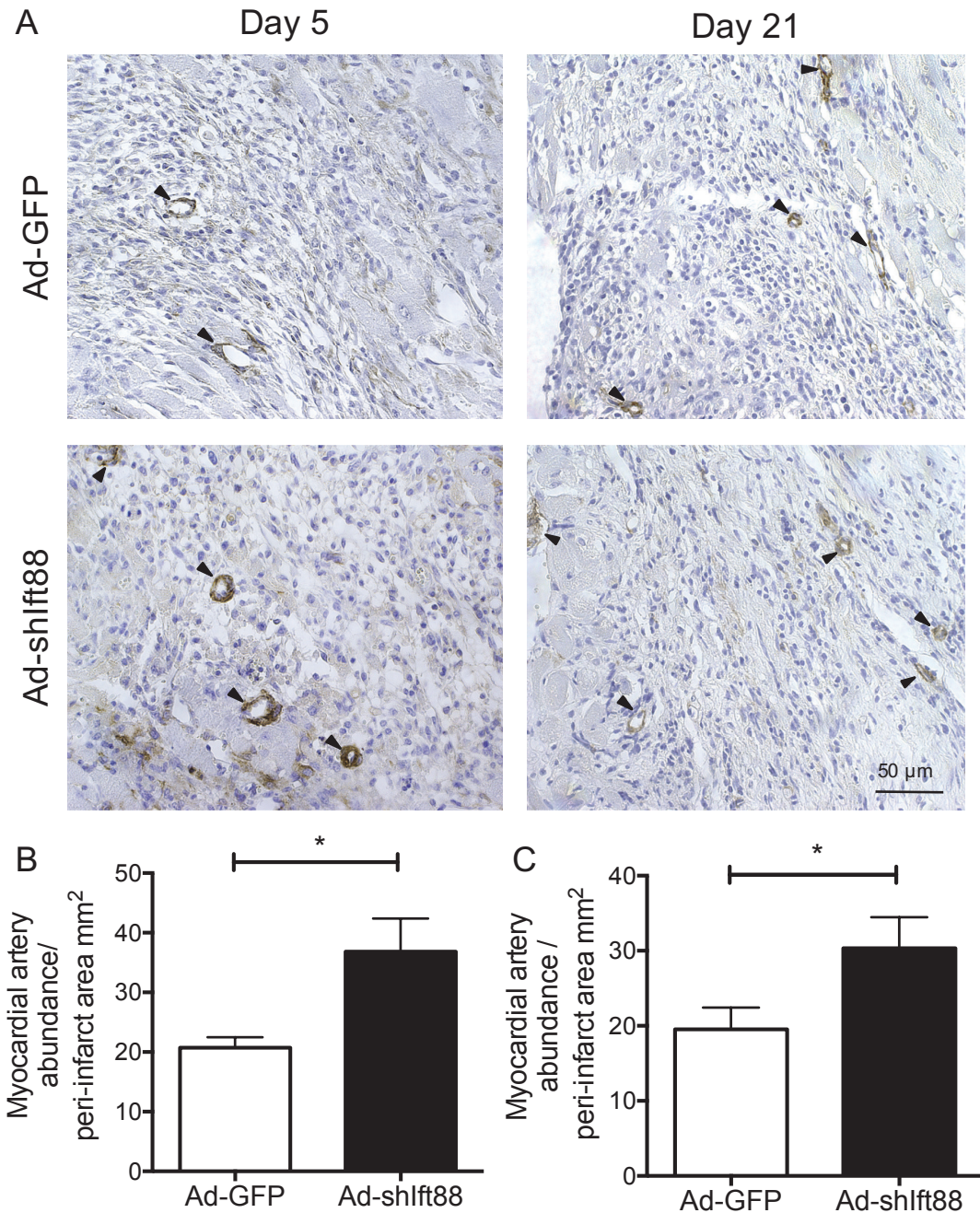


Figure 3.12. Inhibition of Ift88 improves arteriolar density in the peri-infarct area post-MI.

Adult mice were subjected to MI by coronary artery ligation and injected with either Ad-GFP or Ad-shIft88 (10^{10} PFU) in the peri-infarct area. A) Representative images of α -SMA staining. Arterioles were identified as small vessels 10-150 μ m in diameter surrounded by α -SMA positive cells. Black arrows indicate arterioles. Quantification of arteriolar density in the peri-infarct area B) 5 days and C) 21 days post-MI. Data are mean \pm SEM, n = 5-6 mice per group for day 5 and 8-9 mice per group for day 21. * P <0.05 vs. Ad-GFP.

3.4.7 Cardiac hypertrophy 21 days post-MI in adult mice

Hypertrophy of the left ventricular (LV) myocardium is indicative of detrimental cardiac remodeling post-MI and can be assessed by the heart weight/body weight ratio and the thickness of the ventricular septum. Both Ad-GFP and Ad-shIft88 treatment groups had a similar infarct size measured at 21 days post-MI ($39.5 \pm 5.3\%$ vs. $35.6 \pm 3.7\%$, $P=$ n.s.). However, although there were no significant differences in body weight (**Figure 3.13A**), a trend of a lower heart weight/body weight ratio was seen in the Ad-shIft88 treated group as compared to the control Ad-GFP treated group ($P=0.06$, **Figure 3.13B**). Furthermore, the ventricular septum measured at the level of the suture was significantly thinner in the Ad-shift88 group as compared to the Ad-GFP group, indicating an attenuated hypertrophic response by Ad-shIft88 treatment (**Figure 3.13C/D**). To further assess cardiac hypertrophy, cardiomyocyte cell size in the peri-infarct area was studied by measuring the minimum cross-sectional transverse diameter at the nuclear level of hematoxylin/eosin stained heart sections. Treatment with Ad-shIft88 significantly lowered cardiomyocyte cross-sectional diameter as compared to the Ad-GFP treated group ($P<0.05$; **Figure 3.13E/F**).

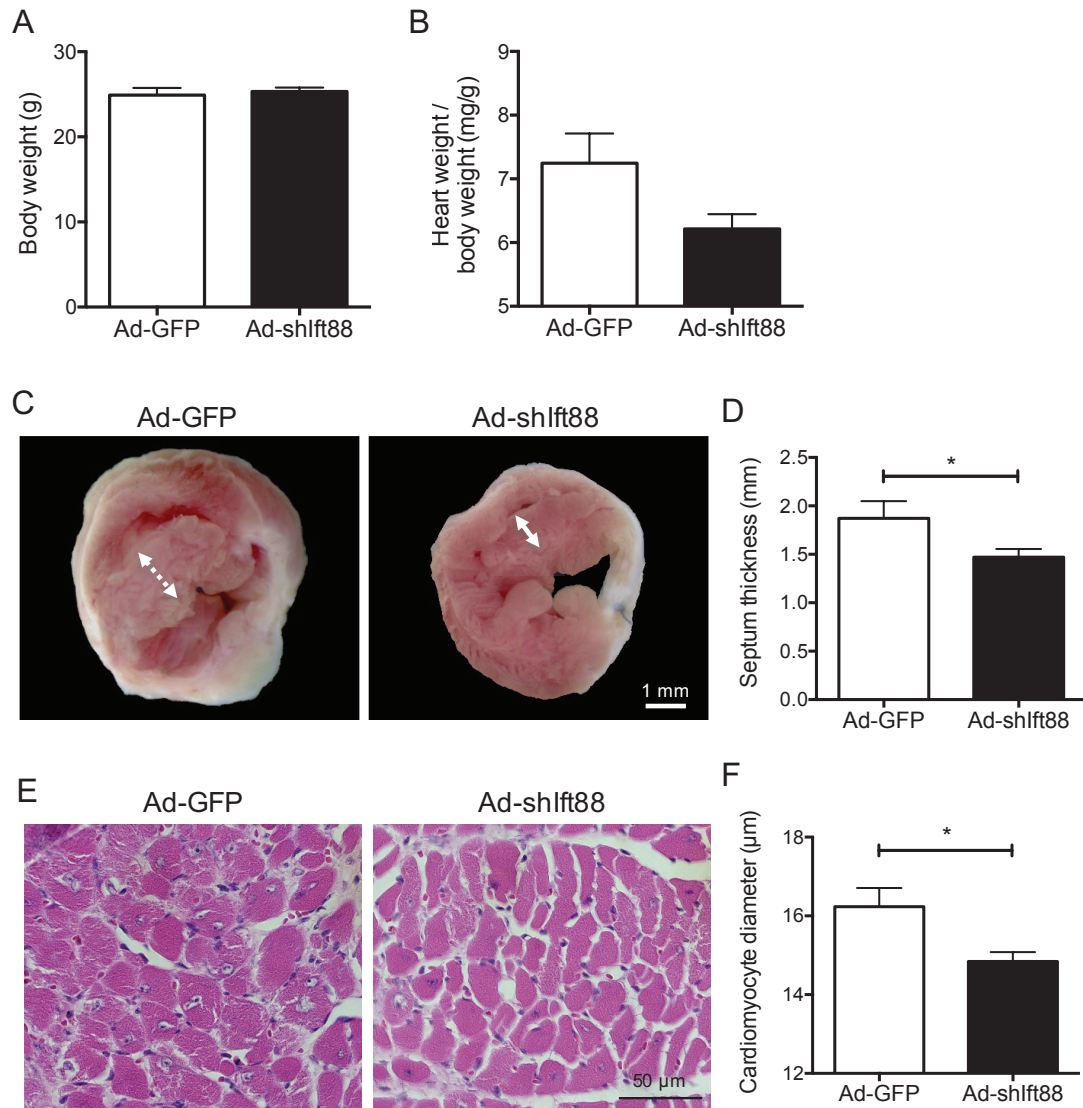


Figure 3.13. Inhibition of Ift88 attenuates cardiac hypertrophy 21 days post-MI.

Adult mice were subjected to MI by coronary artery ligation and injected with either Ad-GFP or Ad-shIf88 (10^{10} PFU) in the peri-infarct area. A) Body weight and B) heart weight / body weight ratio at 21 days post-MI. C) Representative heart sections 21 days post-MI. D) Quantification of ventricular septum thickness. E) Representative photomicrographs of hematoxylin and eosin stained sections showing cross-sections of cardiomyocytes. F) Analysis of cardiomyocyte diameter. Data are mean \pm SEM, n = 8-10 mice per group. * $P < 0.05$ vs Ad-GFP.

3.5 Discussion

The importance of epicardial activation for neovascularization post-MI has been established previously,⁶ however we demonstrate here a novel role for the primary cilium in modulating this process. The results presented herein indicate that knockdown of the required ciliary transport protein Ift88 promotes EMT and neovascularization post-MI, reduces the deleterious remodeling process and improves long-term cardiac function. These data show for the first time that the primary cilium can alter the healing response post-MI, and that primary ciliary disassembly increases EMT in the adult heart. Previous studies demonstrate the ability of Wt1 positive EPDCs to migrate into the infarct and peri-infarct area post-MI to contribute to neovascularization.⁶ However, this activation is not enough to completely salvage the ischemic myocardium post-MI. It is likely that the enhanced Wt1 expression in the epicardium and myocardium in the Ad-shIft88 treated hearts in our study is indicative of increasing numbers of active EPDCs which migrate into the myocardium. Our study suggests that this response improves neovascularization, a hypothesis supported by our observation of increased capillary and arteriole density in the peri-infarct area in the Ad-shIft88 treated group (summarized in **Figure 3.14**). Ad-shIft88 significantly reduced left ventricular chamber dilation, thereby preserving cardiac function. Furthermore, Ad-shIft88 significantly attenuated hypertrophic responses which typically contribute to the deleterious cardiac remodelling process causing cardiomyopathy.

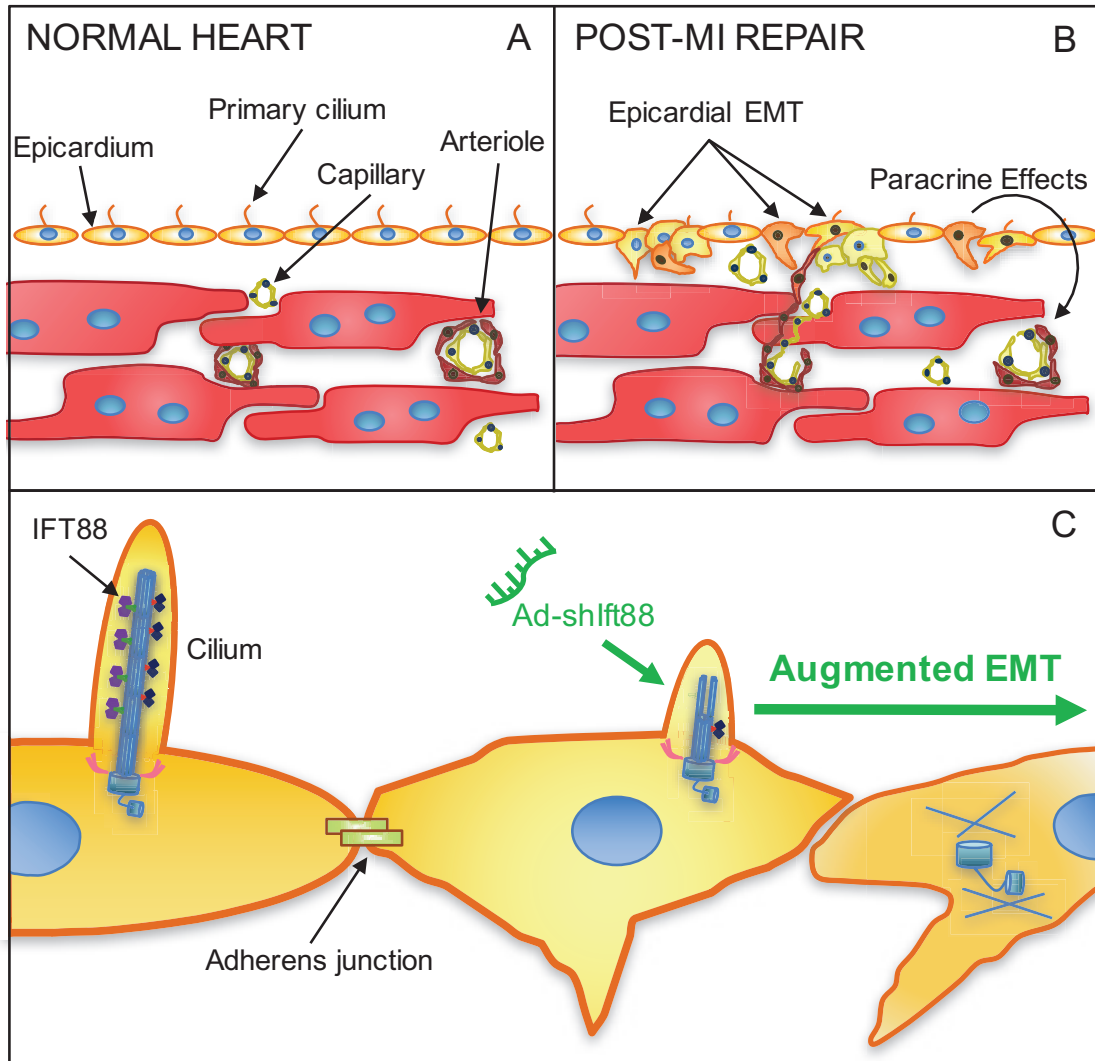


Figure 3.14. Schematic diagram of enhanced epicardial EMT via *Ift88* inhibition post-myocardial infarction (MI).

A) Adult epicardial cells are inherently dormant under normal physiological conditions, however after MI, epicardial cells are activated to undergo EMT. B) Epicardium-derived cells migrate into the myocardium and become mesenchymal cells in support of reparative vasculature. EPDCs also secrete paracrine mediators which aid in cardiac repair. C) *Ift88* knockdown by Ad-shIft88 inhibits primary cilium assembly and augments epicardial EMT post-MI.

Interestingly, cilia are required for proper situs during development, and mutations in ciliary proteins cause congenital heart defects.⁴⁵ Specifically, the primary cilia cannot endure high levels of shear stress, and the loss of cilia actually primes the endocardium to shear-stress induced endothelial-to-mesenchymal transition, which is critical to endocardial cushion formation and compact myocardium development.¹³ Slough *et al.* demonstrated the presence of cilia on the epicardium, but they did not determine the function of these cilia; it was noted however, that epicardial cells from mutant mice without cilia did not exhibit the typical flattened epithelial shape, making them less distinct from the myocardium.⁴⁶ This loss of epicardial phenotype is a feature of EMT. Here we confirm that mouse epicardial cells are indeed ciliated, and that loss of the functional primary cilium supports a transformation from an epithelial phenotype to a mesenchymal phenotype.

Primary cilia are known to modulate Shh, Wnt, and PDGF signalling, and have recently been demarcated as an important site modulating TGF- β mediated responses.⁴⁷ The downstream molecular events regulating the EMT-like effects seen in our study were not investigated, however we postulate that cells without IFT ciliary components may lose inhibition of EMT processes. RT-qPCR analysis demonstrates that several mediators of EMT including *Snail*, *Slug*, and *β -catenin* are indeed higher after Ad-shIft88 treatment. Other groups have established the EMT effects of Shh, Wnt/ *β -catenin*, and PDGF in epicardial cells after cardiac injury.^{35, 48, 49} Furthermore, *β -catenin* mediated upregulation of *Slug* has been demonstrated to be responsible for mesenchymal transformation of aortic endothelial cells lacking primary cilia.¹⁷ Rozycki *et al.* also determined that the combination of TGF- β with deciliation supports EMT, whereas TGF-

β alone was not sufficient to cause EMT in tubular epithelial cells.¹⁵ These data confirm the observation in our study of the ability of the cilium to modulate cellular EMT responses.

Interestingly, studies from zebrafish embryos indicate that endothelial primary cilia are essential in developmental vascular integrity, and embryos with mutant intraflagellar transport genes have leaky vasculature.⁵⁰ It is possible that primary cilia disassembly indeed supports vascular permeability via endothelial junction disassembly, leading to cell migration and movement; thus, primary cilia knockdown would be disadvantageous under normal conditions, and advantageous after postnatal injury. *Sánchez-Duffhues* et al. also demonstrated that cilia are present in endothelial cells of the vasculature. In this study, lack of functional primary cilia potentiated *β -catenin* and *Slug* signaling, sensitizing the endothelium to undergo EMT in aortic endothelial cells.¹⁷

In the work presented here, adenoviral mediated shRNA delivery was used to knockdown the Ift88 transport protein. There are several pitfalls to this experimental approach. Intramyocardial adenoviral injection imparts adenovirus in specific point areas of the myocardium, rather than allowing diffuse expression throughout the heart. To ensure delivery to the area of interest, care was taken to inject within the peri-infarct area at the time of MI. Furthermore, using this approach, we also observed GFP expression in the myocardium, suggesting that some of the observed effects could be attributed to reduction in cardiomyocyte primary cilia function. Cardiomyocytes are ciliated, and knockdown of primary cilia have been demonstrated to support maintenance of a cardiac stem cell like phenotype.⁵¹ Defects in primary cilia have been demonstrated to promote

postnatal cardiomyocyte replication.⁵² Indeed, primary ciliary disassembly is required for progression through the cell cycle.⁵³ However, no difference was observed in the number of proliferating cells in the peri-infarct area in this study (data not shown), suggesting the observed effects are not a result of enhanced cell proliferation. For these reasons, it would be interesting to determine the effects of epicardial specific cilia knockout in the setting of MI in future work. Nevertheless, our study is the first to uncover the importance of primary cilia for cardiac healing.

In summary, intrinsic epicardial activation in response to MI is inadequate to promote sufficient healing. The present investigation showed that Ad-shIft88 treatment to induce primary cilia disassembly potentiated responses to EMT signaling in the epicardium, promoting EMT and neovascularization, and improving cardiac function post-MI. These data reveal the physiological significance of the primary cilium in mediating EMT signaling pathways and highlight the primary cilium as a possible therapeutic target post-MI. This is particularly important since patient mortality post-MI remains high despite current available pharmacological treatments and there is a pressing need for new effective drug therapies.

3.6 References

1. Finegold JA, et al. Mortality from ischaemic heart disease by country, region, and age: statistics from World Health Organisation and United Nations. *Int J Cardiol.* 2013;168:934-45.
2. Bui AL, et al. Epidemiology and risk profile of heart failure. *Nat Rev Cardiol.* 2011;8:30-41.
3. Benjamin EJ, et al. Heart disease and stroke statistics-2017 update: A report from the american heart association. *Circulation.* 2017;135:e146-e603.
4. Cook C, et al. The annual global economic burden of heart failure. *Int J Cardiol.* 2014;171:368-76.
5. Haubner BJ, et al. Complete cardiac regeneration in a mouse model of myocardial infarction. *Aging (Albany NY).* 2012;4:966-77.
6. Xiang FL, et al. Cardiac-specific overexpression of human stem cell factor promotes epicardial activation and arteriogenesis after myocardial infarction. *Circ Heart Fail.* 2014;7:831-42.
7. Smart N, et al. Epicardial progenitor cells in cardiac regeneration and neovascularisation. *Vascul Pharmacol.* 2013;58:164-73.
8. von Gise A and Pu WT. Endocardial and epicardial epithelial to mesenchymal transitions in heart development and disease. *Circ Res.* 2012;110:1628-45.
9. Limana F, et al. Identification of myocardial and vascular precursor cells in human and mouse epicardium. *Circ Res.* 2007;101:1255-65.
10. Porrello ER, et al. Transient regenerative potential of the neonatal mouse heart. *Science.* 2011;331:1078-80.
11. Goetz SC and Anderson KV. The primary cilium: a signalling centre during vertebrate development. *Nat Rev Genet.* 2010;11:331-44.
12. Gonzalez DM and Medici D. Signaling mechanisms of the epithelial-mesenchymal transition. *Sci Signal.* 2014;7:re8.
13. Egorova AD, et al. Lack of primary cilia primes shear-induced endothelial-to-mesenchymal transition. *Circ Res.* 2011;108:1093-101.

14. Hassounah NB, et al. Molecular pathways: the role of primary cilia in cancer progression and therapeutics with a focus on Hedgehog signaling. *Clin Cancer Res.* 2012;18:2429-35.
15. Rozycki M, et al. The fate of the primary cilium during myofibroblast transition. *Mol Biol Cell.* 2014;25:643-57.
16. Pazour GJ, et al. Chlamydomonas IFT88 and its mouse homologue, polycystic kidney disease gene tg737, are required for assembly of cilia and flagella. *J Cell Biol.* 2000;151:709-18.
17. Sanchez-Duffhues G, et al. SLUG is expressed in endothelial cells lacking primary cilia to promote cellular calcification. *Arterioscler Thromb Vasc Biol.* 2015;35:616-27.
18. Blom JN, et al. Myocardial Infarction in Neonatal Mice, A Model of Cardiac Regeneration. *J Vis Exp.* 2016.
19. Feng Q, et al. Increased inducible nitric oxide synthase expression contributes to myocardial dysfunction and higher mortality after myocardial infarction in mice. *Circulation.* 2001;104:700-4.
20. Xin M, et al. Hippo pathway effector Yap promotes cardiac regeneration. *Proc Natl Acad Sci U S A.* 2013;110:13839-44.
21. Liu Y, et al. Nitric oxide synthase-3 promotes embryonic development of atrioventricular valves. *PLoS One.* 2013;8:e77611.
22. Zhang T, et al. Mitogen-activated protein kinase phosphatase-1 inhibits myocardial TNF-alpha expression and improves cardiac function during endotoxemia. *Cardiovasc Res.* 2012;93:471-9.
23. Moazzen H, et al. Pregestational diabetes induces fetal coronary artery malformation via reactive oxygen species signaling. *Diabetes.* 2015;64:1431-43.
24. Ott C and Lippincott-Schwartz J. Visualization of live primary cilia dynamics using fluorescence microscopy. *Curr Protoc Cell Biol.* 2012;Chapter 4:Unit 4 26.
25. Plotnikova OV, et al. Primary cilia and the cell cycle. *Methods Cell Biol.* 2009;94:137-60.
26. Lencinas A, et al. Collagen gel analysis of epithelial-mesenchymal transition in the embryo heart: an in vitro model system for the analysis of tissue interaction, signal transduction, and environmental effects. *Birth Defects Res C Embryo Today.* 2011;93:298-311.

27. Xiang FL, et al. Cardiomyocyte-specific overexpression of human stem cell factor improves cardiac function and survival after myocardial infarction in mice. *Circulation*. 2009;120:1065-74.
28. Vrancken Peeters MP, et al. Smooth muscle cells and fibroblasts of the coronary arteries derive from epithelial-mesenchymal transformation of the epicardium. *Anat Embryol (Berl)*. 1999;199:367-78.
29. Smart N, et al. Thymosin β 4 induces adult epicardial progenitor mobilization and neovascularization. *Nature*. 2007;445:177-82.
30. Potts JD and Runyan RB. Epithelial-mesenchymal cell transformation in the embryonic heart can be mediated, in part, by transforming growth factor beta. *Dev Biol*. 1989;134:392-401.
31. Kraus F, et al. Cloning and expression analysis of the mouse T-box gene Tbx18. *Mechanisms of Development*. 2001;100:83-86.
32. van Wijk B, et al. Cardiac regeneration from activated epicardium. *PLoS One*. 2012;7:e44692.
33. Takeichi M, et al. The transcription factors Tbx18 and Wt1 control the epicardial epithelial-mesenchymal transition through bi-directional regulation of Slug in murine primary epicardial cells. *PLoS One*. 2013;8:e57829.
34. Jing X, et al. Hypoxia induced the differentiation of Tbx18-positive epicardial cells to CoSMCs. *Sci Rep*. 2016;6:30468.
35. Duan J, et al. Wnt1/ β catenin injury response activates the epicardium and cardiac fibroblasts to promote cardiac repair. *EMBO J*. 2012;31:429-42.
36. von Gise A, et al. WT1 regulates epicardial epithelial to mesenchymal transition through beta-catenin and retinoic acid signaling pathways. *Developmental Biology*. 2011;356:421-431.
37. Tao J, et al. Epicardial HIF signaling regulates vascular precursor cell invasion into the myocardium. *Dev Biol*. 2013;376:136-49.
38. Lazarous DF, et al. Effects of chronic systemic administration of basic fibroblast growth factor on collateral development in the canine heart. *Circulation*. 1995;91:145-53.
39. Calvani M, et al. Hypoxic induction of an HIF-1alpha-dependent bFGF autocrine loop drives angiogenesis in human endothelial cells. *Blood*. 2006;107:2705-12.
40. Yoshida D, et al. Hypoxia inducible factor 1-alpha regulates of platelet derived growth factor-B in human glioblastoma cells. *J Neurooncol*. 2006;76:13-21.

41. Itoh N, et al. Roles of FGF signals in heart development, health, and disease. *Front Cell Dev Biol.* 2016;4:110.
42. Vantler M, et al. PDGF-BB protects cardiomyocytes from apoptosis and improves contractile function of engineered heart tissue. *J Mol Cell Cardiol.* 2010;48:1316-23.
43. Bax NA, et al. In vitro epithelial-to-mesenchymal transformation in human adult epicardial cells is regulated by TGFbeta-signaling and WT1. *Basic Res Cardiol.* 2011;106:829-47.
44. Perez-Pomares JM, et al. Origin of coronary endothelial cells from epicardial mesothelium in avian embryos. *Int J Dev Biol.* 2002;46:1005-13.
45. Li Y, et al. Global genetic analysis in mice unveils central role for cilia in congenital heart disease. *Nature.* 2015;521:520-4.
46. Slough J, et al. Monocilia in the embryonic mouse heart suggest a direct role for cilia in cardiac morphogenesis. *Dev Dyn.* 2008;237:2304-14.
47. Bodle JC and Lobo EG. Concise review: Primary cilia: Control centers for stem cell lineage specification and potential targets for cell-based therapies. *Stem Cells.* 2016;34:1445-54.
48. Wang J, et al. Epicardial regeneration is guided by cardiac outflow tract and Hedgehog signalling. *Nature.* 2015;522:226-30.
49. Kim J, et al. PDGF signaling is required for epicardial function and blood vessel formation in regenerating zebrafish hearts. *Proc Natl Acad Sci U S A.* 2010;107:17206-10.
50. Kallakuri S, et al. Endothelial cilia are essential for developmental vascular integrity in zebrafish. *J Am Soc Nephrol.* 2015;26:864-75.
51. Koefoed K, et al. Cilia and coordination of signaling networks during heart development. *Organogenesis.* 2014;10:108-25.
52. Shenje LT, et al. Mutations in Alstrom protein impair terminal differentiation of cardiomyocytes. *Nat Commun.* 2014;5:3416.
53. Pugacheva EN, et al. HEF1-dependent Aurora A activation induces disassembly of the primary cilium. *Cell.* 2007;129:1351-63.

Chapter 4

Malat1 protects the heart from myocardial infarction via inhibition of necroptotic cell death

Blom JN, Lu X, Spector DL, Chakrabarti S, Feng Q.

In preparation for submission

4 Chapter 4

4.1 Chapter summary

The lncRNA *Malat1* is ubiquitously expressed, and has been shown to prevent endothelial cell apoptosis. In patients with myocardial infarction (MI), plasma *MALAT1* levels are elevated. However, the exact role of *MALAT1* after acute MI has not been investigated. Here, we tested the hypothesis that *Malat1* protects the myocardium from ischemic injury. We demonstrated that *Malat1*^{-/-} mice were more susceptible to ischemic damage, evidenced by larger infarct sizes and reduced cardiac function post-MI. Expression of cardioprotective factors, including *bFGF*, *TGF-β* and *SDF-1*, were reduced in *Malat1*^{-/-} mice. Notably, myocardial caspase-3 and caspase-8 activities were not significantly different between knockout and control mice post-MI. However, *Malat1*^{-/-} mice did display increased necrosis in the infarct area as compared to WT controls. Furthermore, expression of both *TNF-α* and RIP3 was increased in the infarct area of *Malat1*^{-/-} mice, suggesting augmented necroptotic cell death. Our study suggests that *Malat1* protects the heart from MI injury via inhibition of necroptosis.

4.2 Introduction

Cardiovascular disease is the leading cause of death worldwide, accounting for over 17.3 million (>30%) deaths per annum.¹ Specifically, myocardial infarction (MI) is a leading cause of death in the industrialized world, with more than 7 million people experiencing MI each year.^{2, 3} It has been argued that the most important contributing event to injury from MI is the initial cell death caused by the infarction. In fact, patients with a larger initial infarct suffer worse outcomes including reduced long-term survival, and higher rates of heart failure.^{4, 5} Thus, to maintain proper function, it is important to study the mechanisms of cell death in the setting of MI in effort to reduce the extent of injury and preserve existing cardiac mass.

In 2002, *Okazaki* et al. revealed that the vast majority of the mammalian transcriptome is non-coding.⁶ Specifically, long non-coding RNAs (lncRNA) represent a significant portion of the non-coding transcriptome. lncRNAs are longer than 200 nucleotides in length and, although present in both the nucleus and cytoplasm, they lack a sufficient open reading frame for protein coding.⁷ However, accumulating evidence indicates that a significant number of lncRNAs are implicated in a diverse array of molecular phenomena including transcriptional, translational and epigenetic regulation.⁸ Recent studies have demonstrated significant changes in lncRNA expression profiles in patients post-MI, suggesting a potential pathological role.⁹

Metastasis associated lung adenocarcinoma transcript 1 (*MALAT1*), also known as nuclear enriched abundant transcript 2 (*NEAT2*), is a nuclear residing, ubiquitously expressed lncRNA with a length of about 8000 nucleotides.¹⁰ Expression of *MALAT1* is associated with cancer progression and metastasis, and is involved in regulating cell

migration, epithelial-to-mesenchymal transition (EMT), and cell proliferation.¹¹ *Malat1* has also been shown to suppress apoptosis in several cell types. Specifically, *MALAT1* has been demonstrated to support PI3K and AKT phosphorylation, and reduce caspase-3 activity.¹² Furthermore, silencing the lncRNA using siRNA or shRNA increases the rate of apoptosis mediated cell death in glioma and endothelial cells.^{13, 14} Similarly, in cervical cancer cells, downregulation of *MALAT1* induced the expression of B-cell lymphoma 2 (Bcl-2)-associated x protein (BAX; pro-apoptotic), as well as caspase-3 and caspase-8, while repressing Bcl-2 expression (anti-apoptotic).¹⁵

Hypoxia upregulates *Malat1* expression.¹⁶ Furthermore, expression of *MALAT1* is increased in the plasma of MI patients, possibly resulting from hypoxia in the ischemic myocardium.¹⁷ Based on these findings, and its role in apoptosis, it is likely that *Malat1* may control cellular responses to affect cell death in the setting of MI. The aim of this study was to investigate the role of *Malat1* in cardiac damage from acute MI. We hypothesized that silencing of the lncRNA *Malat1* would augment apoptosis and cardiac injury post-MI. Our results indicate that deficiency in *Malat1* increases cell death from infarction, causing increased infarct size and reducing cardiac function. However, to our surprise, these results indicate that in the setting of acute MI, *Malat1* does not affect apoptosis, but rather potentiates another regulated mechanism of cell death, necroptosis.

4.3 Methods

4.3.1 Animals

Animal protocols used in this study were approved by the Animal Use Subcommittee at Western University, Canada. A *Malat1*^{-/-} mouse line was provided by

Dr. David L. Spector from Cold Spring Harbor Laboratory, New York.¹⁸ These mice have a homozygous ~3kb deletion in the 5' end and promoter of the *Malat1* gene. The deletion is not conditional, and results in a global knockout with complete depletion of *Malat1* transcript expression in all tissues. To identify *Malat1*^{-/-} mice, genotypes were confirmed by PCR using DNA from tail biopsies. The following primer pairs were used: WT *Malat1* forward: gggaggcaatggtctaactggacctcca, reverse: tcgcacacggcctggcggcaccgtcctgct; *Malat1*^{-/-} forward: gggaggcaatggtctaactggacctcca, reverse: cattcttcttctgggccttggcagtcagc.

4.3.2 Murine model of myocardial ischemia

Male C57Bl/6 and *Malat1*^{-/-} mice (8-12 weeks) underwent left coronary artery ligation as previously described.¹⁹ Briefly, mice were anesthetized by IP injection of a ketamine (50 mg/kg) and xylazine (12.5 mg/kg) mixture. The chest cavity was entered via an anterolateral approach, and MI was induced by surgical occlusion of the left main coronary artery. The surgeon was blinded to the genotype of the mice during surgery. All further experimental procedures were carried out 24 hours post-MI.

4.3.3 Hemodynamic Measurements

One day post-MI, mice were anesthetized by IP injection of ketamine (50 mg/kg) and xylazine (12.5 mg/kg) mixture, and placed on a heat pad. Temperature was monitored to ensure stability at 37 °C. A Millar pressure-conductance catheter (Model SPR-839, Size 1.4F) was inserted into the right carotid artery and baseline arterial pressure was measured. The catheter was then advanced retrograde into the left ventricle through the aorta. The signal was recorded continuously to measure LV pressures, volumes and heart rate. Data was analyzed with a cardiac pressure-volume analysis

program (PVAN 3.2; Millar Instruments, TX).²⁰ After hemodynamics, hearts were excised for use in future experiments.

4.3.4 Infarct Size

Hearts were excised 24 hours post-MI, and the aorta was cannulated to perfuse Evans blue dye solution (1% in PBS) through the coronary arteries. Hearts were then cut into four transverse sections and incubated in 1.5% triphenyl-tetrazolium chloride in PBS (TTC; Sigma-Aldrich, St.Louis, MO) for about 10 minutes at room temperature. Evans blue distinguished the ischemic (white) and non-ischemic (blue) areas of the heart, while TTC stained viable tissue red. Heart sections were weighed and infarct size was calculated by ratio of infarct area (white) to ischemic area (white + red) normalized by tissue weight.²¹

4.3.5 Cell Death by Caspase-3 and Caspase-8 Activity and Propidium Iodide

To determine the involvement of apoptosis, both caspase-3 and caspase-8 activity assays were carried out using a caspase-3 and caspase-8 cellular activity assay kit (BIOMOL, Plymouth Meeting, PA). Cardiac tissue from the ischemic area was collected 24 hours post-MI and homogenized. Protein concentrations were measured and a minimum of 115 µg protein was loaded into a 96-well plate. Protein was incubated in the presence of the caspase substrate Ac-DEVD-AMC (4 µM) with or without the inhibitor for caspase-3 (Ac-DEVD-CHO) or caspase-8 (Ac-IETD-CHO) at 37 °C for 17.5 hours. A Spectra-Max M5 micro-plate reader (Molecular Devices, Sunnyvale, CA) was used to measure fluorescence intensity (excitation at 360 nm and emission at 460 nm). Data are expressed as amount of AMC substrate cleaved per 100 µg protein.

Propidium iodide was used to assess necrotic cell death in the infarct area. To label the necrotic cells, animals received an IP injection of 10 mg/kg propidium iodide (PI; Invitrogen, Grand Island, NY) 2 hours before tissue collection (22 hours post-MI). After collection, hearts were snap-frozen, then embedded in FSC22 frozen section media (Leica) at -20 °C. Hearts were sectioned in the transverse plane at 10 µm thickness, and frozen tissue sections were counterstained with Hoechst 33342 (Invitrogen, Grand Island, NY) to mark nuclei. PI positive cells were quantified and normalized to mm² infarct area.

4.3.6 Quantitative RT-qPCR

Total RNA was isolated from the left ventricular infarct or peri-infarct area using Trizol reagent (Ambion, Foster City, CA) 24 hours after infarction. A minimum of 0.55 µg total RNA was used to synthesize cDNA with Moloney murine leukemia virus (M-MLV) reverse transcriptase in 20 µL reactions. 2 µL cDNA was used for real-time PCR amplification with EvaGreen qPCR MasterMix-S (ABM, Vancouver, BC). An Eppendorf Realplex² Real-Time qPCR machine was used to amplify samples and after 35 cycles, samples were analyzed using cycle threshold (Ct) analysis. Primer sequences for expression analysis are listed in **Table 4.1**. The mRNA levels were determined using a comparative C_T method in relation to murine glyceraldehyde 3-phosphate dehydrogenase (GAPDH) as internal control.

Table 4.1. The PCR primer sequences.

Gene	Accession NM	Forward	Reverse
<i>Malat1</i>	EF177380	ctttgcgggtgttaggtt	acaggagtgaggcttggtg
<i>bFGF</i>	NM_008006	caagggagtgtgtccaacc	tgcccagttcgttcagtgc
<i>TGF-β1</i>	NM_011577	gcccgaagcggactactatg	cactgcttcccgaatgtctg
<i>SDF-1 (CXCL12)</i>	NM_021704	tcagcctgagctaccgatgc	tcttcagccgtgcaacaatc
<i>HIF-1α</i>	NM_001313919	cagcctcaccagacagagca	gtgcacagtcacctgggtgc
<i>RIP3</i>	AF178953	acacggcactccttggtatc	ccgaactgtgcttggtcata
<i>TNF-α</i>	M13049	ccgatgggtgtaccttgc	gggctgggtagagaatggat
<i>GAPDH</i>	NM_001289726	gatgggtgtgaaccacgaga	agtgatggcatggactgtgg

4.3.7 Western Blotting

Total RIP3 expression from the infarct area 1 day post-MI was measured by Western blot analysis. Briefly, 50 µg of protein from isolated left ventricular tissue was separated by 10% SDS-Page gel and transferred onto a polyvinylidene difluoride membrane (PVDF; 0.45µm pore size; Bio-Rad, Hercules, CA). For immunodetection, the following primary antibodies were used: anti-RIP3 (1:100, eBioscience, San Diego, CA) and anti-GAPDH (1:2000, Santa Cruz, Dallas, TX). Blots were then washed and probed

with horseradish peroxidase conjugated secondary antibodies (1:5000, Bio-Rad, Hercules, CA), and detected by using an ECL detection method. Signal quantification was performed by densitometry (AlphaEase FC, Alpha Innotech Corporation, San Leandro, CA).

4.3.8 Statistical Analysis

Data are presented as mean \pm SEM. Differences between groups were analyzed using an unpaired Student's t-test. A one-way ANOVA followed by a Bonferroni test was performed for multiple group comparisons. All tests were two sided using a significance level of $P < 0.05$.

4.4 Results

4.4.1 *Malat1* expression is increased post-MI

Plasma *MALAT1* levels are increased in patients post-MI.¹⁷ To assess *Malat1* expression in the mouse heart, RT-qPCR analysis was employed. *Malat1* was expressed in the mouse heart, and myocardial *Malat1* expression was significantly higher in the infarct area 1 day post-MI as compared to normal hearts ($P < 0.05$, **Figure 4.1**).

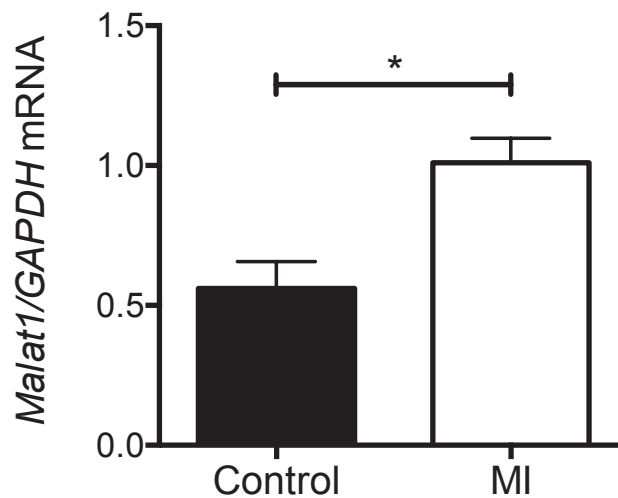


Figure 4.1. *Malat1* expression is significantly increased in the infarct area post-MI.

Real-time qPCR measurements of *Malat1* expression from hearts of control and infarcted WT mice. Data are mean \pm SEM. $n = 4$ mice per group. $*P < 0.05$.

4.4.2 Deficiency in *Malat1* augments myocardial damage post-MI

To determine the role of *Malat1* in infarction, both WT and *Malat1*^{-/-} adult mice were subject to MI by coronary artery ligation. Hearts were collected one day post-MI and perfused with Evans blue dye followed by staining with triphenyl-tetrazolium chloride (TTC) (**Figure 4.2A**). Infarct size was measured as a percent of weight of the infarct to the area at risk, and was significantly larger in *Malat1*^{-/-} mice as compared to WT controls ($P < 0.05$, **Figure 4.2B**). The area at risk was not significantly different between the two groups (**Figure 4.2C**).

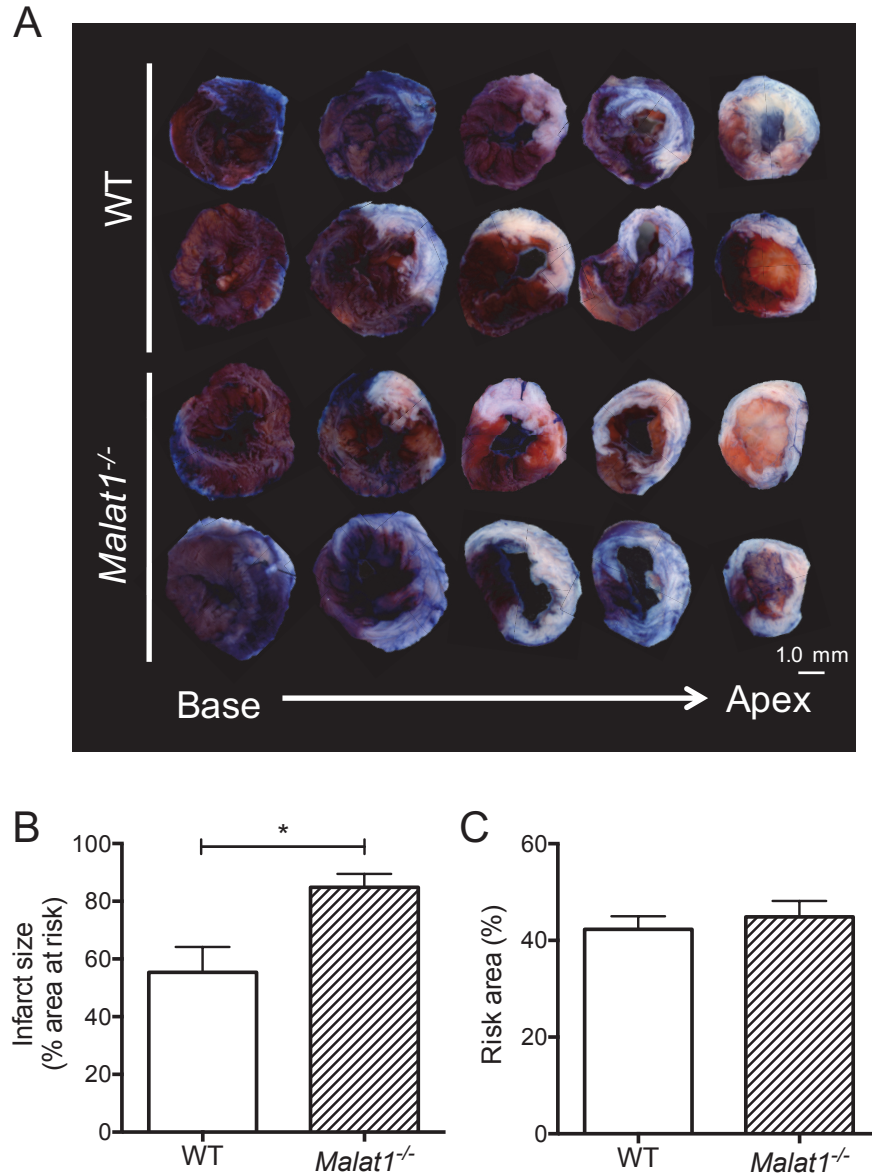


Figure 4.2. *Malat1* deficiency increases infarct size after myocardial infarction.

Myocardial ischemia was induced by occlusion of the left anterior descending coronary artery. A) Representative Evans blue and TTC stained heart sections 1 day post-MI. B) Infarct size expressed as a percent of the weight of the infarct to the area at risk. C) Area at risk after MI. Data are mean \pm SEM, n = 6 mice per group. * $P < 0.05$.

To evaluate cardiac function post-MI, left ventricular hemodynamic parameters were analyzed using a Millar pressure catheter. Apart from a small increase in left ventricular relaxation, there were no significant differences between WT and *Malat1*^{-/-} mice under normal physiological conditions (**Table 4.2**). In mice subject to coronary artery ligation, there were no significant differences in heart rate (HR), mean arterial pressure (MAP), or left ventricular end diastolic pressure (LVEDP) 1 day post-MI. However, *Malat1*^{-/-} mice showed a significant decrease in left ventricular function as determined by left ventricular end systolic pressure (LVSP), as well as left ventricular contractility (LV +dP/dt) and left ventricular relaxation (LV -dP/dt) ($P < 0.05$, **Table 4.2**). These data indicate reduced cardiac function post-MI in *Malat1*^{-/-} mice as compared to WT controls.

Table 4.2. Hemodynamic parameters of WT and *Malat1*^{-/-} mice 1 day after coronary artery ligation (MI) or sham operation.

Parameters	Sham		MI	
	WT	<i>Malat1</i> ^{-/-}	WT	<i>Malat1</i> ^{-/-}
<i>n</i>	6	6	9	9
HR (bpm)	414.0 ± 8.90	455.9 ± 22.4	409.5 ± 12.98	388.6 ± 7.14
MAP (mmHg)	68.25 ± 3.04	67.67 ± 5.44	58.80 ± 1.96	51.33 ± 3.56
LVSP	98.58 ± 5.30	89.45 ± 1.36	79.71 ± 1.95	68.82 ± 3.47*
LVEDP	4.437 ± 1.30	3.199 ± 0.70	8.32 ± 1.56	9.306 ± 1.37
LV +dP/dt (mmHg/s)	7658 ± 516.4	9006 ± 475.6	6466 ± 395.2	4972 ± 523.1*
LV -dP/dt (mmHg/s)	7139 ± 291.7	8142 ± 331.8*	5762 ± 601.5	4249 ± 366.4*

**P*<0.05 as compared to respective WT controls.

4.4.3 Deficiency in *Malat1* reduces expression of cardioprotective genes

To investigate the mechanisms responsible for reduced cardiac function by *Malat1* deletion, the expression of several cardioprotective factors was measured in the peri-infarct area 1 day post-MI. Indeed, there was a significantly lower expression of *bFGF*, *SDF-1* and *TGF- β* in *Malat1*^{-/-} mice as compared to WT controls ($P < 0.05$, **Figure 4.3**). A trend indicates that the pro-survival and pro-angiogenic transcription factor hypoxia inducible factor (*HIF-1 α*) was lower in *Malat1*^{-/-} mice, however this difference was not significant. Thus, *Malat1*^{-/-} mice have a reduced ability to up-regulate cardioprotective factors to prevent cardiac injury.

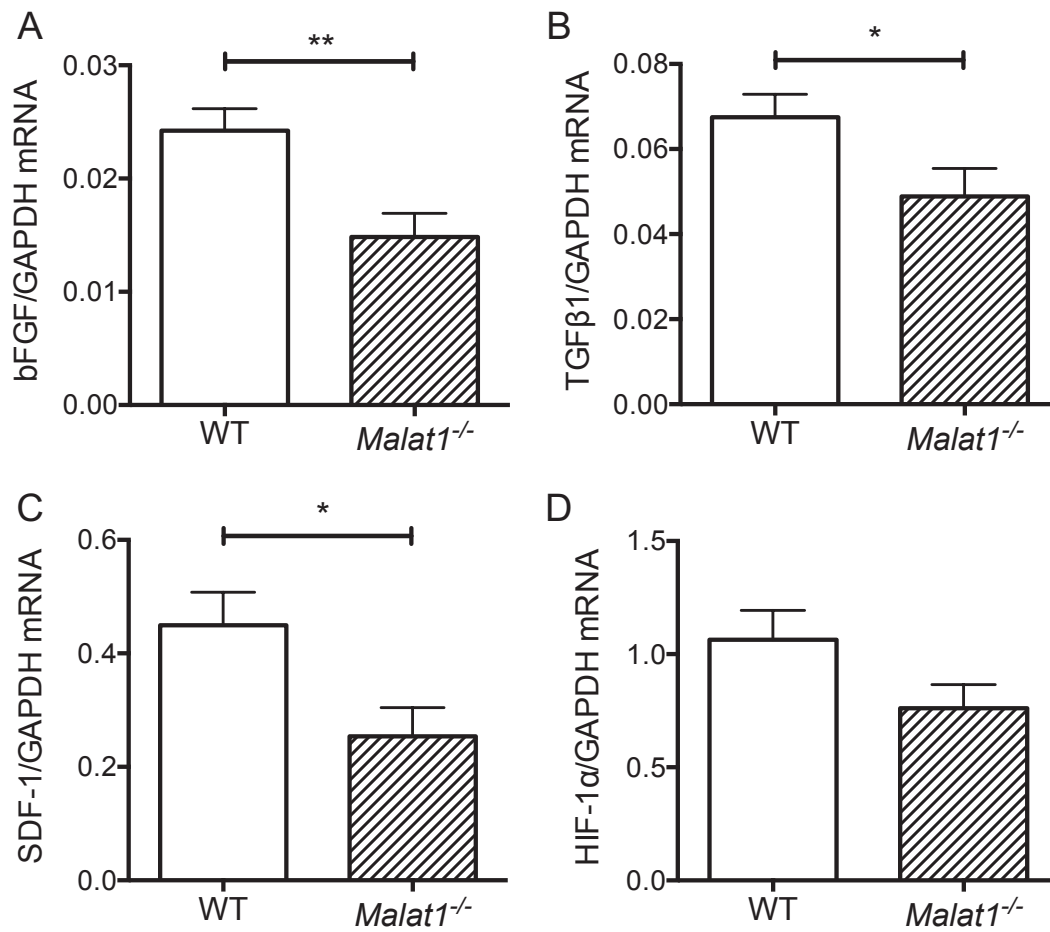


Figure 4.3. *Malat1* deficiency significantly attenuates cardioprotective gene expression in the peri-infarct area post-MI.

Real-time qPCR measurements of A) basic fibroblast growth factor (*bFGF*), B) transforming growth factor-beta (*TGF-β*), C) stromal derived factor-1 (*SDF-1*), and D) hypoxia inducible factor-1 alpha (*HIF-1α*). Data are mean ± SEM. n = 8-9 mice per group. **P* < 0.05, ***P* < 0.01.

4.4.4 Deficiency in *Malat1* does not affect myocardial caspase activity post-MI

To determine the propensity for ischemia related acute damage in the myocardium, myocardial apoptosis was determined using caspase-3 and caspase-8 activity assays. Both caspase-3 and caspase-8 activities were significantly higher in the infarct area of both WT and *Malat1*^{-/-} mice as compared to sham operated WT controls ($P < 0.001$ and $P < 0.01$ for caspase-3 and caspase-8, respectively). However, to our surprise, there was no significant difference between the two MI groups (Figure 4.4).

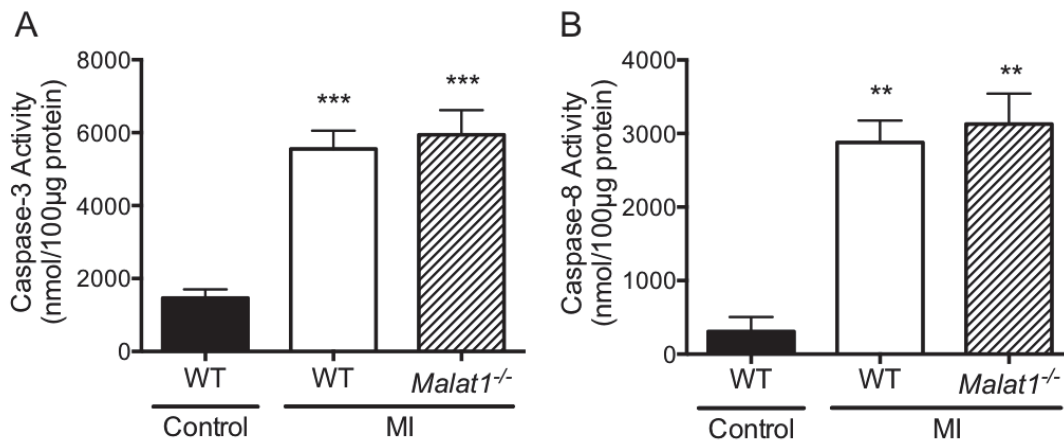


Figure 4.4. *Malat1* deficiency did not affect caspase activity 1 day post-MI.

Myocardial tissues were obtained from the infarct area of WT and *Malat1*^{-/-} mice 1 day post-MI with normal WT left ventricular myocardium serving as controls. Caspase-3 (A) and caspase-8 (B) activity measured by caspase activity assay. Data are mean \pm SEM. $n = 3-8$ mice per group. ** $P < 0.05$, *** $P < 0.001$.

4.4.5 *Malat1* prevents necrotic cell death post-MI

To further elucidate the mechanism causing increased infarct size in *Malat1*^{-/-} mice, myocardial necrosis was assessed by propidium iodide (PI) staining. A significant increase in PI staining was observed in the infarct area of *Malat1*^{-/-} mice as compared to controls one day post-MI ($P < 0.05$, **Figure 4.5**). This suggests an increase in necrotic cell death in *Malat1*^{-/-} mice post-MI.

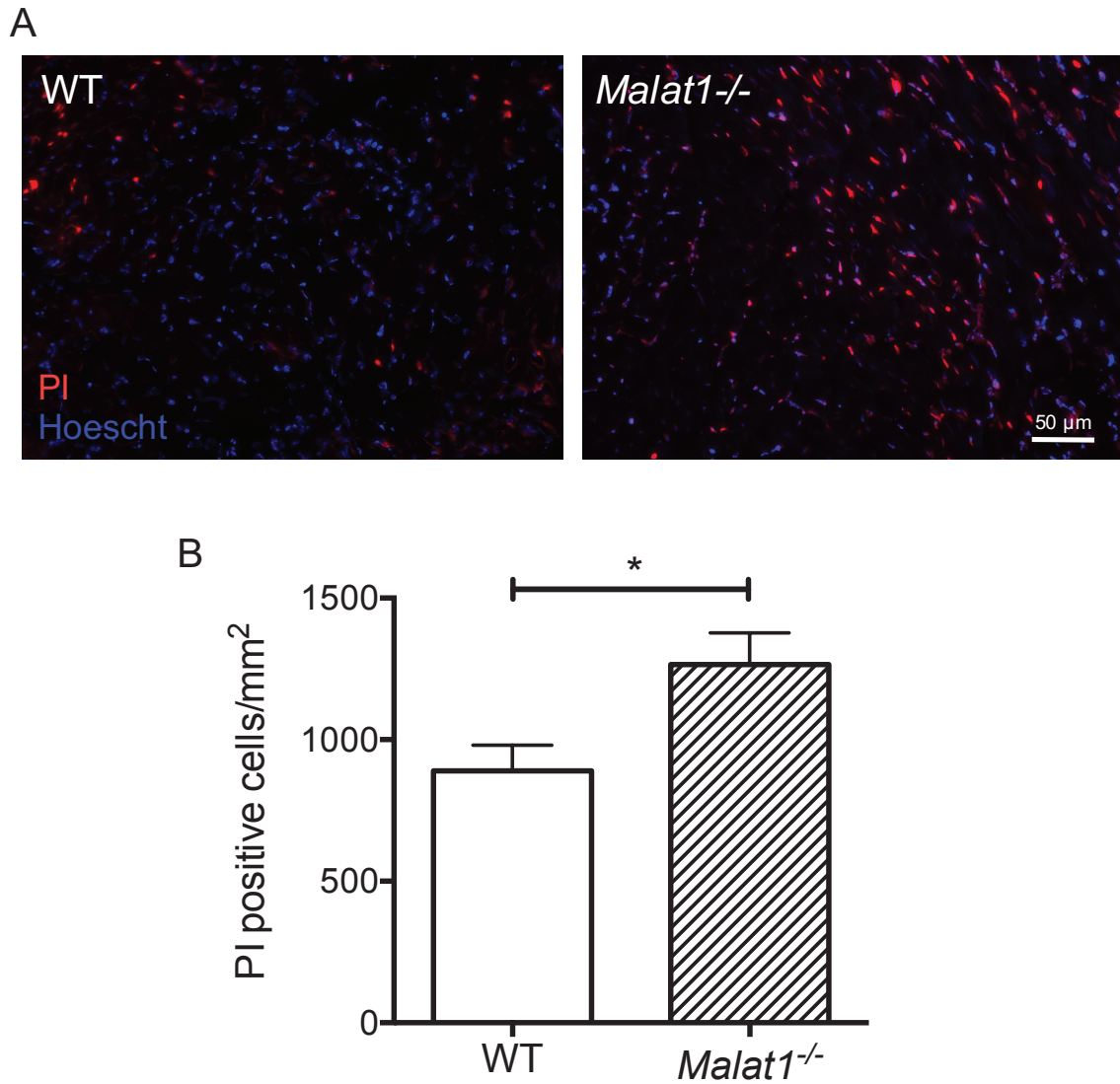


Figure 4.5. *Malat1* deficiency promotes necrotic cell death in the infarct area one day post-MI.

A) Representative images of propidium iodide (PI; red) and nuclear (Hoescht; blue) staining in the infarct area 1 day post-MI. B) Quantification of PI-labelled cells 1 day post-MI. Data are mean \pm SEM. n = 6 mice per group. * P <0.05.

To determine whether necroptosis was altered in *Malat1*^{-/-} mice in response to cardiac injury, *TNF- α* expression was measured 1 day post-MI by RT-qPCR. There was a significantly higher expression of *TNF- α* in the infarct area of *Malat1*^{-/-} mice as compared to WT controls ($P < 0.001$, **Figure 4.6A**). Expression of the downstream mediator of necroptosis, *RIP3*, was also measured 1 day post-MI. Similar to *TNF- α* expression, *RIP3* mRNA levels were significantly higher in the infarct area of *Malat1*^{-/-} mice as compared to WT controls ($P < 0.05$, **Figure 4.6B**). To confirm this effect, Western blotting was performed to detect RIP3 protein levels (**Figure 4.6C**). Densitometric analysis shows that the ratio of RIP3 to GAPDH protein expression was significantly increased in *Malat1*^{-/-} mice as compared to controls ($P < 0.001$, **Figure 4.6D**). These results indicate an enhanced *TNF- α* / *RIP3* signaling pathway, leading to myocardial necroptosis in *Malat1*^{-/-} mice post-MI.

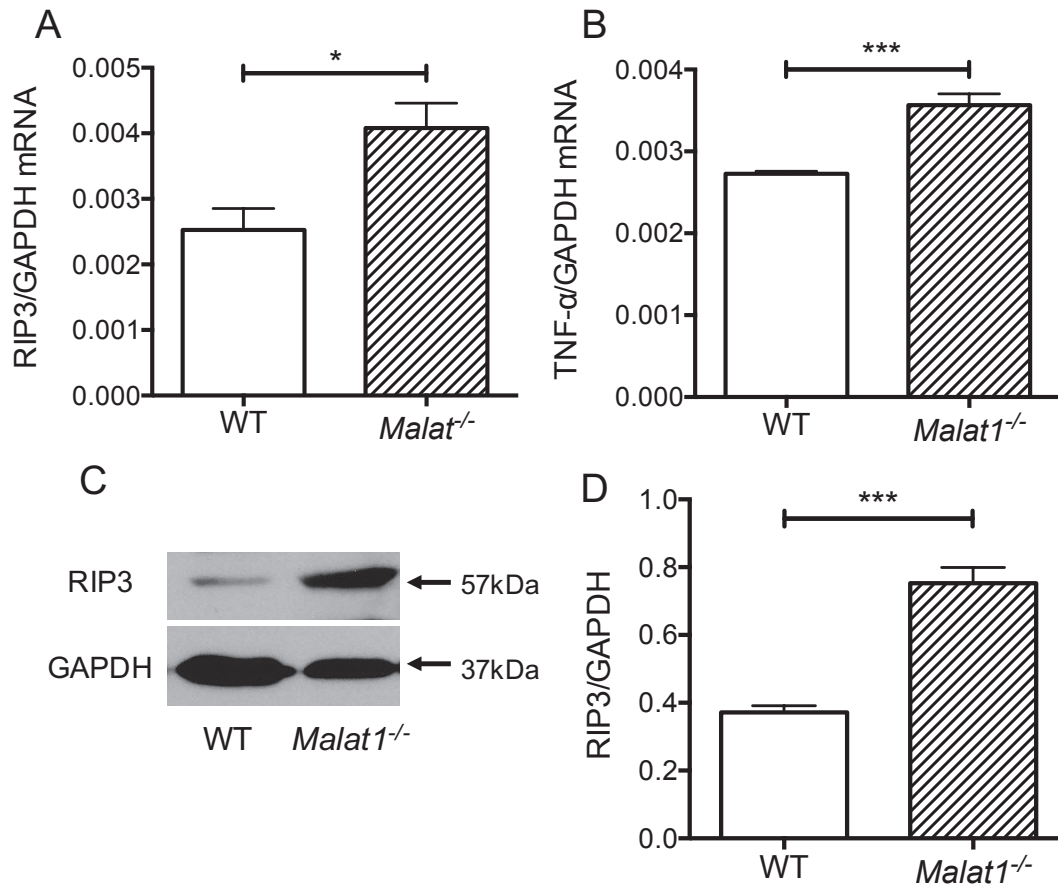


Figure 4.6 *Malat1* deficiency augments *TNF-α* and *RIP3* expression 1 day post-MI.

Real-time qPCR measurements of A) tumor necrosis factor alpha (*TNF-α*) and B) receptor-interacting protein kinase 3 (*RIP3*) expression in infarct area of WT and *Malat1*^{-/-} mice 1 day post-MI. n = 4 mice per group. C) A representative Western blot for *RIP3* and *GAPDH* protein levels in the infarct area of WT and *Malat1*^{-/-} mice. D) Densitometric analysis of *RIP3* protein levels in relation to *GAPDH* protein expression, n = 4-5 mice per group. Data are mean ± SEM. **P*<0.05, ****P*<0.001.

4.5 Discussion

Accumulating evidence indicates that lncRNAs are important regulators of physiological and pathological processes, however their potential importance in cardiac disease is only now emerging. While many lncRNAs have been demonstrated to be differentially expressed in cardiac disease, the mechanisms by which these lncRNAs regulate cardiac functional processes remain poorly understood.²² The present study was carried out to examine the role of the lncRNA *Malat1* in cardiac injury from MI. Using a *Malat1*^{-/-} mouse, we demonstrate for the first time that *Malat1* is important in mitigating cell death from cardiac ischemic injury. Deficiency of *Malat1* was associated with increased myocardial infarct size and reduced cardiac function 1 day post-MI. To our surprise, this was not associated with an increase in apoptosis, but rather enhanced necrotic cell death. This likely occurred as a result of a reduced capacity for expression of cardioprotective factors, as well as higher *TNF- α* and *RIP3* expression.

Cardiac ischemic injury is known to consist of both apoptotic and necrotic cell death.²³ In fact, necrosis may be responsible for the majority of damage not only from the initial infarct, but also contributing to long term deleterious remodelling.²⁴ The contribution of necrosis to infarct-mediated cell death is confirmed in our study by the correlation between increased necrotic cell death and augmented infarct size in the *Malat1*^{-/-} group. While necrosis has been traditionally viewed as an un-regulated, passive form of cell death, recent evidence indicates that it can in fact be actively controlled by *TNF- α* signaling through a process termed necroptosis. Other reports have demonstrated the importance of necroptosis in mediating injury from MI.²⁵

Inappropriate production of TNF- α is implicated in a wide spectrum of pathologies. TNF- α is a pleiotropic cytokine, and depending on environmental conditions, its signaling can cause one of three major processes: inflammation, apoptosis or necroptosis. Through the first pathway, TNF- α binding to its receptor TNFR1 causes ERK/MAPK and NF- κ B mediated pro-inflammatory processes.²⁶ However, in the absence of sufficient ERK/MAPK signaling, TNF- α becomes a potent inducer of cell death. In the second pathway, a complex of death domains forms with caspase-8, which causes apoptosis.²⁷ However, if caspase activity is inhibited or RIP3 levels are high, a third signaling pathway ensues whereby the “necrosome” forms (containing RIP1 and RIP3) and causes necroptosis. The activity of RIP1 and RIP3 is critical to necroptosis as they phosphorylate downstream mediators which disrupt mitochondrial, lysosomal, and plasma membranes.²⁸ This results in uncontrolled ion and solute passage, causing cell swelling and ultimately rupture - the dominant feature of necrosis.

Malat1 is known to support the first ERK/MAPK pathway,^{29, 30} thus its absence may attenuate NF- κ B signaling, and favor cell death. Additionally, knockdown of *Malat1* has been shown to potentiate the expression of TNF- α upon cell stimulation with lipopolysaccharide, suggesting a role for *Malat1* in attenuating overall TNF- α signaling.³¹ In the present study, TNF- α and RIP3 expression was increased in the infarcted myocardium of *Malat1*^{-/-} mice. Our results suggest that *Malat1* inhibits TNF- α /RIP3 signaling and myocardial necroptosis post-MI.

The ubiquitous expression of *Malat1* underscores its functional importance, however its exact mechanism of action is still unknown. Of the diverse roles of *MALAT1*,

it is suggested to mediate processes via binding and sequestration of molecules into nuclear speckles. Specifically, *MALAT1* has been shown to regulate pre-mRNA splicing by bringing RNA-splicing factors to nuclear speckles for assembly, modification, and storage.³² *Malat1* is also thought to play a *cis*-regulatory role by regulating expression of its neighbouring genes.¹⁸ Previous studies have demonstrated a role for *Malat1* in suppressing apoptosis by regulating caspase levels and activity.^{33,34} In 2016, Zhang et al. even confirmed the role of *Malat1* in reducing cardiomyocyte apoptosis in the setting of diabetes.³⁵ Although this group did not discern the mechanism of action, another study suggested that *MALAT1* sponges or sequesters various miRNAs, and that in endothelial cells it modulates the expression of the chemokine receptor CXCR2 by competing with miR-22-3p, a promoter of apoptosis.¹⁴ Unexpectedly, *Malat1* deficiency did not affect caspase activity in the present investigation. Instead, the *Malat1*^{-/-} mice show augmented necroptotic cell death post-MI. While no study has demonstrated a direct relation of *MALAT1* to necroptosis, it is known to downregulate miR-155, the suppression of which attenuates necroptosis.^{36,37} The exact mechanism by which *Malat1* mediates necroptosis in cardiac ischemic cells should be determined in future studies.

In concordance with previous studies, we demonstrate that *Malat1* expression is upregulated in response to ischemia.³⁸ However, the results of the current study are in conflict with two previous reports of the role of *Malat1* in cardiac injury. In one study, *Malat1* reversed the cardioprotective effects of fentanyl in ischemia/reperfusion injury.³⁹ However, the authors only tested fentanyl and *Malat1* co-administration and did not study any effect of *Malat1* alone on ischemia/reperfusion injury. Thus, the effects of *Malat1* on ischemic injury are unknown. In another study, Peters et al. showed that

Malat1 is dispensable during pressure overload-induced cardiac hypertrophy by thoracic aortic constriction (TAC) using a different *Malat1*^{-/-} mouse line.⁴⁰ Although cardiac ischemia may cause cardiac hypertrophy in the long term, this chronic effect was not tested in our study. In future, the role of *Malat1* in long-term cardiac remodeling post-MI should be investigated.

Cardioprotective factors also play an important role in the response to cardiac ischemia. Included in these factors are the ERK1/2 pro-survival kinases, as well as the PI3K/AKT signaling molecules. Upstream of these molecules are mediators of both acute and long term protection including protein tyrosine kinase ligands like bFGF and cytokines like SDF-1 and TGF- β .⁴¹⁻⁴³ Exogenous administration of bFGF, SDF-1 and TGF- β have all been demonstrated to decrease myocardial cell death in the setting of acute ischemic injury.⁴³⁻⁴⁵ This is consistent with previous findings from our lab confirming the role of SDF-1 in myocardial injury.⁴⁶ In the present investigation, we observed reduced expression of *bFGF*, *SDF-1* and *TGF- β* in *Malat1*^{-/-} mice, implicating *Malat1* in the regulation of these cytoprotective factors in the heart. Insufficient cardioprotection in the setting of MI may have contributed to the observed increase in infarct size in *Malat1*^{-/-} mice. The mechanisms by which *Malat1* regulates expression of these cardioprotective factors require further investigation.

In summary, our study suggests that *Malat1* is critical in the regulation of necrotic cell death in cardiac ischemia. A *Malat1* deficiency in the myocardium augments cardiomyocyte necroptosis, leading to increased infarct size and impaired cardiac function one day post-MI. Our results show a cardioprotective role of *Malat1* post-MI,

and suggest that *MALATI* may have therapeutic potential to reduce cardiac injury in the setting of acute MI.

4.6 References

1. Benjamin EJ, et al. Heart disease and stroke statistics-2017 update: A report from the american heart association. *Circulation*. 2017;135:e146-e603.
2. World Health Organization. Global status report on noncommunicable diseases. 2014:volumes.
3. Reed GW, et al. Acute myocardial infarction. *Lancet*. 2017;389:197-210.
4. Sobel BE, et al. Estimation of infarct size in man and its relation to prognosis. *Circulation*. 1972;46:640-8.
5. Miller TD, et al. Infarct size after acute myocardial infarction measured by quantitative tomographic 99mTc sestamibi imaging predicts subsequent mortality. *Circulation*. 1995;92:334-41.
6. Okazaki Y, et al. Analysis of the mouse transcriptome based on functional annotation of 60,770 full-length cDNAs. *Nature*. 2002;420:563-73.
7. Niazi F and Valadkhan S. Computational analysis of functional long noncoding RNAs reveals lack of peptide-coding capacity and parallels with 3' UTRs. *RNA*. 2012;18:825-43.
8. Wang KC and Chang HY. Molecular mechanisms of long noncoding RNAs. *Mol Cell*. 2011;43:904-14.
9. Archer K, et al. Long non-coding rnas as master regulators in cardiovascular diseases. *Int J Mol Sci*. 2015;16:23651-67.
10. Ji P, et al. MALAT-1, a novel noncoding RNA, and thymosin β 4 predict metastasis and survival in early-stage non-small cell lung cancer. *Oncogene*. 2003;22:8031-41.
11. Gutschner T, et al. MALAT1 -- a paradigm for long noncoding RNA function in cancer. *J Mol Med (Berl)*. 2013;91:791-801.
12. Xin JW and Jiang YG. Long noncoding RNA MALAT1 inhibits apoptosis induced by oxygen-glucose deprivation and reoxygenation in human brain microvascular endothelial cells. *Exp Ther Med*. 2017;13:1225-1234.
13. Xiang J, et al. Silencing of long non-coding rna MALAT1 promotes apoptosis of glioma cells. *J Korean Med Sci*. 2016;31:688-94.
14. Tang Y, et al. The lncRNA MALAT1 protects the endothelium against ox-LDL-induced dysfunction via upregulating the expression of the miR-22-3p target genes CXCR2 and AKT. *FEBS Lett*. 2015;589:3189-96.

15. Guo F, et al. Inhibition of metastasis-associated lung adenocarcinoma transcript 1 in CaSki human cervical cancer cells suppresses cell proliferation and invasion. *Acta Biochim Biophys Sin (Shanghai)*. 2010;42:224-9.
16. Lelli A, et al. Induction of long noncoding RNA MALAT1 in hypoxic mice. *Hypoxia*. 2015;2015:45-52.
17. Vausort M, et al. Long noncoding RNAs in patients with acute myocardial infarction. *Circ Res*. 2014;115:668-77.
18. Zhang B, et al. The lncRNA Malat1 is dispensable for mouse development but its transcription plays a cis-regulatory role in the adult. *Cell Rep*. 2012;2:111-23.
19. Feng Q, et al. Increased inducible nitric oxide synthase expression contributes to myocardial dysfunction and higher mortality after myocardial infarction in mice. *Circulation*. 2001;104:700-4.
20. Detombe SA, et al. Longitudinal follow-up of cardiac structure and functional changes in an infarct mouse model using retrospectively gated micro-computed tomography. *Invest Radiol*. 2008;43:520-9.
21. Burger D, et al. Role of heme oxygenase-1 in the cardioprotective effects of erythropoietin during myocardial ischemia and reperfusion. *Am J Physiol Heart Circ Physiol*. 2009;296:H84-93.
22. Ounzain S, et al. Genome-wide profiling of the cardiac transcriptome after myocardial infarction identifies novel heart-specific long non-coding RNAs. *Eur Heart J*. 2015;36:353-68a.
23. Konstantinidis K, et al. Mechanisms of cell death in heart disease. *Arterioscler Thromb Vasc Biol*. 2012;32:1552-62.
24. Szobi A, et al. Analysis of necroptotic proteins in failing human hearts. *J Transl Med*. 2017;15:86.
25. Luedde M, et al. RIP3, a kinase promoting necroptotic cell death, mediates adverse remodelling after myocardial infarction. *Cardiovasc Res*. 2014;103:206-16.
26. Pasparakis M and Vandenabeele P. Necroptosis and its role in inflammation. *Nature*. 2015;517:311-20.
27. Marques-Fernandez F, et al. TNFalpha induces survival through the FLIP-L-dependent activation of the MAPK/ERK pathway. *Cell Death Dis*. 2013;4:e493.
28. Wang H, et al. Mixed lineage kinase domain-like protein MLKL causes necrotic membrane disruption upon phosphorylation by RIP3. *Mol Cell*. 2014;54:133-46.

29. Chen L, et al. Long non-coding RNA Malat1 promotes neurite outgrowth through activation of ERK/MAPK signalling pathway in N2a cells. *J Cell Mol Med.* 2016;20:2102-2110.
30. Wu XS, et al. MALAT1 promotes the proliferation and metastasis of gallbladder cancer cells by activating the ERK/MAPK pathway. *Cancer Biol Ther.* 2014;15:806-14.
31. Zhao G, et al. The long noncoding RNA MALAT1 regulates the lipopolysaccharide-induced inflammatory response through its interaction with NF-kappaB. *FEBS Lett.* 2016;590:2884-95.
32. Tripathi V, et al. The nuclear-retained noncoding RNA MALAT1 regulates alternative splicing by modulating SR splicing factor phosphorylation. *Mol Cell.* 2010;39:925-38.
33. Zhang X, et al. Long noncoding rna malat1 regulates cerebrovascular pathologies in ischemic stroke. *J Neurosci.* 2017;37:1797-1806.
34. Chen H, et al. Long non-coding RNA MALAT-1 is downregulated in preeclampsia and regulates proliferation, apoptosis, migration and invasion of JEG-3 trophoblast cells. *Int J Clin Exp Pathol.* 2015;8:12718-27.
35. Zhang M, et al. Down-regulation of lncRNA MALAT1 reduces cardiomyocyte apoptosis and improves left ventricular function in diabetic rats. *Int J Cardiol.* 2016;203:214-6.
36. Liu J, et al. MicroRNA-155 prevents necrotic cell death in human cardiomyocyte progenitor cells via targeting RIP1. *J Cell Mol Med.* 2011;15:1474-82.
37. Cao S, et al. Tumor-suppressive function of long noncoding RNA MALAT1 in glioma cells by suppressing miR-155 expression and activating FBXW7 function. *Am J Cancer Res.* 2016;6:2561-2574.
38. Salle-Lefort S, et al. Hypoxia upregulates Malat1 expression through a CaMKK/AMPK/HIF-1alpha axis. *Int J Oncol.* 2016;49:1731-6.
39. Zhao ZH, et al. Long non-coding RNA MALAT1 functions as a mediator in cardioprotective effects of fentanyl in myocardial ischemia-reperfusion injury. *Cell Biol Int.* 2017;41:62-70.
40. Peters T, et al. Long non-coding rna malat-1 is dispensable during pressure overload-induced cardiac remodeling and failure in mice. *PLoS One.* 2016;11:e0150236.
41. Hausenloy DJ and Yellon DM. Cardioprotective growth factors. *Cardiovasc Res.* 2009;83:179-94.

42. Veldkamp CT, et al. Monomeric structure of the cardioprotective chemokine SDF-1/CXCL12. *Protein Sci.* 2009;18:1359-69.
43. Bujak M and Frangogiannis NG. The role of TGF-beta signaling in myocardial infarction and cardiac remodeling. *Cardiovasc Res.* 2007;74:184-95.
44. Horrigan MC, et al. Reduction in myocardial infarct size by basic fibroblast growth factor after temporary coronary occlusion in a canine model. *Circulation.* 1996;94:1927-33.
45. Hu X, et al. Stromal cell derived factor-1 alpha confers protection against myocardial ischemia/reperfusion injury: role of the cardiac stromal cell derived factor-1 alpha CXCR4 axis. *Circulation.* 2007;116:654-63.
46. Li N, et al. Endothelial nitric oxide synthase promotes bone marrow stromal cell migration to the ischemic myocardium via upregulation of stromal cell-derived factor-1alpha. *Stem Cells.* 2009;27:961-70.

Chapter 5

5 Chapter 5

5.1 Summary of Major Findings

The overall objective of this thesis was to assess the capacity for cardiac regeneration in neonatal mice, and investigate the contributions of the primary cilium and the lncRNA *Malat1* in responses to cardiac ischemic injury. Specifically, these studies aimed to determine the importance of *Wt1* and *Malat1* in neonatal cardiac regeneration, the role of the primary cilium in epicardial EMT, and the functional importance of *Malat1* in cardiac cell death. To achieve this goal, experimental approaches included *in vitro* cell culture and *in vivo* animal studies. MI was used as a model of cardiac injury in both adult and neonatal mice. The regenerative capacity in the neonatal mouse was assessed by attempting to perturb regeneration through reductions in *Wt1* and *Malat1* expression. The role of the primary cilium was investigated using an adenoviral construct containing shRNA for the Ift88 transport protein, while the importance of *Malat1* in ischemic injury was studied using a *Malat1*^{-/-} mouse.

In **Chapter 2**, the effects of *Wt1* knockdown and *Malat1* deficiency on the cardiac regenerative response were investigated using a *Wt1*^{CreER} mouse heterozygous for *Wt1*, and a *Malat1*^{-/-} mouse line. A protocol to cause reproducible cardiac injury was established in neonatal mice. Critical to the implementation of this protocol is the control of mouse temperature during the surgical procedure such that the coronary vasculature is still perfused and is thus visible during hypothermic anesthesia. Reproducible cardiac injury was demonstrated by 100% infarction rate with a consistent infarct size of ~ 49%

of the area at risk. All mice subject to coronary artery ligation exhibited reduced cardiac function (EF and FS) measured by echocardiography. Complete cardiac regeneration was evident 21 days post-MI as demonstrated by a normal ventricular architecture and lack of scarring after Masson's trichrome staining. Interestingly, neither *Wt1* knockdown nor *Malat1* deficiency affected the cardiac regenerative response; regardless of genotype, all mice exhibited 100% cardiac regeneration. These data further support the notion that the mammalian neonate possesses a powerful capacity for cardiac regeneration.

EMT is a key regulator of the cardiac response to MI.¹ In **Chapter 3**, the effects of primary ciliary disassembly on EMT and cardiac function post-MI were assessed. To carry out this aim, an adenoviral construct containing shRNA for *Ift88* was employed to disassemble the primary cilium. *In vitro* cultures of epicardium derived cells (EPDCs) treated with Ad-sh*Ift88* had fewer cells possessing cilia, and cilia that were present were shorter in length. The primary cilium is known to mitigate EMT and affect cardiogenesis,^{2,3} however its role in epicardial activation in the adult heart has apparently never been investigated. We demonstrate for the first time that *Ift88* knockdown potentiates epicardial activation and EMT both *in vitro* and *in vivo* post-MI. Molecular analysis demonstrated increased expression levels of the key EMT transcription factors *Wt1*, *Snail*, *Slug* and β -catenin in the peri-infarct area of hearts injected with Ad-sh*Ift88*. This resulted in improved neovascularization as compared to the control group. Overall, primary ciliary disassembly was associated with the attenuation of adverse remodeling post-MI, improved cardiac function, and reduced cardiomyocyte hypertrophy.

Myocardial injury causing loss of functional cardiomyocytes within a few hours after ischemia produces pathological changes in the heart which may ultimately lead to

heart failure. In **Chapter 4** the role of *Malat1* in acute myocardial ischemia was investigated. To carry out this aim, a *Malat1*^{-/-} mouse line was obtained for use in *in vivo* experiments. On initial experimental analysis, it was noted that 24 hours post-MI *Malat1*^{-/-} mice had larger infarcts than their WT counterparts. Importantly, this led to reduced cardiac function. Surprisingly, myocardial apoptosis was not affected in this model, but rather *Malat1*^{-/-} mice exhibited reduced expression of cardioprotective factors and augmented necrosis. We further demonstrated the involvement of regulated necroptotic signaling via *TNF- α* and RIP3 expression. Thus, we provide novel evidence that *Malat1* may affect the necroptosis pathway, and that its deficiency enhances injury from cardiac ischemia.

In summary, we have validated the ability of neonates to recover from MI, and observed evidence of the involvement of the primary cilium and the lncRNA *Malat1* as mediators of the damaging responses to this type of cardiac injury. Knockdown of the primary ciliary intraflagellar transport protein *Ift88* enhances endogenous repair mechanisms by supporting EPDC EMT. This leads to neovascularization, which mitigates adverse cardiac remodeling post-MI. Contrastingly, deficiency of *Malat1* augments cell death from cardiac ischemic injury. These studies provide important information for developing novel strategies for both the treatment of MI, and identifying factors which may place patients at risk for increased damage in the face of MI. A summary of the findings from these studies is shown in **Figure 5.1**.

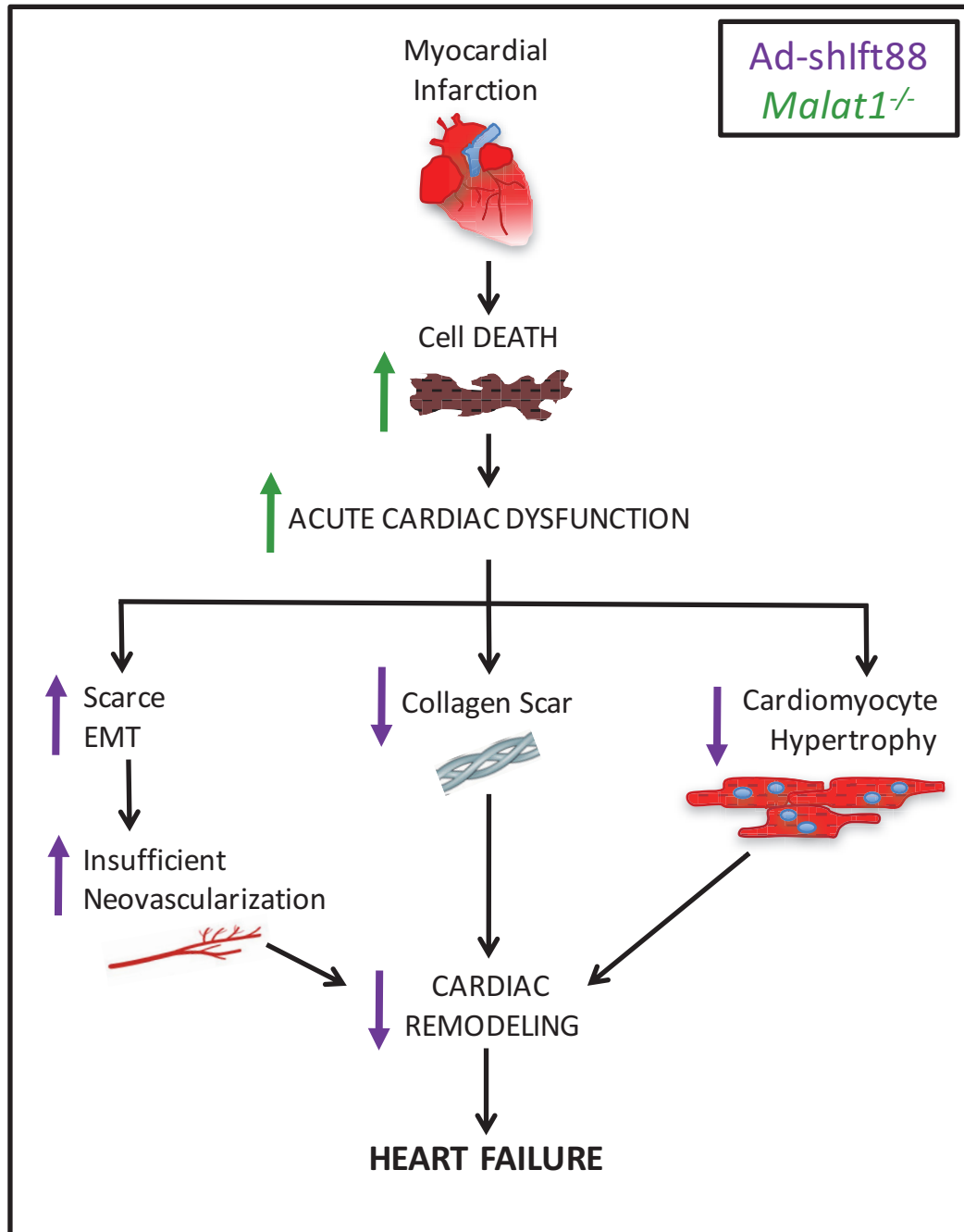


Figure 5.1. Summary of the cardiac response to myocardial infarction and the effects of primary ciliary disassembly and *Malat1* deficiency.

Myocardial infarction causes cell death, which results in cardiac dysfunction. An insufficient epithelial-to-mesenchymal transition (EMT) response to support neovascularization, coupled with collagen deposition and hypertrophy in remaining viable cardiomyocytes causes cardiac remodeling and heart failure. Effects of Ad-shIft88 and *Malat1* deficiency are shown by purple and green arrows, respectively.

5.2 Study Limitations

5.2.1 Mouse models

To evaluate the basic pathophysiological changes and potential therapies for any disease, it is necessary to simulate the human entity using a model that is both physiologically similar to humans, with conserved biological processes, and offers high throughput with minimal cost. The mouse genome has 99% homology with that of the human,⁴ and the use of mouse models offers the great advantage of possible genetic manipulation through knockout or overexpression mouse lines. Advancements in comparative genomics and the understanding of how small genetic mutations alter mouse response to disease may offer potential targets for therapeutics for humans and may be applied to identify individuals at risk for disease. However, the mouse genome does not completely recapitulate that of the human, and differences in gene isoform expression can cause major physiological changes. For example, the predominant ventricular sarcomeric protein in humans is β -myosin heavy chain (β -MyHC), whereas ventricular protein composition in mouse is >95% α -MyHC.⁵ Thus, genetic alterations may result in different physiological effects which may cause drastic phenotypic consequences in response to stressful stimuli in mice as compared to that in observed in humans with similar genetic mutations.

Another advantage of murine disease modelling is the ability to ensure disease conditions are the same in all groups studied, while also observing phenomena at any time point in the disease process. The work presented here made use of an animal model of MI by surgically ligating the left anterior descending coronary artery (LAD). This is advantageous over other animal models of cardiac injury such as transverse aortic

constriction (TAC) or electrocautery as the effects on the myocardium are physiologically very similar to those which occur from a coronary artery block in humans. Furthermore, although harm from acute reperfusion injury invokes further myocyte cell death in the setting of ischemia/reperfusion,⁶ permanent occlusion of the LAD was chosen over an ischemia/reperfusion model in our studies. As duration of occlusion increases, the risk of stunned myocardium becoming infarcted increases, producing a larger, long lasting irreversible cardiac injury in the setting of permanent occlusion.^{7, 8} Thus, any beneficial effects demonstrated by shIft88 or *Malat1* could be critically important, particularly for the development of therapeutics for patients who are unable to receive reperfusion therapy.

Unfortunately, this approach does involve some inherent disadvantages. The most common cause of human MI is blockage of the LAD by rupture of an atherosclerotic plaque.⁹ Most patients with this form of MI carry a significant burden of comorbid conditions such as dyslipidemia, hypertension or diabetes.¹⁰ Many of these patients have already progressed to a late stage of cardiac disease, having already experienced angina, sometimes intermittent ischemia, and moderate cardiac remodeling by hypertrophy.¹¹ Furthermore, a disproportionately high percentage of patients experiencing coronary artery disease are older individuals.¹² Thus, the myocardium of a typical MI patient is already moderately damaged, and the repair capabilities of this tissue would be inferior to that of a murine heart from our model of MI. Despite these shortcomings, cardiac research continues to depend heavily on mouse models of MI for the development of therapeutics and the understanding of molecular processes contributing to heart failure.

5.2.2 Genetically altered mice

The ease with which the mouse genome can be manipulated makes it an invaluable model to study the mechanisms of cardiovascular disease. In this study, the $Wt1^{CreER}$ mouse heterozygous for the $Wt1$ allele was used. However, heterozygous deficiency of $Wt1$ may not be sufficient to perturb the regenerative capacity in neonates. $Wt1$ expression by the remaining endogenous allele could be responsible for the lack of any observable effects in $Wt1^{CreER}$ mice on cardiac regeneration. In 1993, *Kreidberg et al.* reported on the developmental deficiencies of mice with a homozygous deletion for $Wt1$.¹³ Even epicardial specific $Wt1$ mutants die from cardiovascular defects between E16.5 and E18.5.¹⁴ Although the $Wt1$ homozygous deletion cannot be used to study the role of $Wt1$ in the postnatal animal, $Wt1$ conditional knockout has been demonstrated in the study of glomerulosclerosis.¹⁵

Interestingly, $Wt1$ mutations have been observed in the human population, and mutations in an exon from 11q13 causes Wilms' tumors, a kidney tumor typically presenting in childhood.¹⁶ Larger mutations in this gene may cause WAGR syndrome, a more serious syndrome with a spectrum of defects including Wilms' tumours, aniridia, genitourinary abnormalities and mental retardation, or Denys-Drash syndrome in which patients present with ambiguous genitalia, dysgenic gonads, nephropathy and Wilms' tumors.¹⁷ Although mouse models of these syndromes using $Wt1$ deletion strategies identified the importance of $Wt1$ in the epicardium,¹⁸ cardiac abnormalities have only been reported in one patient with WAGR or Denys-Drash syndrome.¹⁹ However, Meacham syndrome is another rare multiple formation syndrome with an association to $Wt1$ mutations.¹⁹ Abnormalities, including congenital heart defects, have presented in

proepicardium derived tissues in these patients.¹⁹ Whether homozygous deletion of other parts of this gene in humans results in severe cardiac defects causing spontaneous abortion early in development has not been investigated.

The differential effects observed in *Wt1* mutant mice as compared to human patients with *Wt1* mutations exemplifies a disadvantage of genetic knockout or knockdown mutant mice. Full genetic knockout or knockdown mutations may cause different phenotypes from point mutations in a gene. Proteins, such as *Wt1*, are created from multiple exons, and variants of a gene can produce different isoforms, causing differential effects on protein structure and function.²⁰ Thus, while genetic knockouts may cause a drastic effect in development, point variants found in humans may have different consequences.

Like the lack of effect on cardiac regeneration in *Wt1*^{CreER} neonatal mice, knockout of the lncRNA *Malat1* had no observed effect on the cardiac regenerative capacity in the neonatal mouse. While there were no observable effects in the heart at this early time point in postnatal life, in **Chapter 4** we did observe detrimental effects of *Malat1* deficiency on cardiac function after MI in the adult. The differences in these studies underline the importance of differential gene expression signatures, causing interactions during development which are different from those in the adult mammal. For example, epigenetic regulators cause changes in expression profiles of proteins from development to post-natal life.²¹ Furthermore, *Malat1* is known to be affected by methylation status, and while it is ubiquitously expressed in all tissues during early embryonic development, its expression varies markedly in adult tissue.^{22, 23}

As *Malat1* is expressed in numerous cell types, the effects observed in the whole body knockout could be the result of *Malat1* deficiency in non-cardiac cells. Although no morphological differences between WT and *Malat1*^{-/-} mice have been reported, we cannot definitively rule out that *Malat1* deficiency in other cell types may have contributed to the effects observed in **Chapter 4**. TNF- α and other pro-inflammatory cytokines are known to play a role in the response to MI.²⁴ It is possible that the role of *Malat1* in TNF- α mediated inflammation could affect macrophage and neutrophil response to infarction. Neutrophil recruitment peaks 1 day post-infarction and contributes to the production of reactive oxygen species.²⁵ It is possible that *Malat1* deficiency in neutrophils may have altered the response to MI in our study. Other inflammatory cells such as macrophages are known to be recruited to the infarct region several days after MI.²⁵ As such, it is unlikely that reduced *Malat1* in these inflammatory cells is a major player in the responses observed at the early 1 day time point in this study. It would be interesting to observe the effects of a cardiac specific *Malat1* knockout or *Malat1* knockdown in cardiomyocyte culture to further clarify these processes. In previous studies, siRNA has been used to knockdown *Malat1* in a stable cardiomyocyte cell line *in vitro*.²⁶ Furthermore, *Malat1* expression has been reduced in the *in vivo* setting using antisense GapmeR reduction.²⁷ However, a cardiac specific knockout or knockdown has yet to be published.

To the best of our knowledge, there are no reported cases of humans with *MALATI* null mutations. However, *MALATI* expression is known to be upregulated in various types of cancer.²⁸ A recent study demonstrated that a genetic variant on the *MALATI* allele was associated with better survival for advanced lung adenocarcinoma

patients.²⁹ It would be interesting to determine whether patients with this allele suffer worse outcomes in the face of an MI. Furthermore, the *MALATI* gene produces a very long transcript (6700 nt),³⁰ thus, determining the structural and functional effects of this mutation should be the subject of future work.

5.2.3 Methods for Ift88 knockdown

In **Chapter 3**, the Ift88 transport protein was knocked down using an adenoviral construct containing short hairpin RNA. This approach has several pitfalls. Firstly, as noted in **Chapter 3**, uptake of the adenoviral construct was not restricted to epicardial cells. Thus, the observed effects could be partially the result of Ift88 knockdown in other cell types. This could be improved upon using an epicardial specific promoter (e.g., Wt1 promoter) in future work. Secondly, an intramyocardial injection was used to deliver the Ad-shIft88 vector. This method would be suboptimal in the clinical setting as the myocardium is not directly approachable without opening of the thoracic cavity. Intravenous (IV) adenoviral delivery may be more a more clinically translatable method, as opening of the chest cavity would not be required. Tissue specific adenoviral targeting has been used previously to target the myocardium via IV injection.³¹ Catheter-based intramyocardial gene delivery by transendocardial injection is another superior approach which may be advantageous in the clinical setting. Using this less invasive approach, *Kornowski et al.* demonstrated that transgenes can be effectively delivered to precise regions of the myocardium.³² Finally, adenoviral administration can stimulate the immune system, causing activation of the interferon pathway.³³ The safety profiles of adeno-associated viruses (AAVs) and biological nanoparticles (BNPs) have been demonstrated to be superior to those of adenoviral, retroviral and lentiviral vectors, and

may be more suitable approaches for clinical translation.^{34, 35} In fact, AAVs have been shown to have a higher and longer lasting infection efficiency than adenoviruses in the heart.³⁶

In addition to vector delivery, method of gene silencing can affect the efficiency of knockdown. While shRNA provides more efficient knockdown than other methods like siRNA, shRNA itself can cause unexpected cellular effects.³⁷ Cell toxicity can arise from excess shRNA due to competition with normal cellular miRNA for processing machinery.³⁸ This has been demonstrated by fatality in mice from oversaturation of the endogenous RNA processing machinery due to sustained high doses of shRNA via IV infusion.³⁹ Thus, this type of cell injury should be controlled for in future work using another shRNA in combination with the control adenovirus. Other methods of RNA knockdown should also be considered. For example, CRISPR/Cas9 was recently demonstrated to efficiently knockdown *Ift88* in zebrafish.⁴⁰

5.2.4 Suggestions for future research

This thesis demonstrated the extraordinary capacity for regeneration in neonatal cardiac tissue, and the roles of EMT, primary cilia and *Malat1* in supporting repair and mitigating injury. However, other aspects of EMT signaling through the primary cilium and the mechanisms of action of *Malat1* should be investigated in future studies to gain a further understanding of their roles in MI.

In **Chapter 2**, the remarkable capacity of cardiac regeneration in neonatal mice was demonstrated; WT, *Wt1^{CreER}*, and *Malat1^{-/-}* neonates were able to completely regenerate their hearts post-MI. As mentioned above, the heterozygous deletion of *Wt1* in

the $Wt1^{CreER}$ mouse may not be sufficient to perturb the regenerative response in the neonatal heart. Although conditional Cre-mediated $Wt1$ deletion is not 100% effective,¹⁴ it is possible that the use of an inducible $Wt1$ knockout may provide superior $Wt1$ knockdown and could thus resolve this issue. Furthermore, *Malat1* was demonstrated to play a role in necroptosis mediated cell death in **Chapter 4**, however the effect of necroptosis in neonatal cardiac regeneration has not been investigated. It would be interesting to determine whether perturbing the necroptosis pathway by another downstream mediator would affect regenerative capacity. For example, overexpression of RIP3 is known to augment ischemic injury from MI,⁴¹ thus it is possible that RIP3 overexpression would reduce the regenerative capacity in neonatal mice.

In **Chapter 3** of this thesis, knockdown of the primary cilium was demonstrated to augment EMT, neovascularization and cardiac repair post-MI. In addition to the suggested future work mentioned above, there are several experiments which could further support our findings. We demonstrated augmented EPDC EMT on a collagen gel *in vitro* by primary ciliary disassembly. When activated EPDCs are seeded next to cardiomyocytes in a transwell assay, they migrate towards the cardiomyocytes, reflecting their migratory capacity.⁴² To distinguish migratory ability from mesenchymal like differentiation, EPDCs could be treated with Ad-shIft88 in a transwell assay. Additionally, we demonstrated a significantly higher density of arterioles and capillaries in the peri-infarct area post-MI in our Ad-shIft88 treated group. To confirm the effect of shIft88 on neovascularization, an *in vivo* cardiac Matrigel plug assay could be performed to definitively establish an angiogenic response. Given the role of the primary cilium in EMT, it is expected that Ad-shIft88 administration with the Matrigel plug would enhance

vessel-like formation. Furthermore, to definitively establish whether EPDCs were responsible for the increased formation of vasculature, a lineage tracing study could be performed to track Wt1 positive cells. Our laboratory has previously demonstrated the contribution of Wt1 positive EPDCs to arteriogenesis using ROSA^{mTmG};Wt1^{CreER} mice,⁴² which express membrane-targeted tandem dimer Tomato (mT) globally prior to Cre-mediated excision, and membrane-targeted enhanced green fluorescent protein (mG) upon Cre-mediated excision in Wt1 positive cells. If this study were to be performed, an adenoviral construct containing shIfi88 without an eGFP tag would be required.

In **Chapter 4**, deficiency of *Malat1* was demonstrated to augment injury from MI. The protective role of *Malat1* observed in our study conflicts with the report by *Peters et al.* which demonstrated that *Malat1* was dispensable in cardiac hypertrophy.⁴³ Specifically, this group did not observe any effects of *Malat1* deficiency in long term cardiac hypertrophic remodeling in response to pressure overload. The long term effects of MI induced cardiac remodeling and hypertrophy in *Malat1*^{-/-} mice were not investigated in our study; this should be the subject of future work. Given the role of *Malat1* in EMT and angiogenesis,^{27, 44} it is expected that *Malat1* deficiency will attenuate neovascularization, augment deleterious remodeling, and enhance hypertrophy, thereby worsening cardiac function as compared to controls post-MI.

Furthermore, to definitively discern the role of *Malat1* in cardiac ischemic injury, the mechanism of action of *Malat1* should be established. An attempt was made in the present investigation to determine the mechanism by which *Malat1* affects cardiac cell death. Although we demonstrated the upregulation of mediators of necroptosis in *Malat1*^{-/-} mice, future work is required to study the molecular mechanism by which *Malat1*

regulates the necroptotic pathway. A model of hypoxic injury in cardiomyocytes *in vitro* may be helpful in elucidating this mechanism. Other studies have demonstrated a role for necroptosis in cardiomyocyte death *in vitro*, however the response to hypoxia in these cells was not studied.⁴¹

Differential enzymatic processing of the *MALAT1* transcript has recently been demonstrated to yield a small RNA molecule, *mascRNA*, which consists of 61 nucleotides, and localizes to the cytoplasm.⁴⁵ High levels of *mascRNA* have been demonstrated in human immunoregulatory cells.⁴⁶ *Gast et al.* further showed differential expression patterns of *MALAT1* and *mascRNA*.⁴⁶ Furthermore, in a monocyte cell line, anti-*mascRNA* treatment enhanced caspase activity and TNF- α expression. Interestingly, however, they demonstrate that *mascRNA* enhances innate immunity gene expression in cardiomyocytes. This suggests that the loss of *mascRNA* may contribute to the detrimental effects of *Malat1* deficiency in our study. *mascRNA* levels should be measured in future work.

5.2.5 Conclusions

This thesis provides the first evidence for the roles of the primary cilium and *Malat1* in cardiac ischemic injury. Knockdown of the primary cilium offers cardiac protection and improves cardiac repair post-MI, while *Malat1* deficiency augments cardiac injury from MI. Although *Malat1* and EMT were demonstrated to be important for mitigating injury from cardiac ischemia, perturbing their activity did not affect the capacity for neonatal cardiac regeneration (**Chapter 2**). Further investigation is required to determine the therapeutic potential of Ad-shIft88 in humans, however it is clear that primary ciliary disassembly and EMT are beneficial post-MI in the adult (**Chapter 3**).

This work has provided valuable insight into the mechanisms by which the primary cilium mitigates differentiation and migration of EPDCs. Furthermore, while future studies are required to determine the exact mechanism by which *Malat1* affects cardiomyocyte viability, this work demonstrates its importance in mitigating injury from MI (**Chapter 4**). Whether *MALAT1* expression may play a role in determining infarct size in human MI remains to be determined. Overall, the doctoral research presented herein has broadened the understanding of the primary cilium and the lncRNA *Malat1* in the response to MI, and resultant cardiac function post-ischemic injury, and may open up new strategies in the development of therapeutics for the treatment of MI.

5.3 References

1. von Gise A and Pu WT. Endocardial and epicardial epithelial to mesenchymal transitions in heart development and disease. *Circ Res*. 2012;110:1628-45.
2. Egorova AD, et al. Lack of primary cilia primes shear-induced endothelial-to-mesenchymal transition. *Circ Res*. 2011;108:1093-101.
3. Hassounah NB, et al. Molecular pathways: the role of primary cilia in cancer progression and therapeutics with a focus on Hedgehog signaling. *Clin Cancer Res*. 2012;18:2429-35.
4. Mouse Genome Sequencing C, et al. Initial sequencing and comparative analysis of the mouse genome. *Nature*. 2002;420:520-62.
5. Marian AJ. On mice, rabbits, and human heart failure. *Circulation*. 2005;111:2276-9.
6. Yellon DM and Hausenloy DJ. Myocardial reperfusion injury. *N Engl J Med*. 2007;357:1121-35.
7. Reimer KA, et al. The wavefront phenomenon of ischemic cell death. 1. Myocardial infarct size vs duration of coronary occlusion in dogs. *Circulation*. 1977;56:786-94.
8. Miura H, et al. Limitation of infarct size and ventricular remodeling in patients with completely reperfused anterior acute myocardial infarction--the potential role of ischemia time. *Clin Cardiol*. 2002;25:566-71.
9. Baron T, et al. Type 2 myocardial infarction in clinical practice. *Heart*. 2015;101:101-6.
10. Sachdev M, et al. The prognostic importance of comorbidity for mortality in patients with stable coronary artery disease. *J Am Coll Cardiol*. 2004;43:576-82.
11. Cupples LA, et al. Preexisting cardiovascular conditions and long-term prognosis after initial myocardial infarction: the Framingham Study. *Am Heart J*. 1993;125:863-72.
12. Rogers WJ, et al. Trends in presenting characteristics and hospital mortality among patients with ST elevation and non-ST elevation myocardial infarction in the National Registry of Myocardial Infarction from 1990 to 2006. *Am Heart J*. 2008;156:1026-34.
13. Kreidberg JA, et al. WT-1 is required for early kidney development. *Cell*. 1993;74:679-91.

14. Martinez-Estrada OM, et al. Wt1 is required for cardiovascular progenitor cell formation through transcriptional control of Snail and E-cadherin. *Nat Genet.* 2010;42:89-93.
15. Gebeshuber CA, et al. Focal segmental glomerulosclerosis is induced by microRNA-193a and its downregulation of WT1. *Nat Med.* 2013;19:481-7.
16. Haber DA, et al. An internal deletion within an 11p13 zinc finger gene contributes to the development of Wilms' tumor. *Cell.* 1990;61:1257-69.
17. Dome JS and Huff V. Wilms tumor predisposition. In: R. A. Pagon, M. P. Adam, H. H. Ardinger, S. E. Wallace, A. Amemiya, L. J. H. Bean, T. D. Bird, N. Ledbetter, H. C. Mefford, R. J. H. Smith and K. Stephens, eds. *GeneReviews(R)* Seattle (WA); 1993.
18. Moore AW, et al. YAC complementation shows a requirement for Wt1 in the development of epicardium, adrenal gland and throughout nephrogenesis. *Development.* 1999;126:1845-57.
19. Suri M, et al. WT1 mutations in Meacham syndrome suggest a coelomic mesothelial origin of the cardiac and diaphragmatic malformations. *Am J Med Genet A.* 2007;143A:2312-20.
20. Mrowka C and Schedl A. Wilms' tumor suppressor gene WT1: from structure to renal pathophysiologic features. *J Am Soc Nephrol.* 2000;11 Suppl 16:S106-15.
21. Yuen RK, et al. Extensive epigenetic reprogramming in human somatic tissues between fetus and adult. *Epigenetics Chromatin.* 2011;4:7.
22. Guo F, et al. MALAT1 is an oncogenic long non-coding RNA associated with tumor invasion in non-small cell lung cancer regulated by DNA methylation. *Int J Clin Exp Pathol.* 2015;8:15903-10.
23. Nakagawa S, et al. Malat1 is not an essential component of nuclear speckles in mice. *RNA.* 2012;18:1487-99.
24. Nah DY and Rhee MY. The inflammatory response and cardiac repair after myocardial infarction. *Korean Circ J.* 2009;39:393-8.
25. Liu J, et al. Inflammation and Inflammatory Cells in Myocardial Infarction and Reperfusion Injury: A Double-Edged Sword. *Clin Med Insights Cardiol.* 2016;10:79-84.
26. Zhao ZH, et al. Long non-coding RNA MALAT1 functions as a mediator in cardioprotective effects of fentanyl in myocardial ischemia-reperfusion injury. *Cell Biol Int.* 2017;41:62-70.

27. Michalik KM, et al. Long noncoding RNA MALAT1 regulates endothelial cell function and vessel growth. *Circ Res*. 2014;114:1389-97.
28. Yoshimoto R, et al. MALAT1 long non-coding RNA in cancer. *Biochim Biophys Acta*. 2016;1859:192-9.
29. Wang JZ, et al. A genetic variant in long non-coding RNA MALAT1 associated with survival outcome among patients with advanced lung adenocarcinoma: a survival cohort analysis. *BMC Cancer*. 2017;17:167.
30. Zhang B, et al. The lncRNA Malat1 is dispensable for mouse development but its transcription plays a cis-regulatory role in the adult. *Cell Rep*. 2012;2:111-23.
31. Pacak CA, et al. Tissue specific promoters improve specificity of AAV9 mediated transgene expression following intra-vascular gene delivery in neonatal mice. *Genet Vaccines Ther*. 2008;6:13.
32. Kornowski R, et al. Electromagnetic guidance for catheter-based transendocardial injection: a platform for intramyocardial angiogenesis therapy. Results in normal and ischemic porcine models. *J Am Coll Cardiol*. 2000;35:1031-9.
33. Thaci B, et al. The challenge for gene therapy: innate immune response to adenoviruses. *Oncotarget*. 2011;2:113-21.
34. Kawase Y, et al. Rescuing the failing heart by targeted gene transfer. *J Am Coll Cardiol*. 2011;57:1169-80.
35. Daka A and Peer D. RNAi-based nanomedicines for targeted personalized therapy. *Adv Drug Deliv Rev*. 2012;64:1508-21.
36. Vassalli G, et al. Adeno-associated virus (AAV) vectors achieve prolonged transgene expression in mouse myocardium and arteries in vivo: a comparative study with adenovirus vectors. *Int J Cardiol*. 2003;90:229-38.
37. Boudreau RL, et al. Minimizing variables among hairpin-based RNAi vectors reveals the potency of shRNAs. *RNA*. 2008;14:1834-44.
38. van Gestel MA, et al. shRNA-induced saturation of the microRNA pathway in the rat brain. *Gene Ther*. 2014;21:205-11.
39. Grimm D, et al. Fatality in mice due to oversaturation of cellular microRNA/short hairpin RNA pathways. *Nature*. 2006;441:537-41.
40. Chen X, et al. Cilia control vascular mural cell recruitment in vertebrates. *Cell Rep*. 2017;18:1033-1047.

41. Luedde M, et al. RIP3, a kinase promoting necroptotic cell death, mediates adverse remodelling after myocardial infarction. *Cardiovasc Res.* 2014;103:206-16.
42. Xiang FL, et al. Cardiac-specific overexpression of human stem cell factor promotes epicardial activation and arteriogenesis after myocardial infarction. *Circ Heart Fail.* 2014;7:831-42.
43. Peters T, et al. Long non-coding rna malat-1 is dispensable during pressure overload-induced cardiac remodeling and failure in mice. *PLoS One.* 2016;11:e0150236.
44. Yang S, et al. Long non-coding rna malat1 mediates transforming growth factor beta1-induced epithelial-mesenchymal transition of retinal pigment epithelial cells. *PLoS One.* 2016;11:e0152687.
45. Wilusz JE, et al. 3' end processing of a long nuclear-retained noncoding RNA yields a tRNA-like cytoplasmic RNA. *Cell.* 2008;135:919-32.
46. Gast M, et al. Long noncoding RNA MALAT1-derived mascRNA is involved in cardiovascular innate immunity. *J Mol Cell Biol.* 2016;8:178-81.

Appendix



AUP Number: [REDACTED]

PI Name: [REDACTED]

AUP Title: Modulation Of Myocardial Function In Myocardial Infarction, Sepsis And Diabetes

Approval Date: 11/28/2016

Official Notice of Animal Use Subcommittee (AUS) Approval: Your new Animal Use Protocol (AUP) entitled "Modulation Of Myocardial Function In Myocardial Infarction, Sepsis And Diabetes" has been APPROVED by the Animal Use Subcommittee of the University Council on Animal Care. This approval, although valid for four years, and is subject to annual Protocol Renewal.2016-099::1

1. This AUP number must be indicated when ordering animals for this project.
2. Animals for other projects may not be ordered under this AUP number.
3. Purchases of animals other than through this system must be cleared through the ACVS office. Health certificates will be required.

The holder of this Animal Use Protocol is responsible to ensure that all associated safety components (biosafety, radiation safety, general laboratory safety) comply with institutional safety standards and have received all necessary approvals. Please consult directly with your institutional safety officers.

Submitted by: Copeman, Laura
on behalf of the Animal Use Subcommittee
University Council on Animal Care



Curriculum Vitae

Jessica Blom

**Post-secondary
Education and
Degrees:**

University of Guelph
Guelph, Ontario, Canada
2006-2010
BSc, Biomedical Science.

University of Edinburgh
Edinburgh, Scotland
2010 -2011
MSc by Research in Cardiovascular Biology.

Western University
London, Ontario, Canada
2012-2017
MD/PhD Candidate
2014-2017
PhD Candidate, Physiology and Pharmacology

**Honours and
Awards:**

Biomedical Sciences Research Award of Merit
University of Guelph
Guelph, Ontario, Canada
2010

Young Investigator Prize for Best Oral Presentation
Scottish Cardiovascular Forum
Aberdeen, Scotland
2010

Jack Banham Hargreaves/ Jessie Louisa Florence Hargreaves
MD/PhD Award
School of Graduate and Postdoctoral Studies and Schulich School
of Medicine and Dentistry
2012-2014

Western Graduate Research Scholarship
Western University
2014-2015, 2015-2016, 2016-2017

Queen Elizabeth II Graduate Scholarship in Science and
Technology

Ministry of Training, Colleges and Universities
Western University
2015-2016, 2016-2017

Ontario Graduate Scholarship
Ontario Council on Graduate Studies
2014-2015, 2015-2016, 2016-2017

Malcolm Arnold Presentation Award in Cardiovascular Sciences
Physiology & Pharmacology Research Day (1st Place Poster)
Department of Physiology and Pharmacology
Western University
2015 & 2016

3MT (Three Minute Thesis) 3rd Place Winner
Western University
2016

CIHR Canadian Student Health Research Forum – Poster
Competition Silver Award
2016

Invited Oral Presentations: London Health Research Day
London, Ontario
2017

National & International Conference Poster Presentations: CITAC AGM
Clinician Investigator Trainee Association of Canada
Toronto, Ontario
2015 & 2016

Experimental Biology
San Diego, CA, USA
2016

Related Work Experience Teaching Assistant – Cardiovascular Pharmacology 4320A
Western University
2014-2015, 2015-2016

Publications:

Blom JN, Lu X, Arnold P, Feng Q. Myocardial infarction in neonatal mice, a model of cardiac regeneration. *Journal of Visualized Experiments*. **2016; 111: e54100**